



Search for pair production of scalar leptoquarks decaying into first- or second-generation leptons and top quarks in proton–proton collisions at $\sqrt{s} = 13$ TeV with the ATLAS detector

ATLAS Collaboration*

CERN, 1211 Geneva 23, Switzerland

Received: 6 October 2020 / Accepted: 25 February 2021 / Published online: 12 April 2021
© CERN for the benefit of the ATLAS collaboration 2021

Abstract A search for pair production of scalar leptoquarks, each decaying into either an electron or a muon and a top quark, is presented. This is the first leptoquark search using ATLAS data to investigate top-philic cross-generational couplings that could provide explanations for recently observed anomalies in B meson decays. This analysis targets high leptoquark masses which cause the decay products of each resultant top quark to be contained within a single high- p_T large-radius jet. The full Run 2 dataset is exploited, consisting of 139 fb^{-1} of data collected from proton–proton collisions at $\sqrt{s} = 13$ TeV from 2015 to 2018 with the ATLAS detector at the CERN Large Hadron Collider. In the absence of any significant deviation from the background expectation, lower limits on the leptoquark masses are set at 1480 GeV and 1470 GeV for the electron and muon channel, respectively.

1 Introduction

The quark and lepton sectors of the standard model (SM) are interestingly similar, motivating one to hypothesize a fundamental symmetry between the two sectors. Such a symmetry can be found in many grand unified theories, such as grand unified SU(5) [1], the Pati–Salam model based on SU(4) [2], or R-parity-violating (RPV) supersymmetry (SUSY) models [3]. These models predict a new class of bosons carrying both lepton and baryon number, called leptoquarks (LQs). LQs are hypothetical colour-triplet bosons which couple directly to quarks and leptons. They can be of either scalar or vector nature, and carry fractional electric charge. The production cross section of vector LQs could be enhanced relative to that of scalar LQs due to the existence of a massive gluon partner in the minimal set of vector companions [4].

LQs have recently gained attention as they provide an attractive explanation of the recent hints of possible lepton-flavour-universality violation from the observed B meson decay anomalies in BaBar [5], Belle [6] and LHCb [7–9]. Single scalar (S_3) or vector (U_3) LQ triplet models [10], as well as a mixed model of a doublet and a singlet LQ ($R_2 + \tilde{U}_1$) [11] are possible solutions to the flavour-changing neutral current B anomaly. LQs are also motivated by a long-standing deviation from the SM in the anomalous muon magnetic dipole moment measured with the E821 experiment at Brookhaven National Laboratory [12, 13]. At the Large Hadron Collider (LHC) [14], LQs could be produced in pairs, or singly in association with a lepton.

This analysis targets LQ pair production, which is dominated by strong interactions and largely insensitive to the Yukawa coupling at a LQ–lepton–quark vertex. The lowest-order Feynman diagrams are shown in Fig. 1. Gluon-initiated processes dominate for LQ masses less than 1.5 TeV. The t -channel lepton exchange process contributes to the cross section at the 10% level, and is thus neglected in this analysis [15–18]. Only scalar LQ production is considered because this is less model dependent than vector LQ production. The LQ–lepton–quark couplings are determined by two parameters: a model parameter β , that controls the branching ratio into charged leptons or neutrinos, and the coupling parameter λ . The coupling to charged leptons is given by $\sqrt{\beta}\lambda$, and the coupling to neutrinos by $\sqrt{1-\beta}\lambda$.

Most previous searches have assumed that leptoquarks couple to quarks and leptons of the same generation. Recently, there have been dedicated searches at the LHC for LQ pair production in the $LQ \rightarrow q\ell$, $LQ \rightarrow c\ell$, $LQ \rightarrow b\ell$, and $LQ \rightarrow t\tau$ channels using the full Run 2 proton–proton (pp) collision dataset collected at $\sqrt{s} = 13$ TeV [19, 20]. The results presented here pertain to the search for cross-generational leptoquarks with decays into a top quark and an electron or a top quark and a muon, in which both top quarks decay hadronically. It is optimized for LQ masses larger than 1 TeV, for which the top quarks tend to be boosted. Therefore,

* e-mail: atlas.publications@cern.ch

the signature considered is a pair of same-flavour opposite-sign leptons and a pair of large-radius (large- R) jets. Simultaneous couplings of LQs to the first- and second-generation leptons are tightly constrained by the measurements of rare lepton-flavour-violating decays [21], and thus not considered in this paper. A boosted decision tree (BDT) approach, based on kinematic variables and jet substructure variables, is applied to classify events as originating from the signal or background processes in the signal region. Dedicated control regions are constructed to control the normalization of the dominant backgrounds: $t\bar{t}$ and $Z + \text{jets}$ production. The extraction of the signal strength is performed through a simultaneous likelihood fit to the BDT discriminant distribution and the control region yields. The LQ $\rightarrow t\mu$ and LQ $\rightarrow te$ channels have not been examined previously in ATLAS. The CMS Collaboration has published a search using 35.9 fb^{-1} of data collected in 2015–2016 that excluded masses below 1420 GeV for scalar LQs decaying exclusively into $t\mu$ [22].

2 ATLAS detector

The ATLAS detector [23–25] at the LHC is a multipurpose particle detector with a forward–backward symmetric cylindrical geometry that covers nearly the entire solid angle around the collision point. It consists of an inner detector (ID) surrounded by a thin superconducting solenoid providing a 2 T axial magnetic field, electromagnetic and hadronic calorimeters, and a muon spectrometer. The inner detector covers the pseudorapidity range¹ $|\eta| < 2.5$. It consists of a silicon pixel detector, including the insertable B-layer installed after Run 1 of the LHC, and a silicon microstrip detector surrounding the pixel detector, followed by a transition radiation straw-tube tracker. Lead/liquid-argon sampling calorimeters provide electromagnetic energy measurements with high granularity and a steel/scintillator-tile hadron calorimeter covers the central pseudorapidity range ($|\eta| < 1.7$). The endcap and forward regions are instrumented with liquid-argon calorimeters for both the electromagnetic and hadronic energy measurements up to $|\eta| = 4.9$. The outer part of the detector consists of a muon spectrometer (MS) with high-precision tracking chambers for coverage up to $|\eta| = 2.7$, fast detectors for triggering over $|\eta| < 2.4$, and three large superconducting toroid magnets with eight coils

¹ The ATLAS Collaboration uses a right-handed coordinate system with its origin at the nominal interaction point (IP) in the centre of the detector and the z -axis along the beam pipe. The x -axis points from the IP to the centre of the LHC ring, and the y -axis points upwards. Cylindrical coordinates (r, ϕ) are used in the transverse plane, ϕ being the azimuthal angle around the beam pipe. The pseudorapidity is defined in terms of the polar angle θ as $\eta = -\ln \tan(\theta/2)$. Angular distance is measured in units of $\Delta R \equiv \sqrt{(\Delta\eta)^2 + (\Delta\phi)^2}$.

each. The ATLAS detector has a two-level trigger system to select events for offline analysis [26].

3 Data and simulation samples

The data utilized in this search correspond to 139 fb^{-1} of integrated luminosity from pp collisions at $\sqrt{s} = 13 \text{ TeV}$ collected with the ATLAS detector. Only data collected during stable beam conditions with all ATLAS detector subsystems operational are considered.

Simulated events with pair-produced scalar LQs were generated at next-to-leading order (NLO) in quantum chromodynamics (QCD) with MADGRAPH5_aMC@NLO 2.6.0 [27] using the LQ model of Ref. [16] that adds parton showers to previous fixed-order NLO QCD calculations [17, 18], and the NNPDF3.0nlo [28] parton distribution function (PDF) set with $\alpha_S = 0.118$. MADGRAPH was interfaced with PYTHIA 8.230 [29] using the A14 set of tuned parameters (tune) [30] and the NNPDF2.3lo set of PDFs [31] for the underlying-event description, parton showering, and hadronization. Matching of the matrix element with parton showering was performed following the CKKW-L prescription [32], with a matching scale set to one quarter of the leptoquark mass. The LQ pair-production cross sections were obtained from the calculation of direct top-squark pair production, as they are both massive, coloured, scalar particles with the same production modes, computed at approximate next-to-next-to-leading order (NNLO) in QCD with resummation of next-to-next-to-leading logarithmic (NNLL) soft gluon terms [33–36]. The cross sections do not include lepton t -channel contributions, which are neglected in Ref. [16] and may lead to corrections at the 10% level [15]. Theoretical uncertainties were evaluated from variations of factorization and renormalization scales, α_S , and PDFs. Only LQs coupling to the third-generation quarks and either exclusively to the first-generation leptons or exclusively to the second-generation leptons were considered. To ensure that LQs decay promptly, the coupling parameter λ was set to give a LQ width of about 0.2% of its mass. MADSPIN [37, 38] was used to decay top quarks while preserving the spin-correlation and finite-width effects. For this analysis, signal samples were produced for LQ mass values from 900 to 2000 GeV, with a 100 GeV step size in general and a finer 50 GeV step size near the expected LQ mass exclusion limits, and $\beta = 1.0$ with fully hadronic top decays.

The dominant backgrounds in this search are $Z + \text{jets}$ and $t\bar{t}$ production, with two leptons in the final state. Sources of smaller backgrounds considered include single top quark, $t\bar{t}V$ ($V = W, Z$), diboson (WZ, ZZ, WW), and $W + \text{jets}$ production. The background contribution from multi-jet production was found to be negligible and is not considered in this search.

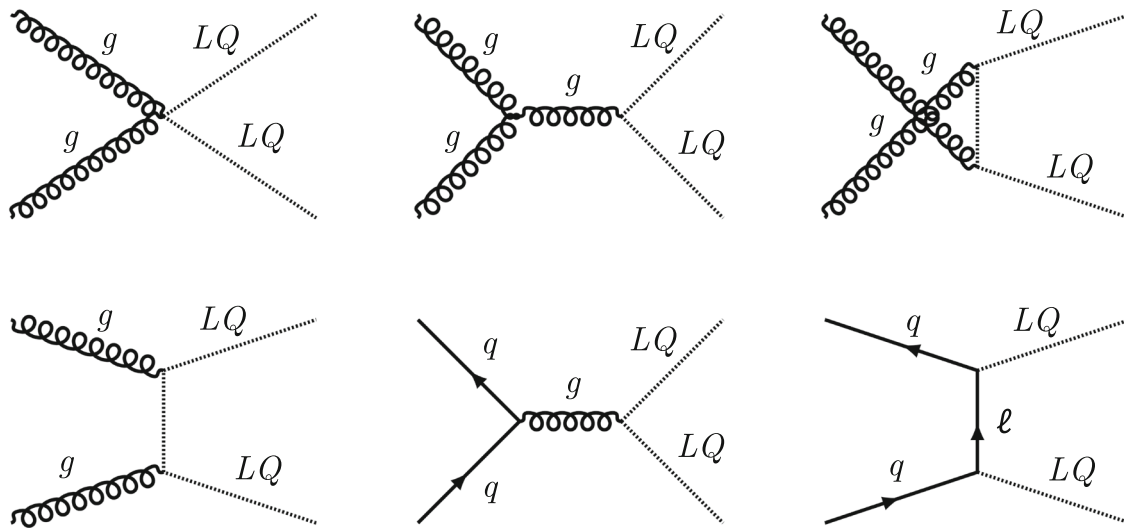


Fig. 1 The lowest-order Feynman diagrams for LQ pair production. In this paper, the t-channel lepton exchange diagram is ignored

The $Z + \text{jets}$, $W + \text{jets}$ and diboson samples were generated using SHERPA 2.2.1 [39] with the NNPDF3.0nlo PDF set. The $Z + \text{jets}$ and $W + \text{jets}$ samples were normalized to the NNLO cross sections calculated with FEWZ [40]. Matrix elements were calculated for up to two partons at NLO and four partons at leading order (LO) using COMIX [41] and OPENLOOPS [42–44] matrix-element generators, and merged with the SHERPA parton shower [45] using the ME+PS@NLO prescription [46–49]. For the diboson samples, matrix elements were calculated for up to one parton at NLO and three partons at LO using COMIX and OPENLOOPS matrix-element generators, and merged with the SHERPA parton shower using the ME+PS@NLO prescription.

The nominal $t\bar{t}$ and single-top event samples in the Wt -, t - and s -channels were simulated with POWHEG-BOX v2 [50–55] which provides matrix elements at NLO in α_S with the NNPDF3.0nlo PDF set. The POWHEG-BOX event generator was interfaced with PYTHIA 8.230 for the parton shower and hadronization, using the A14 tune and the NNPDF2.3lo PDF set. The NLO radiation factor, h_{damp} , was set to 1.5 times the mass of the top quark, m_{top} . The diagram removal (DR) method was used to remove the interference between Wt -channel single-top production and $t\bar{t}$ production [56]. The related uncertainty is estimated by comparison with an alternative sample generated using the diagram subtraction (DS) scheme [56, 57]. The $t\bar{t}$ samples were normalized to the NNLO cross section with soft-gluon resummation to NNLL accuracy using TOP++ 2.0 [58–64]. The single-top cross sections for the t - and s -channels are normalized to their NLO predictions using HATHOR 2.1 [65, 66], while for the Wt -channel the cross section is normalized to its NLO+NNLL prediction [67, 68]. To estimate the modelling uncertainties from the choice of generator and parton shower, alternative

samples were generated at NLO for both the $t\bar{t}$ and single-top events using MADGRAPH5_aMC@NLO 2.6.0 interfaced to PYTHIA 8.230, and POWHEG-BOX v2 interfaced to HERWIG 7.04 [69, 70], respectively.

The $t\bar{t}V$ samples were simulated using MADGRAPH5_aMC@NLO v2.3.3 [27] at NLO in α_S with the NNPDF3.0nlo PDF set. MADGRAPH was interfaced with PYTHIA 8.210 [29] using the A14 tune and NNPDF2.3lo PDF set for parton showering and hadronization. The cross sections of the samples were calculated at NLO QCD and NLO EW accuracy using MADGRAPH5_aMC@NLO as reported in Ref. [71]. In the case of $t\bar{t}\ell\ell$ the cross section is additionally scaled by an off-shell correction estimated at one-loop level in α_S .

The $t\bar{t}V$ events used EVTGEN v1.2.0 [72] to simulate the modelling of b - and c -hadron decays, and all other simulated events, except those generated by SHERPA, used EVTGEN v1.6.0.

All simulated event samples for the nominal predictions were passed through the ATLAS simulation infrastructure [73], using the full GEANT4 [74] simulation of the ATLAS detector. The alternative $t\bar{t}$ and single-top generator samples were processed with a fast simulation [75] of the ATLAS detector with parameterized showers in the calorimeters. Simulated events were then reconstructed using the same software as used for the data, and overlaid with additional pp collisions in the same or nearby bunch crossings (pile-up) simulated using the soft QCD processes of the PYTHIA 8.186 [76] generator with the NNPDF2.3lo PDF set and the A3 tune [77]. The Monte Carlo samples were reweighted to match the distribution of the number of pile-up interactions to the data.

4 Analysis object selection

A set of physics objects (electrons, muons, jets, and missing transverse momentum) are reconstructed using an optimized combination of information from the various subsystems of the ATLAS detector. The reconstructed primary vertex of the event is required to have at least two associated ID tracks with $p_T > 0.5$ GeV. If more than one primary vertex candidate is reconstructed in an event, the vertex with the largest $\sum p_T^2$ of all associated tracks is considered as the hard-scatter vertex.

Electron candidates are reconstructed from clusters of energy deposits in the electromagnetic calorimeter associated with a charged-particle track reconstructed in the ID. To ensure that electron candidates originate from the primary vertex, they are required to possess $|d_0|/\sigma_{d_0} < 5$ and $|z_0 \sin \theta| < 0.5$ mm, where d_0 (z_0) is the transverse (longitudinal) impact parameter relative to the primary vertex and σ_{d_0} is the uncertainty in d_0 . The electron candidates are required to satisfy the *Tight* likelihood identification criteria for high purity [78]. High-purity candidates must fulfil the *Loose* isolation criteria with fixed cuts on isolation variables to further suppress background contributions from hadrons that are misidentified as electrons [78]. Additionally, the electrons are required to have $p_T > 30$ GeV and pseudorapidity $|\eta| < 2.47$, while excluding those in the barrel–endcap transition region ($1.37 < |\eta| < 1.52$) of the electromagnetic calorimeters.

Muon candidates are reconstructed from a combined measurement of tracks in the inner detector and the muon spectrometer. The associated tracks must point to the primary vertex by satisfying $|d_0|/\sigma_{d_0} < 3$ and $|z_0 \sin \theta| < 0.5$ mm. The muon candidates are required to satisfy the *Medium* muon identification selection criteria [79] if the leading muon's p_T is below 800 GeV; otherwise, tighter *High-Pt* muon identification requirements [79] are applied to guarantee the best muon resolution and removal of poorly measured tracks in the high- p_T regime. To reject background from muons originating from hadron decays, the *FixedCutTightTrackOnly* track-based isolation criterion is applied, with a wider isolation cone used for $p_T > 50$ GeV [79]. The muons are required to have $p_T > 30$ GeV and $|\eta| < 2.5$.

Small-radius (Small- R) jets are reconstructed using the anti- k_r algorithm [80,81] with a radius parameter of $R = 0.4$ and with particle-flow objects [82,83] as inputs. These particle-flow objects are typically either charged-particle tracks that originate from the hard-scatter vertex and are matched to a set of topo-clusters in the calorimeters [84], or the remaining calorimeter energy clusters after the subtraction of calorimeter energy associated with those charged-particle tracks. Small- R jets are considered if they satisfy $p_T > 25$ GeV and $|\eta| < 2.5$. For small- R jets with $p_T < 60$ GeV and $|\eta| < 2.4$, a multivariate jet vertex tag-

ger is employed to reduce contamination by jets coming from pile-up [85]. Small- R jets are only used for the object overlap removal discussed below and for the event kinematic reconstruction discussed in Sect. 5.2.

Large- R jets are reconstructed from topo-clusters of energy deposits in the calorimeters using the anti- k_r algorithm with a radius parameter of $R = 1.0$. To remove contributions from pile-up, the k_r -based trimming algorithm [86–89] is employed to recluster jet constituents into subjets with a finer R -parameter value of 0.2 and discard subjets with energy less than 5% of the large- R jet's energy [90]. Trimmed large- R jets are required to have $p_T > 200$ GeV, $|\eta| < 2.0$ and jet mass $m > 50$ GeV. To identify large- R jets that are likely to have originated from the hadronic decay of a top quark, jet substructure information is exploited as inputs to the BDT model in the muon channel, as discussed in Sect. 5.2, using the N-subjettiness ratio τ_{32} [91,92], the splitting measure $\sqrt{d_{23}}$ [93] and the Q_W variables [94].

The missing transverse momentum, E_T^{miss} , in a given reconstructed event is computed as the magnitude of the negative vector sum of the p_T of all reconstructed leptons and small- R jets. A track-based soft term is also included in the E_T^{miss} calculation to account for the ‘soft’ energy from inner detector tracks that are not matched to any of the selected objects but are consistent with originating from the primary vertex [95,96].

To avoid double counting of the same object in different reconstructed object types, an overlap removal procedure is applied to specific pairs of objects that either share a track or have small separation in ΔR . Electron candidates are discarded if they are found to share a track with a more energetic electron or a muon. For overlapping small- R jets and electrons, small- R jets within $\Delta R = 0.2$ of a reconstructed electron are removed. If the nearest surviving small- R jet is within $\Delta R = 0.4$ of the electron, then the electron is discarded. To reject hadronic jet candidates produced by bremsstrahlung from very energetic muons, the jet is required to have at least three associated tracks if it lies within a cone of $\Delta R = 0.2$ around a muon candidate. However, if a surviving jet is separated from the nearest muon with transverse momentum p_T^μ by $\Delta R < 0.04 + 10 \text{ GeV}/p_T^\mu$ up to a maximum of 0.4, the small- R jet is kept and the muon is removed instead; this reduces the background contributions due to muons from hadron decays. No dedicated overlap-removal procedure between large- R and small- R jets is performed. As high- p_T electrons could deposit significant amounts of energy in the calorimeter to form large- R jets, the electron energy is removed from any overlapping large- R jets before the jet momentum requirements are applied to avoid double counting the electrons as large- R jets. This approach has a 20% better signal efficiency compared to rejecting large- R jets that overlap with a reconstructed electron.

5 Analysis strategy

5.1 Event selection

In the signal region (SR), events were recorded using either a set of single-electron triggers or a set of single-muon triggers. The single-electron triggers imposed a p_T threshold of 26 GeV (24 GeV in 2015) and isolation requirements, or a p_T threshold of 60 GeV and no isolation requirements [97]. The single-muon triggers accepted an isolated muon with $p_T > 26$ GeV (20 GeV in 2015) or any muon with $p_T > 50$ GeV [98]. Events with exactly two opposite-sign, same-flavour leptons with p_T above 100 GeV are considered. Events must also have at least two large- R jets. In addition, events containing a lepton pair with invariant mass below 120 GeV are removed to reduce background contributions from low-mass resonances. In the SR, the dominant backgrounds are from the $t\bar{t}$ and $Z + \text{jets}$ processes. The LQ signal, $t\bar{t}$ and $Z + \text{jets}$ events which satisfy these SR criteria are used to train a BDT for signal and background classification.

Dedicated control regions (CRs) are defined in order to extract the normalization of the $t\bar{t}$ and $Z + \text{jets}$ backgrounds from data. For the $t\bar{t}$ -enriched CR, the selection criteria are the same as in the SR, except that either a single-electron trigger or a single-muon trigger must be satisfied and events must contain exactly one opposite-sign electron–muon pair. The $Z + \text{jets}$ -enriched CR is kept orthogonal to the SR by selecting data in a dilepton invariant mass window $70 < m_{\ell\ell} < 110$ GeV around the Z boson mass. A summary of the event selections for the signal and control regions is given in Table 1.

The expected numbers of events in the SR for the background processes and signal hypothesis with mass $m_{LQ} = 1500$ GeV are shown in Table 2. For a signal model with $\beta = 1$ and a fully hadronic top-quark final state, the acceptance times efficiency of the SR selection, for LQ masses from $m_{LQ} = 900$ to 2000 GeV, ranges from 32 to 49% in the electron channel, and from 36 to 43% in the muon channel.

5.2 Signal region BDT classification

A BDT classifier is trained in the SR to further separate the signal from the backgrounds. A gradient boosting approach is used with the XGBOOST framework [99] as the back end for mathematical computations.

The gradient boosting algorithm contains at most 1000 trees with a maximal tree depth of 3, while early stopping is employed if no improvement in the classification is found after 10 iterations of the trees. To avoid overtraining the classifier, nested cross validation [100] was performed to obtain an unbiased evaluation of the classifier performance. The classifier produces an output score referring to the predicted

probability that the event contains LQs, which is then used as the final discriminant to separate LQ signal events from the SM backgrounds.

A natural basis of kinematic observables can be created, utilizing Lorentz symmetry to reduce unnecessary duplication of observables, in the rest frames of intermediate particle states, conditioned on the hypotheses of LQ pair, dileptonic $t\bar{t}$ or $Z + \text{jets}$ decay processes. A suite of such discriminating variables is constructed using the recursive jigsaw reconstruction technique [101], and is provided as inputs to the classifier. The dileptonic $t\bar{t}$ reconstruction scheme is based on the ‘min ΔM_{top} approach’ of the recursive jigsaw reconstruction technique, in which the two leading small- R jets are used as the b -quark candidates from the top-quark decays. Variables related to hadronic and leptonic activity, missing transverse momentum and jet substructure are also used to provide additional separation power. Large- R jet substructure variables are only used in the muon channel. As discussed in Sect. 4, the energy of electrons overlapping with large- R jets is subtracted from the jet four-momentum to avoid double counting. Such kinematic modification of large- R jets is incompatible with the use of substructure variables. In total, 29 inputs are used in the BDT classifier in the electron channel and 32 in the muon channel. The top five discriminating variables are the dilepton invariant mass, the scalar p_T sum of the two leptons, the two large- R jet masses, and the reconstructed LQ mass. Figure 2 shows the distributions of the dilepton invariant mass in the $Z + \text{jets}$ CR of the muon channel, and the reconstructed W mass based on a dileptonic $t\bar{t}$ hypothesis in the $t\bar{t}$ CR of the electron channel. In general, the kinematic variables show good agreement between data and the background expectation in the CRs. A complete list of the input variables is provided in Table 3.

In order to maximize the sensitivity of the BDT over a wide mass range, and ensure a smooth interpolation of the signal efficiency between the mass points where it was trained, a parameterized machine-learning approach [102] is implemented. The inputs to the BDT classifier are expanded to include the theoretical LQ mass, resulting in a single BDT classifier that smoothly provides optimized discrimination across a range of masses, from 900 to 2000 GeV. The parameterized BDT was trained with large samples of simulated signal events at m_{LQ} values from 900 to 1900 GeV, with a 200 GeV step size. The modelling of the BDT distribution of the main backgrounds is validated using events in the $Z + \text{jets}$ and $t\bar{t}$ control regions, as shown in Fig. 3. The number of bins and their boundaries in the SR are optimized to maximize the expected scalar leptoquark sensitivity while ensuring a minimum of three background events in the highest BDT bin. It was found that having three bins in the SR was optimal, which are defined as the low, mid and high BDT SR. Of the signal events which enter the signal

Table 1 Summary of event selections applied in the signal and control regions. Leptons and large- R jets are, respectively, denoted by ℓ and J

| | $t\bar{t}$ CR | Z + jets CR | SR |
|-------------------------|--------------------------|--|--------------------------|
| Leptons | | $p_T^\ell > 100$ GeV, $ \eta_e < 2.47$, $ \eta_\mu < 2.5$ $N_\ell = 2$; opposite-sign | |
| Large- R jets | | $p_T^J > 200$ GeV, $ \eta_J < 2.0$, $m_J > 50$ GeV $N_J \geq 2$ | |
| Dilepton invariant mass | $m_{\ell\ell} > 120$ GeV | 70 GeV $< m_{\ell\ell} < 110$ GeV | $m_{\ell\ell} > 120$ GeV |
| Lepton flavour | $e\mu$ | ee or $\mu\mu$ | |

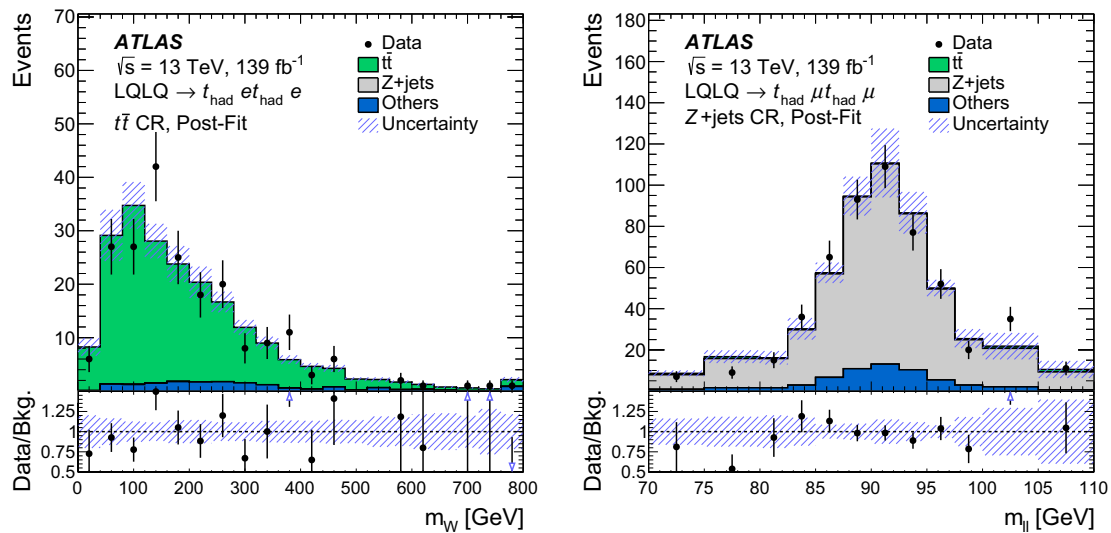


Fig. 2 Distributions of the reconstructed W mass associated with the leading lepton assuming a dileptonic hypothesis in the $t\bar{t}$ CR after the simultaneous background-only fit of the electron channel CRs (left), and the dilepton invariant mass $m_{\ell\ell}$ in the Z + jets CR after the simulta-

neous background-only fit of the muon channel CRs (right). The bottom panels show the ratio of data to expected background. The hatched band represents the total uncertainty. The blue triangles indicate points that are outside the vertical range

region, over 94% fall into the high BDT SR while only 1% and 8% of the $t\bar{t}$ and Z + jets background do so, respectively.

6 Systematic uncertainties

The systematic uncertainties are broken down into three broad categories: luminosity and cross-section uncertainties, detector-related experimental uncertainties, and modelling uncertainties in simulated background processes. The uncertainty from each source is treated as a Gaussian-distributed or log-normal nuisance parameter in a profile-likelihood fit of the CR normalizations and BDT output score distributions, and shape effects are taken into account where relevant. Due to the tight selection criteria applied and resultant statistical limitation to the sensitivity, the systematic uncertainties only mildly degrade the sensitivity of the search.

6.1 Luminosity and normalization uncertainties

The uncertainty in the combined 2015–2018 integrated luminosity is 1.7% [103], obtained using the LUCID-2 detector [104] for the primary luminosity measurements.

Theoretical cross-section uncertainties are applied to the various simulated samples. For the LQ signal, PDF, α_S and scale uncertainties are considered in the approximate NNLO + NNLL calculation of the cross section. The PDF and α_S uncertainties are estimated from the PDF4LHC15 error set [105]. The effect of uncertainties in the renormalization and factorization scales is estimated from variations by a factor of two about the central scales. The overall uncertainty ranges from 10% at low LQ masses to 25% at 2 TeV [33–36]. This cross-section uncertainty is not included in the profile-likelihood fit, but represented by an uncertainty band around the theoretical prediction in the cross-section limit plots in Sect. 8. The uncertainties for W +jets and diboson production are both assumed to be 50% [106, 107]. For single top quark and $t\bar{t}V$ production, the uncertainties are taken as 7% [65, 66]

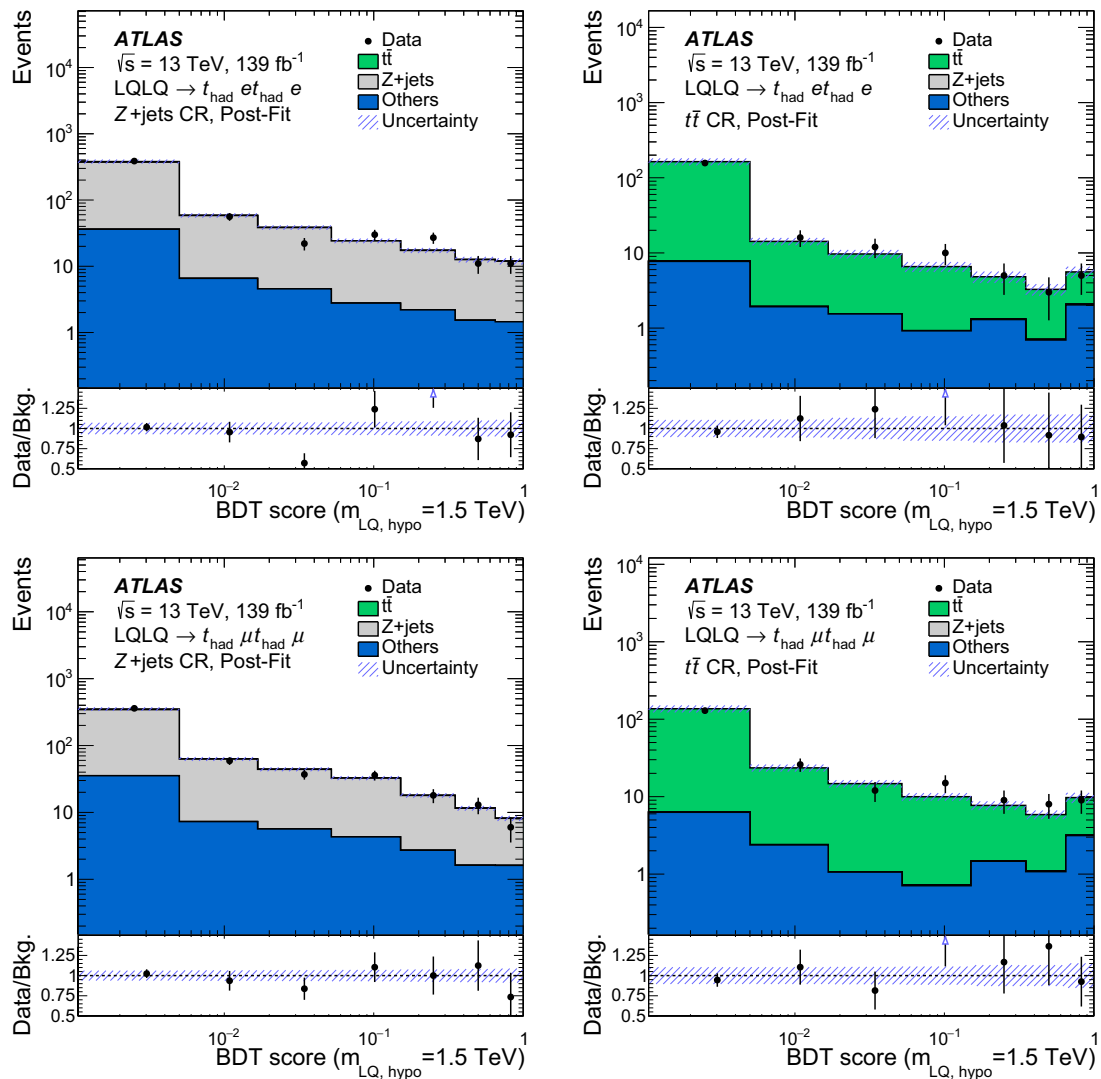


Fig. 3 Distributions of the BDT output score in the $Z + \text{jets}$ and $t\bar{t}$ CRs for the electron (top row) and muon (bottom row) channel after the simultaneous background-only fit of the CRs. The bottom panels show the ratio of data to expected background. The hatched band represents the total uncertainty. The blue triangles indicate points that are outside the vertical range. All BDT scores correspond to the theoretical LQ mass parameter $m_{LQ, \text{hypo}}$ set to 1.5 TeV. The first bin contains all underflow events

resents the total uncertainty. The blue triangles indicate points that are outside the vertical range. All BDT scores correspond to the theoretical LQ mass parameter $m_{LQ, \text{hypo}}$ set to 1.5 TeV. The first bin contains all underflow events

and 30% [108], respectively. The normalizations of $t\bar{t}$ and $Z + \text{jets}$ are determined from data via unconstrained normalization parameters.

6.2 Detector-related uncertainties

The dominant sources of detector-related uncertainties in the signal and background yields relate to the lepton identification efficiency scale factors that are used to correct for the difference between the Monte Carlo simulation and data. These uncertainties have an impact on the fitted signal yield of roughly 12% and 5% in the electron and muon channel respectively. Additional uncertainties to account for the degradation of the muon momentum resolution due to the

impact of possible misalignment between layers of the MS, as well as between the MS and the ID, were estimated to be 5%.

Uncertainties in the small- R and large- R jet energy scales and resolutions are also considered. The small- R and large- R jet energy scales and their uncertainties are derived by combining information from test-beam data, LHC collision data and simulation [109]. The uncertainties in the jet energy scale have an impact of up to $\sim 4\%$ on the fitted signal yield. Moreover, in the case where an electron overlaps with a large- R jet, the impact on the jet energy scale calibration due to the analysis-specific removal of the electron energy from the large- R jets was evaluated. The jet axis shift and the fraction of calibrated jet energy contributed by the overlapping

electrons were studied in simulated events. These additional jet systematic uncertainties have an impact of $< 3\%$ on the signal yield.

Other detector-related uncertainties come from uncertainties in the large- R jet mass scales and resolutions; lepton isolation and reconstruction; lepton trigger efficiencies, energy scales, and resolutions; the E_T^{miss} reconstruction; pile-up modelling; and the jet-vertex-tagger requirement. Uncertainties in the object momenta are propagated to the E_T^{miss} measurement, and additional uncertainties in E_T^{miss} arising from the ‘soft’ energy are also considered. These all have negligible impact on the fitted signal yield ($< 3\%$ each).

6.3 Generator modelling uncertainties

Modelling uncertainties are estimated for the signal as well as Z +jets, $t\bar{t}$ and single-top-quark backgrounds. The modelling uncertainties are estimated by comparing simulated samples generated with different configurations, described in Sect. 3.

For the LQ signal, in addition to the cross-section uncertainties, the impact on the acceptance due to variations of the QCD scales, PDF and shower parameters was studied. These uncertainties were estimated from the envelope of independent pairs of renormalization and factorization scale variations by a factor of 0.5 and 2, by propagating the PDF and α_S uncertainties following the PDF4LHC15 prescription, and by considering two alternative samples generated with settings that increase or decrease the amount of QCD radiation. Both the PDF and scale variations have an impact below 15% for all bins considered, while variations of the underlying-event modelling have only a 1–2% effect.

For the Z +jets backgrounds, scale, PDF and α_S variations are considered and their effects are evaluated within the SHERPA event generator. Seven variations are considered for the renormalization and factorization scales, with the maximum shift within the envelope of those variations taken to estimate the effect of the scale uncertainty. The PDF variations include the variation of the nominal NNPDF3.0nnlo PDF as well as the central values of two other PDF sets, MMHT2014nnlo68cl [110] and CT14nnlo [111]. The intra-PDF uncertainty is estimated as the standard deviation of the 100 variations of the NNPDF3.0nnlo set. The envelope of the differences between the nominal and alternative PDF sets is used as an additional nuisance parameter. The effect of varying α_S from its nominal value of 0.118 by ± 0.001 is also considered. The dominant effect is from the renormalization and factorization scale variations and is about 6% of the signal yield.

For the $t\bar{t}$ background, four sources of modelling uncertainties are considered. The uncertainty in the matrix-element calculation is estimated by comparing events generated with two different Monte Carlo generators, MADGRAPH5_aMC@NLO and POWHEG-BOX, while keeping the

same parton shower model. The uncertainty in the fragmentation, hadronization and underlying-event modelling is estimated by comparing two different parton shower models, PYTHIA and HERWIG, while keeping the same hard-scatter matrix-element calculation. The effects of extra initial- and final-state gluon radiation are estimated by comparing simulated samples generated with enhanced or reduced initial-state radiation, doubling the h_{damp} parameter, and using different values of the radiation parameters [57]. The PDF uncertainty is estimated from the PDF4LHC15 error set. The dominant effect is from the final-state radiation estimation uncertainty and is about 6% of the signal yield.

In this analysis, the single-top-quark background comes mainly from the Wt -channel and is a minor background. Similarly to $t\bar{t}$, uncertainties in the hard-scatter generation, the fragmentation and hadronization, the amount of additional radiation, and the PDF are considered. In addition, the uncertainty due to the treatment of the overlap between Wt -channel single top quark production and $t\bar{t}$ production is considered by comparing samples using the DS and DR methods (see Sect. 3). The dominant effect is from the uncertainty in the fragmentation and hadronization and is about 7% of the signal yield.

7 Statistical interpretation

The binned distributions of the BDT score in the SR and the overall number of events in the $t\bar{t}$ and Z + jets CR are used to test for the presence of a signal. Hypothesis testing is performed using a modified frequentist method as implemented in ROOSTATS [112, 113] and is based on a profile likelihood that takes into account the systematic uncertainties as nuisance parameters that are fitted to the data. A simultaneous fit is performed in the SR and the two CRs, but done separately for the electron and muon channel. As the $t\bar{t}$ CR is built requiring an electron and muon, the same events are considered in the independent electron and muon channel fits.

The statistical analysis is based on a binned likelihood function $\mathcal{L}(\mu, \theta)$ constructed as a product of Poisson probability terms over all bins considered in the search. This function depends on the signal strength parameter μ , a multiplicative factor applied to the theoretical signal production cross section, and θ , a set of nuisance parameters that encode the effect of systematic uncertainties in the signal and background expectations and are implemented in the likelihood function as Gaussian and log-normal constraints. Uncertainties in each bin due to the finite size of the simulated samples are also taken into account via dedicated constrained fit parameters. There are enough events in the CRs and the lowest BDT bin in the SR, where the signal contribution is small, to obtain a data-driven estimate of the $t\bar{t}$ and Z + jets normalizations and hence the normalizations of those two

Table 2 Event yields in the signal and control regions before and after the background-only fit to data in the electron and muon channel. The quoted uncertainties include statistical and systematic uncertainties; for the $t\bar{t}$ and $Z + \text{jets}$ backgrounds no cross-section uncertainty is included since it is a free parameter of the fit. The contributions from single top, $t\bar{t}V$, diboson and $W + \text{jets}$ production are included in the ‘Others’ cate-

gory. In the post-fit case, the uncertainties in the individual background components can be larger than the uncertainty in the sum of the backgrounds, due to the correlations between the fit parameters. Both signal models correspond to $m_{LQ} = 1500$ GeV assuming 100% branching ratio into a hadronically decaying top quark and a charged lepton

| Sample | $t\bar{t}$ CR | $Z + \text{jets}$ CR | SR: low BDT | SR: mid BDT | SR: high BDT |
|-------------------------------|-----------------|----------------------|-----------------|-------------------|---------------|
| Electron Channel | | | | | |
| Pre-fit | | | | | |
| $t\bar{t}$ | 222 ± 58 | 9.6 ± 7.8 | 90 ± 30 | 4.3 ± 1.9 | 0.6 ± 0.3 |
| $Z + \text{jets}$ | 0.3 ± 0.1 | 520 ± 100 | 32.7 ± 5.9 | 8.2 ± 1.8 | 2.9 ± 0.8 |
| Others | 16.1 ± 5.3 | 55 ± 18 | 6.7 ± 3.6 | 2.1 ± 1.1 | 0.3 ± 0.1 |
| Total background | 238 ± 60 | 590 ± 110 | 130 ± 36 | 14.6 ± 3.4 | 3.7 ± 0.9 |
| Signal ($m_{LQ} = 1500$ GeV) | < 0.001 | 0.006 ± 0.002 | < 0.001 | 0.015 ± 0.004 | 7.4 ± 1.6 |
| Post-fit | | | | | |
| $t\bar{t}$ | 200 ± 19 | 10.3 ± 5.3 | 86 ± 10 | 4.4 ± 1.0 | 0.6 ± 0.1 |
| $Z + \text{jets}$ | 0.22 ± 0.04 | 493 ± 43 | 30.7 ± 2.9 | 8.0 ± 0.9 | 2.8 ± 0.3 |
| Others | 19.1 ± 5.7 | 53 ± 19 | 9.6 ± 5.2 | 3.1 ± 1.6 | 0.3 ± 0.1 |
| Total background | 219 ± 18 | 556 ± 38 | 126 ± 12 | 15.4 ± 2.0 | 3.7 ± 0.3 |
| Data | 208 | 544 | 130 | 22 | 6 |
| Muon Channel | | | | | |
| Pre-fit | | | | | |
| $t\bar{t}$ | 222 ± 58 | 8.9 ± 6.9 | 112 ± 23 | 8.3 ± 5.0 | 0.8 ± 0.5 |
| $Z + \text{jets}$ | 0.3 ± 0.1 | 532 ± 45 | 31.7 ± 2.8 | 11.7 ± 1.3 | 2.9 ± 0.3 |
| Others | 16.1 ± 6.9 | 59 ± 19 | 7.6 ± 4.1 | 2.2 ± 1.7 | 0.6 ± 0.4 |
| Total background | 238 ± 60 | 600 ± 53 | 152 ± 24 | 22.2 ± 6.2 | 4.2 ± 1.0 |
| Signal ($m_{LQ} = 1500$ GeV) | < 0.001 | 0.013 ± 0.003 | < 0.001 | 0.031 ± 0.007 | 7.0 ± 1.4 |
| Post-fit | | | | | |
| $t\bar{t}$ | 187 ± 19 | 7.9 ± 4.1 | 92.2 ± 9.3 | 7.6 ± 2.9 | 0.7 ± 0.3 |
| $Z + \text{jets}$ | 0.22 ± 0.03 | 463 ± 36 | 27.6 ± 2.2 | 10.2 ± 1.0 | 2.5 ± 0.3 |
| Others | 17.9 ± 7.5 | 59 ± 18 | 8.1 ± 4.1 | 2.5 ± 1.8 | 0.6 ± 0.5 |
| Total background | 205 ± 19 | 530 ± 32 | 127.9 ± 9.3 | 20.4 ± 3.1 | 3.8 ± 0.5 |
| Data | 208 | 529 | 123 | 20 | 6 |

backgrounds are included as unconstrained nuisance parameters, $\mu_{t\bar{t}}$ and μ_Z . Nuisance parameters representing systematic uncertainties are only included in the likelihood if either of the following conditions are met: the overall impact on the normalization in a given region is larger than 3%, or any single bin within the region has at least a 3% uncertainty. This is done separately for each region and for each template (signal or background). When the bin-by-bin statistical variation of a given uncertainty is significant, a smoothing algorithm is applied.

The test statistic q_μ is defined as the profile likelihood ratio, $q_\mu = -2\ln(\mathcal{L}(\mu, \hat{\theta}_\mu)/\mathcal{L}(\hat{\mu}, \hat{\theta}))$, where $\hat{\mu}$ and $\hat{\theta}$ are the values of the parameters that maximize the likelihood function, and $\hat{\theta}_\mu$ are the values of the nuisance parameters that maximize the likelihood function for a given value of μ . The compatibility of the observed data with the background-only

hypothesis is tested by setting $\mu = 0$ in the profile likelihood ratio: $q_0 = -2\ln(\mathcal{L}(0, \hat{\theta}_0)/\mathcal{L}(\hat{\mu}, \hat{\theta}))$. Upper limits on the signal production cross section for each of the signal scenarios considered are derived by using q_μ in the so-called CL_s method [114, 115]. For a given signal scenario, values of the production cross section (parameterized by μ) yielding CL_s < 0.05, where CL_s is computed using the asymptotic approximation [116], are excluded at $\geq 95\%$ confidence level (CL).

8 Results

8.1 Likelihood fit results

The expected and observed event yields in the signal and control regions before and after fitting the background-only hypothesis to data, including all uncertainties, are listed in

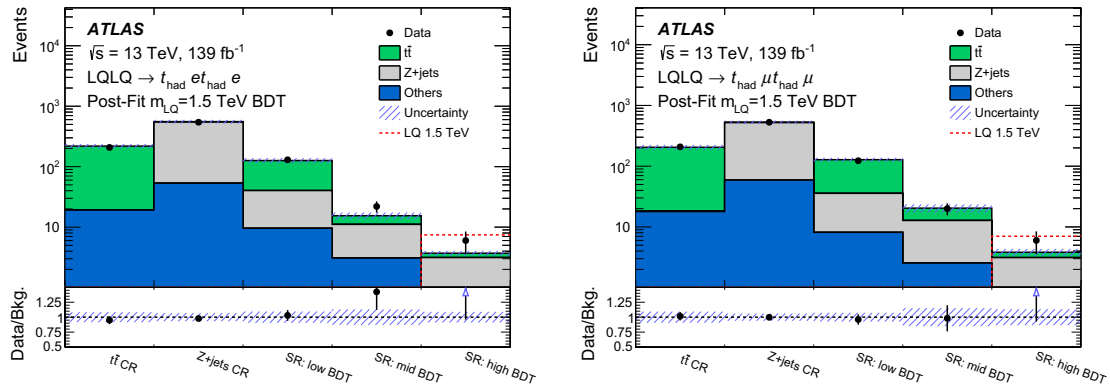


Fig. 4 Fit results (background-only) for the binned BDT output score distribution in the signal region of the electron (left) and muon (right) channel, and the overall number of events in the $t\bar{t}$ and $Z + \text{jets}$ control

regions. The lower panel shows the ratio of data to the fitted background yields. The band represents the systematic uncertainty after the maximum-likelihood fit

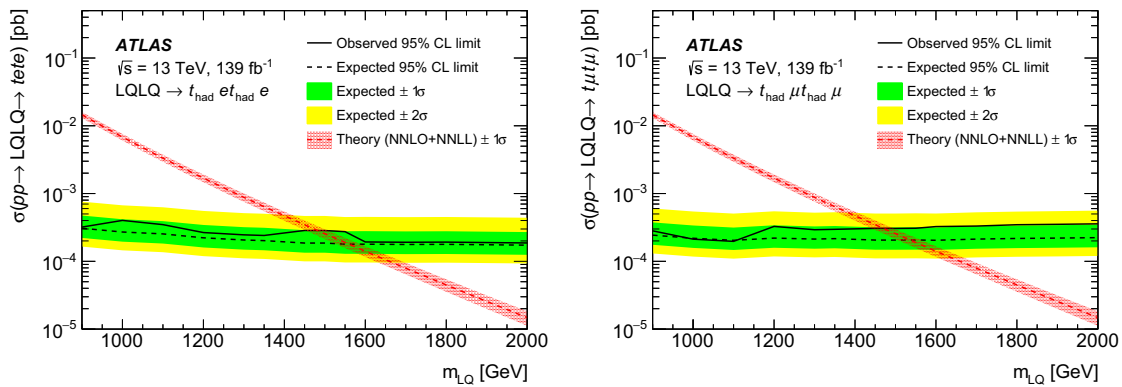


Fig. 5 Upper limits at 95% CL on the cross section of LQ pair production as a function of LQ mass, assuming a branching ratio $B(LQ \rightarrow t\ell^\pm) = 1$, for the electron (left) and muon (right) channel. Observed limits are shown as a black solid line and expected limits

as a black dashed line. The green and yellow shaded bands correspond to ± 1 and ± 2 standard deviations, respectively, around the expected limit. The red curve and band show the nominal theoretical prediction and its ± 1 standard deviation uncertainty

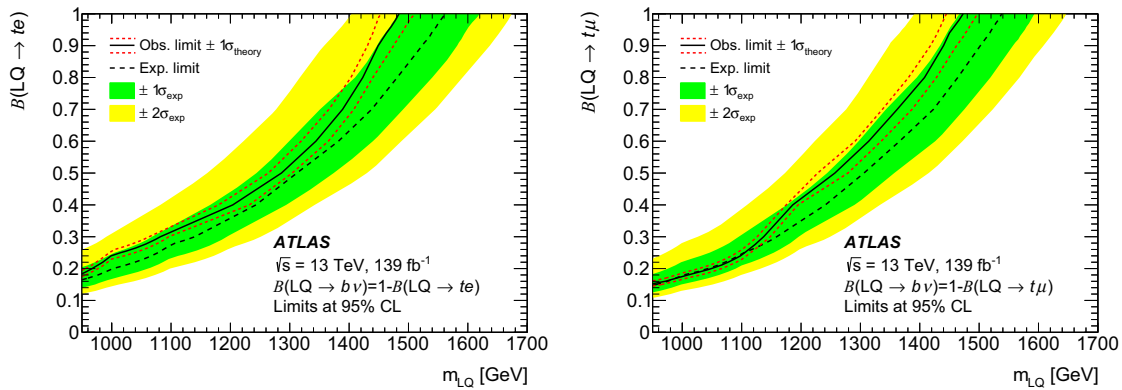


Fig. 6 Lower exclusion limits on the leptoquark mass for scalar leptoquark pair production as a function of the branching ratio into a top quark and an electron (left) or a muon (right) at 95% CL. The observed nominal limits are indicated by a black solid curve, with the surrounding red dotted lines obtained by varying the signal cross section by

uncertainties from PDFs, renormalization and factorization scales, and the strong coupling constant α_s . Expected limits are indicated with a black dashed curve, with the yellow and green bands indicating the ± 1 standard deviation and ± 2 standard deviation excursions due to experimental and modelling uncertainties

Table 2. The total uncertainty shown in the table is the uncertainty obtained from the full fit, and is therefore not identical to the sum in quadrature of each component, due to the correlations between the fit parameters. A comparison of the post-fit agreement between data and prediction for the signal and control regions is shown in Fig. 4. In the electron (muon) channel, the ratio of the $t\bar{t}$ total post-fit yield over the pre-fit yield is 0.90 ± 0.25 (0.84 ± 0.24). The ratio of the $Z + \text{jets}$ total post-fit yield over the pre-fit yield is 0.95 ± 0.20 (0.87 ± 0.10). None of the individual uncertainties are significantly constrained by data.

The probability that the data is compatible with the background-only hypothesis is estimated by integrating the distribution of the test statistic, approximated using the asymptotic formulae, above the observed value of q_0 .² This value is computed for each signal scenario considered, defined by the assumed mass of the leptoquark. The lowest local p -value is found to be $\sim 11\%$ (10%), for a LQ mass of 1450 (1600) GeV in the electron (muon) channel. Thus no significant excess above the background expectation is found.

8.2 Limits on LQ pair production

Upper limits at the 95% CL on the LQ pair-production cross section, for an assumed value of $\beta = 1$, are set as a function of the LQ mass m_{LQ} and compared with the theoretical prediction (Fig. 5). The resulting lower limit on m_{LQ} is determined using the central value of the theoretical NNLO+NNLL cross-section prediction. The observed (expected) lower limits on m_{LQ} are found to be 1480 (1560) GeV and 1470 (1540) GeV for the electron and muon channel respectively. The sensitivity of the analysis is limited by the statistical uncertainty of the data. Including all systematic uncertainties degrades the expected mass limits by only around 10 GeV, and for a mass of 1.5 TeV the cross-section limits increase by less than 7% in both the electron and muon channel.

Exclusion limits on LQ pair production are also obtained for different values of m_{LQ} as a function of the branching ratio (\mathcal{B}) into a charged lepton and a top quark (Fig. 6). The theoretical cross section was scaled by the branching ratio, and then used to obtain the corresponding limit. The full statistical interpretation is performed for each 0.1 step in \mathcal{B} , covering the full plane.

² Cross-checks with sampling distributions generated using pseudo-experiments were performed to test the accuracy of the asymptotic approximation for the whole probed leptoquark mass spectrum. The approximation is found to lead to limits that are slightly stronger than those obtained with pseudo-experiments, up to 10% in general for both channels. The impact of this approximation on the mass limits is below 5 GeV.

9 Conclusion

A search for pair production of scalar leptoquarks, each decaying into a top quark and either an electron or a muon has been presented, targeting the high-mass region in which the decay products of each top quark are contained within a single large-radius jet. The analysis is based on tight selection criteria to reduce the SM backgrounds. The normalizations of the dominant $Z + \text{jets}$ and $t\bar{t}$ backgrounds were determined simultaneously in a profile likelihood fit to the binned output score of a boosted decision tree in the signal region and two dedicated control regions. The data used in this search correspond to an integrated luminosity of 139 fb^{-1} of pp collisions with a centre-of-mass energy $\sqrt{s} = 13 \text{ TeV}$ recorded by the ATLAS experiment in the whole of Run 2 of the LHC. The observed data distributions are compatible with the expected Standard Model background and no significant excess is observed. Lower limits on the leptoquark masses are set at 1480 GeV and 1470 GeV for the electron and muon channel, respectively.

Acknowledgements We thank CERN for the very successful operation of the LHC, as well as the support staff from our institutions without whom ATLAS could not be operated efficiently.

We acknowledge the support of ANPCyT, Argentina; YerPhI, Armenia; ARC, Australia; BMWFW and FWF, Austria; ANAS, Azerbaijan; SSTC, Belarus; CNPq and FAPESP, Brazil; NSERC, NRC and CFI, Canada; CERN; ANID, Chile; CAS, MOST and NSFC, China; COLCIENCIAS, Colombia; MSMT CR, MPO CR and VSC CR, Czech Republic; DNRF and DNSRC, Denmark; IN2P3-CNRS and CEA-DRF/IRFU, France; SRNSFG, Georgia; BMBF, HGF and MPG, Germany; GSRT, Greece; RGC and Hong Kong SAR, China; ISF and Benozio Center, Israel; INFN, Italy; MEXT and JSPS, Japan; CNRS, Morocco; NWO, Netherlands; RCN, Norway; MNI/SW and NCN, Poland; FCT, Portugal; MNE/IFA, Romania; JINR; MES of Russia and NRC KI, Russian Federation; MESTD, Serbia; MSSR, Slovakia; ARRS and MIZŠ, Slovenia; DST/NRF, South Africa; MICINN, Spain; SRC and Wallenberg Foundation, Sweden; SERI, SNSF and Cantons of Bern and Geneva, Switzerland; MOST, Taiwan; TAEK, Turkey; STFC, United Kingdom; DOE and NSF, United States of America. In addition, individual groups and members have received support from BCKDF, CANARIE, Compute Canada, CRC and IVADO, Canada; Beijing Municipal Science & Technology Commission, China; COST, ERC, ERDF, Horizon 2020 and Marie Skłodowska-Curie Actions, European Union; Investissements d'Avenir Labex, Investissements d'Avenir Idex and ANR, France; DFG and AvH Foundation, Germany; Herakleitos, Thales and Aristeia programmes co-financed by EU-ESF and the Greek NSRF, Greece; BSF-NSF and GIF, Israel; La Caixa Banking Foundation, CERCA Programme Generalitat de Catalunya and PROMETEO and GenT Programmes Generalitat Valenciana, Spain; Göran Gustafssons Stiftelse, Sweden; The Royal Society and Leverhulme Trust, United Kingdom.

The crucial computing support from all WLCG partners is acknowledged gratefully, in particular from CERN, the ATLAS Tier-1 facilities at TRIUMF (Canada), NDGF (Denmark, Norway, Sweden), CC-IN2P3 (France), KIT/GridKA (Germany), INFN-CNAF (Italy), NL-T1 (Netherlands), PIC (Spain), ASGC (Taiwan), RAL (UK) and BNL (USA), the Tier-2 facilities worldwide and large non-WLCG resource providers. Major contributors of computing resources are listed in Ref. [118].

Data Availability Statement This manuscript has no associated data or the data will not be deposited. [Authors' comment: "All ATLAS scientific output is published in journals, and preliminary results are made available in Conference Notes. All are openly available, without restriction on use by external parties beyond copyright law and the standard conditions agreed by CERN. Data associated with journal publications are also made available: tables and data from plots (e.g. cross section values, likelihood profiles, selection efficiencies, cross section limits, ...) are stored in appropriate repositories such as HEPDATA (<http://hepdata.cedar.ac.uk/>). ATLAS also strives to make additional material related to the paper available that allows a reinterpretation of the data in the context of new theoretical models. For example, an extended encapsulation of the analysis is often provided for measurements in the framework of RIVET (<http://rivet.hepforge.org/>)."] This information is taken from the ATLAS Data Access Policy, which is a public document that can be downloaded from <http://opendata.cern.ch/record/413>[opendata.cern.ch].]

Open Access This article is licensed under a Creative Commons Attribution 4.0 International License, which permits use, sharing, adaptation,

distribution and reproduction in any medium or format, as long as you give appropriate credit to the original author(s) and the source, provide a link to the Creative Commons licence, and indicate if changes were made. The images or other third party material in this article are included in the article's Creative Commons licence, unless indicated otherwise in a credit line to the material. If material is not included in the article's Creative Commons licence and your intended use is not permitted by statutory regulation or exceeds the permitted use, you will need to obtain permission directly from the copyright holder. To view a copy of this licence, visit <http://creativecommons.org/licenses/by/4.0/>.
Funded by SCOAP³.

Appendix

Table 3 The discriminating variables used in the signal–background discrimination training can be classified into five different groups. The first three groups include kinematic variables that are physics-based rather than detector-based, conditioned on different physics process hypotheses: LQ, dileptonic $t\bar{t}$ and leptonic Z decay hypothesis. These physics-based kinematic variables include the invariant masses and the momenta of intermediate and final-state particles in their parent's rest frame. In the dileptonic $t\bar{t}$ decay hypothesis, the combinatoric ambiguity in the small- R -jet–lepton pairing is resolved using the 'min ΔM_{top}

approach' of the recursive jigsaw reconstruction technique [101]. The reconstructed hemisphere of the decay process associated with the leading (subleading) lepton is labelled with 1 (2). The fourth group of variables is detector-based and defined in the lab frame. These variables are related to the event-level activity of visible objects or missing transverse momentum. The last group of variables is used to identify the three-prong jet structure of hadronic top-quark decays and is used only in the muon channel

Input variables

| | | |
|---------------------------|--|---|
| LQ hypothesis | $m_{\text{LQ LQ}}$ | Invariant mass of LQ pair system, reconstructed from two leptons and two large- R jets |
| | $m_{\ell 1, \text{J}1}^{\text{max}}$ | The higher mass of the two LQ candidates, with the lepton–jet pair labelled as $\ell 1$ and J1. |
| | $m_{\ell 2, \text{J}2}^{\text{min}}$ | The lower mass of the two LQ candidates, with the lepton–jet pair labelled as $\ell 2$ and J2. |
| | $m_{\ell 2, \text{J}1}$ | Invariant mass of lepton–jet pair $\ell 2$ and J1 |
| | $m_{\ell 1, \text{J}2}$ | Invariant mass of lepton–jet pair $\ell 1$ and J2 |
| | $m_{\text{J}1}$ | Invariant mass of large- R jet J1 |
| | $m_{\text{J}2}$ | Invariant mass of large- R jet J2 |
| | $E_{\ell 1}^{\text{LQ}}$ | Energy of lepton $\ell 1$ in its LQ parent's rest frame |
| | $E_{\ell 2}^{\text{LQ}}$ | Energy of lepton $\ell 2$ in its LQ parent's rest frame |
| | $E_{\text{J}1}^{\text{LQ}}$ | Energy of large- R jet J1 in its LQ parent's rest frame |
| | $E_{\text{J}2}^{\text{LQ}}$ | Energy of large- R jet J2 in its LQ parent's rest frame |
| | Dilepton $t\bar{t}$ hypothesis | $m_{t\bar{t}}$ |
| $m_{t1'}$ | | Invariant mass of top quark $t1'$, reconstructed from W boson $W1'$ and b -quark $b1'$ |
| $m_{t2'}$ | | Invariant mass of top quark $t2'$, reconstructed from W boson $W2'$ and b -quark $b2'$ |
| $m_{t1', \text{swapped}}$ | | Invariant mass of top quark $t1'$, with its b -quark child $b1'$ swapped with that of top quark $t2'$ |
| $m_{t2', \text{swapped}}$ | | Invariant mass of top quark $t2'$, with its b -quark child $b2'$ swapped with that of top quark $t1'$ |
| $m_{W1'}$ | | Invariant mass of W boson $W1'$, reconstructed from the leading lepton $\ell 1'$ and $E_{\text{T}}^{\text{miss}}$ |
| $m_{W2'}$ | | Invariant mass of W boson $W2'$, reconstructed from the subleading lepton $\ell 2'$ and $E_{\text{T}}^{\text{miss}}$ |
| $E_{b1'}^t$ | | Energy of small- R jet j1 as b -quark candidate $b1'$ in its top quark parent ($t1'$) rest frame |
| $E_{b2'}^t$ | | Energy of small- R jet j2 as b -quark candidate $b2'$ in its top quark parent ($t2'$) rest frame |
| $E_{\ell 1'}^W$ | | Energy of the leading lepton $\ell 1'$ in its W boson parent ($W1'$) rest frame |
| $E_{\ell 2'}^W$ | Energy of the subleading lepton $\ell 2'$ in its W boson parent ($W2'$) rest frame | |

Table 3 continued

| Input variables | | |
|-------------------------------------|-------------------------------|---|
| $Z \rightarrow \ell\ell$ hypothesis | $m_{\ell\ell}$ | Invariant mass of the dilepton system |
| | $p_{T,\ell\ell}^{\text{lab}}$ | Transverse momentum of the dilepton system in the lab frame |
| Detector-based | L_T | Scalar p_T sum of the two leptons |
| | H_T | Scalar p_T sum of the two leading large- R jets |
| | S_T | Scalar p_T sum of the two leptons and the two leading large- R jets |
| | E_T^{miss} | Missing transverse momentum |
| | E_T^{miss} sig. | Missing transverse momentum significance, defined as $E_T^{\text{miss}}/\sqrt{H_T}$ |
| Jet substructure | sd_{23} | k_t splitting scale for the 2nd and 3rd subjet, defined as $\text{sd}_{23} = \min(p_{T,2}, p_{T,3}) \times \Delta R_{23}$ |
| | τ_{32}^{WTA} | The ratio of τ_3 to τ_2 , where N-subjettiness variable τ_N is defined as $\tau_N = \frac{1}{d_0} \sum_{i \in \text{jet constituents}} p_{T,i} \times \min(\delta R_{1i}, \dots, \delta R_{Ni})$ with $d_0 = \sum_{i \in \text{jet constituents}} p_{T,i} \times R$, where R is the radius parameter of the jet, and δR_{ji} is the distance between the subjet j and the constituent i . WTA denotes the winner-take-all (WTA) recombination scheme [117] used in subjet reconstruction. |
| | Q_w | The minimum invariant mass of the two subjets in the second-to-last reclustering step of the k_t algorithm, applied to a large- R jet |
| MVA parameterization | $m_{\text{LQ, hypo}}$ | Set to the test mass point at which the model is utilized. In the training phase, this parameter is set to the corresponding LQ mass for the signal samples, and a uniformly distributed random value from the training set of LQ mass points for the background samples. |

References

- W. Buchmuller, D. Wyler, Constraints on SU(5)-type leptoquarks. Phys. Lett. B **177**, 377 (1986). [https://doi.org/10.1016/0370-2693\(86\)90771-9](https://doi.org/10.1016/0370-2693(86)90771-9), ISSN:0370-2693
- J.C. Pati, A. Salam, Lepton number as the fourth “color”, Phys. Rev. D **10**, 275, (1974) <https://doi.org/10.1103/PhysRevD.10.275>. Erratum: Phys. Rev. D **11**, 703-703 (1975). <https://doi.org/10.1103/PhysRevD.11.703.2>
- R. Barbier et al., R-Parity-violating supersymmetry. Physics Reports **420**, 1 (2005). <https://doi.org/10.1016/j.physrep.2005.08.006>. ISSN: 0370-1573
- M.J. Baker, J. Fuentes-Martín, G. Isidori, M. König, p_T signatures in vector-leptoquark models. Eur. Phys. J. C **79**, 334 (2019). <https://doi.org/10.1140/epjc/s10052-019-6853-x>. arXiv:1901.10480
- BaBar Collaboration, Measurement of an excess of $\bar{B} \rightarrow D^{(*)} \tau^- \bar{\nu}_\tau$ decays and implications for charged Higgs bosons. Phys. Rev. D **88**, 072012 (2013). <https://doi.org/10.1103/PhysRevD.88.072012>. arXiv:1303.0571
- Belle Collaboration, Measurement of the branching ratio of $\bar{B} \rightarrow D^{(*)} \tau^- \bar{\nu}_\tau$ relative to $\bar{B} \rightarrow D^{(*)} \ell^- \bar{\nu}_\ell$ decays with hadronic tagging at Belle. Phys. Rev. D **92**, 072014 (2015). <https://doi.org/10.1103/PhysRevD.92.072014>. arXiv:1507.03233
- LHCb Collaboration, Measurement of the Ratio of Branching Fractions $\mathcal{B}(\bar{B}^0 \rightarrow D^{*+} \tau^- \bar{\nu}_\tau)/\mathcal{B}(\bar{B}^0 \rightarrow D^{*+} \mu^- \bar{\nu}_\mu)$, Phys. Rev. Lett. **115**, 111803, (2015). <https://doi.org/10.1103/PhysRevLett.115.111803>, arXiv:1506.08614, Erratum: Phys. Rev. Lett. **115**, 159901, (2015). <https://doi.org/10.1103/PhysRevLett.115.159901>
- LHCb Collaboration, Test of lepton universality with $B^0 \rightarrow K^{*0} \ell^+ \ell^-$ decays, JHEP **08**, 055, (2017). [https://doi.org/10.1007/JHEP08\(2017\)055](https://doi.org/10.1007/JHEP08(2017)055), arXiv:1705.05802
- LHCb Collaboration, Search for Lepton-Universality Violation in $B^+ \rightarrow K^+ \ell^+ \ell^-$ Decays, Phys. Rev. Lett. **122**, 191801, (2019). <https://doi.org/10.1103/PhysRevLett.122.191801>, arXiv:1903.09252
- G. Hiller, D. Loose, I. Nišandžić, Flavorful leptoquarks at hadron colliders. Phys. Rev. D **97**, 075004 (2018). <https://doi.org/10.1103/PhysRevD.97.075004>. arXiv:1801.09399
- A.C.J. Camargo-Molina, D. Faroughy, Anomalies in bottom from new physics in top. Phys. Lett. B **784**, 284 (2018). <https://doi.org/10.1016/j.physletb.2018.07.051>. arXiv:1805.04917
- C.-H. Chen, T. Nomura, H. Okada, Excesses of muon $g - 2$, $R_{D^{(*)}}$, and $R_{K^{(*)}}$ in a leptoquark model. Phys. Lett. B **774**, 456 (2017). <https://doi.org/10.1016/j.physletb.2017.10.005>. arXiv:1703.03251
- Muon $g-2$ Collaboration, Final report of the E821 muon anomalous magnetic moment measurement at BNL, Phys. Rev. D **73**, 072003, (2006). <https://doi.org/10.1103/PhysRevD.73.072003>, arXiv:hep-ex/0602035
- L. Evans, P. Bryant, LHC Machine. JINST **3**, S08001 (2008). <https://doi.org/10.1088/1748-0221/3/08/S08001>
- C. Borschensky, B. Fuks, A. Kulesza, D. Schwartländer, Scalar leptoquark pair production at hadron colliders. Phys. Rev. D **101**, 115017 (2020). <https://doi.org/10.1103/PhysRevD.101.115017>. arXiv:2002.08971 [hep-ph]
- T. Mandal, S. Mitra, S. Seth, Pair production of scalar leptoquarks at the LHC to NLO parton shower accuracy. Phys. Rev. D **93**, 035018 (2016). <https://doi.org/10.1103/PhysRevD.93.035018>. arXiv:1506.07369 [hep-ph]
- M. Kramer, T. Plehn, M. Spira, P. Zerwas, Pair production of scalar leptoquarks at the CERN LHC. Phys. Rev. D **71**, 057503 (2005). <https://doi.org/10.1103/PhysRevD.71.057503>. arXiv:hep-ph/0411038
- M. Kramer, T. Plehn, M. Spira, P. Zerwas, Pair Production of Scalar Leptoquarks at the Fermilab Tevatron. Phys. Rev. Lett. **79**, 341 (1997). <https://doi.org/10.1103/PhysRevLett.79.341>. arXiv:hep-ph/9704322
- ATLAS Collaboration, Search for pairs of scalar leptoquarks decaying into quarks and electrons or muons in $\sqrt{s} = 13$ TeV

- pp collisions with the ATLAS detector, (2020). [https://doi.org/10.1007/JHEP10\(2020\)112](https://doi.org/10.1007/JHEP10(2020)112), arXiv:2006.05872
20. ATLAS Collaboration, Search for pair production of third-generation scalar leptoquarks decaying into a top quark and a τ -lepton in pp collisions at $\sqrt{s} = 13$ TeV with the ATLAS detector, (2021). arXiv:2006.05872
 21. R. Mandal, A. Pich, Constraints on scalar leptoquarks from lepton and kaon physics. *JHEP* **12**, 089 (2019). [https://doi.org/10.1007/JHEP12\(2019\)089](https://doi.org/10.1007/JHEP12(2019)089). arXiv:1908.11155 [hep-ph]
 22. CMS Collaboration, Search for Leptoquarks Coupled to Third-Generation Quarks in Proton-Proton Collisions at $\sqrt{s} = 13$ TeV, *Phys. Rev. Lett.* **121**, 241802, (2018), <https://doi.org/10.1103/PhysRevLett.121.241802>, arXiv:1809.05558
 23. ATLAS Collaboration, The ATLAS Experiment at the CERN Large Hadron Collider, *JINST* **3**, S08003, (2008) <https://doi.org/10.1088/1748-0221/3/08/S08003>
 24. ATLAS Collaboration, ATLAS Insertable B-Layer Technical Design Report, ATLAS-TDR-19; CERN-LHCC-2010-013, 2010, URL: <https://cds.cern.ch/record/1291633>
 25. B. Abbott et al., Production and integration of the ATLAS Insertable B-Layer. *JINST* **13**, T05008 (2018). <https://doi.org/10.1088/1748-0221/13/05/T05008>. arXiv:1803.00844 [physics.ins-det]
 26. ATLAS Collaboration, Performance of the ATLAS trigger system in 2015, *Eur. Phys. J. C* **77**, 317, (2017), <https://doi.org/10.1140/epjc/s10052-017-4852-3>, arXiv:1611.09661 [hep-ex]
 27. J. Alwall et al., The automated computation of tree-level and next-to-leading order differential cross sections, and their matching to parton shower simulations. *JHEP* **07**, 079 (2014). [https://doi.org/10.1007/JHEP07\(2014\)079](https://doi.org/10.1007/JHEP07(2014)079). arXiv:1405.0301
 28. R.D. Ball et al., Parton distributions for the LHC run II. *JHEP* **04**, 040 (2015). [https://doi.org/10.1007/JHEP04\(2015\)040](https://doi.org/10.1007/JHEP04(2015)040). arXiv:1410.8849
 29. T. Sjöstrand et al., An introduction to PYTHIA 8.2. *Comput. Phys. Commun.* **191**, 159 (2015). <https://doi.org/10.1016/j.cpc.2015.01.024>. arXiv:1410.3012
 30. ATLAS Collaboration, ATLAS Pythia 8 tunes to 7 TeV data, tech. rep. ATL-PHYS-PUB-2014-021, CERN, 2014, URL: <https://cds.cern.ch/record/1966419>
 31. R.D. Ball et al., Parton distributions with LHC data. *Nucl. Phys. B* **867**, 244 (2013). <https://doi.org/10.1016/j.nuclphysb.2012.10.003>. arXiv:1207.1303 [hep-ph]
 32. L. Lönnblad, S. Prestel, Merging multi-leg NLO matrix elements with parton showers. *JHEP* **03**, 166 (2013). [https://doi.org/10.1007/JHEP03\(2013\)166](https://doi.org/10.1007/JHEP03(2013)166). arXiv:1211.7278 [hep-ph]
 33. W. Beenakker, C. Borschensky, M. Krämer, A. Kulesza, E. Laenen, NNLL-fast: predictions for coloured supersymmetric particle production at the LHC with threshold and Coulomb resummation. *JHEP* **12**, 133 (2016). [https://doi.org/10.1007/JHEP12\(2016\)133](https://doi.org/10.1007/JHEP12(2016)133). arXiv:1607.07741 [hep-ph]
 34. W. Beenakker, M. Kramer, T. Plehn, M. Spira, P. Zerwas, Stop production at hadron colliders. *Nucl. Phys. B* **515**, 3 (1998). [https://doi.org/10.1016/S0550-3213\(98\)00014-5](https://doi.org/10.1016/S0550-3213(98)00014-5). arXiv:hep-ph/9710451
 35. W. Beenakker et al., Supersymmetric top and bottom squark production at hadron colliders. *JHEP* **08**, 098 (2010). [https://doi.org/10.1007/JHEP08\(2010\)098](https://doi.org/10.1007/JHEP08(2010)098). arXiv:1006.4771 [hep-ph]
 36. W. Beenakker et al., NNLL resummation for stop pair-production at the LHC. *JHEP* **05**, 153 (2016). [https://doi.org/10.1007/JHEP05\(2016\)153](https://doi.org/10.1007/JHEP05(2016)153). arXiv:1601.02954 [hep-ph]
 37. S. Frixione, E. Laenen, P. Motylinski, B.R. Webber, Angular correlations of lepton pairs from vector boson and top quark decays in Monte Carlo simulations. *JHEP* **04**, 081 (2007). <https://doi.org/10.1088/1126-6708/2007/04/081>. arXiv:hep-ph/0702198
 38. P. Artoisenet, R. Frederix, O. Mattelaer, R. Rietkerk, Automatic spin-entangled decays of heavy resonances in Monte Carlo simulations. *JHEP* **03**, 015 (2013). [https://doi.org/10.1007/JHEP03\(2013\)015](https://doi.org/10.1007/JHEP03(2013)015). arXiv:1212.3460
 39. E. Bothmann et al., Event generation with Sherpa 2.2. *SciPost Phys.* **7**, 034 (2019). <https://doi.org/10.21468/SciPostPhys.7.3.034>. arXiv:1905.09127
 40. C. Anastasiou, L.J. Dixon, K. Melnikov, F. Petriello, High-precision QCD at hadron colliders: Electroweak gauge boson rapidity distributions at next-to-next-to leading order. *Phys. Rev. D* **69**, 094008 (2004). <https://doi.org/10.1103/PhysRevD.69.094008>. arXiv:hep-ph/0312266
 41. T. Gleisberg, S. Höche, Comix, a new matrix element generator. *JHEP* **12**, 039 (2008). <https://doi.org/10.1088/1126-6708/2008/12/039>. arXiv:0808.3674
 42. F. Buccioni et al., OpenLoops 2. *Eur. Phys. J. C* **79**, 866 (2019). <https://doi.org/10.1140/epjc/s10052-019-7306-2>. arXiv:1907.13071
 43. F. Cascioli, P. Maierhöfer, S. Pozzorini, Scattering Amplitudes with Open Loops. *Phys. Rev. Lett.* **108**, 111601 (2012). <https://doi.org/10.1103/PhysRevLett.108.111601>. arXiv:1111.5206
 44. A. Denner, S. Dittmaier, L. Hofer, COLLIER: A fortran-based complex one-loop library in extended regularizations. *Comput. Phys. Commun.* **212**, 220 (2017). <https://doi.org/10.1016/j.cpc.2016.10.013>. arXiv:1604.06792
 45. S. Schumann, F. Krauss, A parton shower algorithm based on Catani-Seymour dipole factorisation. *JHEP* **03**, 038 (2008). <https://doi.org/10.1088/1126-6708/2008/03/038>. arXiv:0709.1027
 46. S. Höche, F. Krauss, M. Schönherr, F. Siegert, A critical appraisal of NLO+PS matching methods. *JHEP* **09**, 049 (2012). [https://doi.org/10.1007/JHEP09\(2012\)049](https://doi.org/10.1007/JHEP09(2012)049). arXiv:1111.1220
 47. S. Höche, F. Krauss, M. Schönherr, F. Siegert, QCD matrix elements + parton showers. The NLO case, *JHEP* **04**, 027 (2013). [https://doi.org/10.1007/JHEP04\(2013\)027](https://doi.org/10.1007/JHEP04(2013)027). arXiv:1207.5030
 48. S. Catani, F. Krauss, R. Kuhn, B.R. Webber, QCD Matrix Elements + Parton Showers. *JHEP* **11**, 063 (2001). <https://doi.org/10.1088/1126-6708/2001/11/063>. arXiv:hep-ph/0109231
 49. S. Höche, F. Krauss, S. Schumann, F. Siegert, QCD matrix elements and truncated showers. *JHEP* **05**, 053 (2009). <https://doi.org/10.1088/1126-6708/2009/05/053>. arXiv:0903.1219
 50. P. Nason, A new method for combining NLO QCD with shower Monte Carlo algorithms. *JHEP* **11**, 040 (2004). <https://doi.org/10.1088/1126-6708/2004/11/040>. arXiv:hep-ph/0409146
 51. S. Frixione, P. Nason, C. Oleari, Matching NLO QCD computations with parton shower simulations: the POWHEG method. *JHEP* **11**, 070 (2007). <https://doi.org/10.1088/1126-6708/2007/11/070>. arXiv:0709.2092
 52. S. Alioli, P. Nason, C. Oleari, E. Re, A general framework for implementing NLO calculations in shower Monte Carlo programs: the POWHEG BOX. *JHEP* **06**, 043 (2010). [https://doi.org/10.1007/JHEP06\(2010\)043](https://doi.org/10.1007/JHEP06(2010)043). arXiv:1002.2581
 53. S. Frixione, P. Nason, G. Ridolfi, A positive-weight next-to-leading-order Monte Carlo for heavy flavour hadroproduction. *JHEP* **09**, 126 (2007). <https://doi.org/10.1088/1126-6708/2007/09/126>. arXiv:0707.3088
 54. E. Re, Single-top Wt-channel production matched with parton showers using the POWHEG method. *Eur. Phys. J. C* **71**, 1547 (2011). <https://doi.org/10.1140/epjc/s10052-011-1547-z>. arXiv:1009.2450
 55. S. Alioli, P. Nason, C. Oleari and E. Re, NLO single-top production matched with shower in POWHEG: s- and t-channel contributions, *JHEP* **09**, 111, (2009). <https://doi.org/10.1088/1126-6708/2009/09/111>, arXiv:0907.4076, Erratum: *JHEP* **02**, 011, (2010). [https://doi.org/10.1007/JHEP02\(2010\)011](https://doi.org/10.1007/JHEP02(2010)011)
 56. S. Frixione, E. Laenen, P. Motylinski, B.R. Webber, C.D. White, Single-top hadroproduction in association with a W boson. *JHEP*

- 07, 029 (2008). <https://doi.org/10.1088/1126-6708/2008/07/029>. arXiv:0805.3067
57. ATLAS Collaboration, Studies on top-quark Monte Carlo modelling for Top2016, ATL-PHYS-PUB-2016-020, 2016, URL: <https://cds.cern.ch/record/2216168>
58. M. Beneke, P. Falgari, S. Klein, C. Schwinn, Hadronic top-quark pair production with NNLL threshold resummation. Nucl. Phys. B **855**, 695 (2012). <https://doi.org/10.1016/j.nuclphysb.2011.10.021>. arXiv:1109.1536
59. M. Cacciari, M. Czakon, M. Mangano, A. Mitov, P. Nason, Top-pair production at hadron colliders with next-to-next-to-leading logarithmic soft-gluon resummation. Phys. Lett. B **710**, 612 (2012). <https://doi.org/10.1016/j.physletb.2012.03.013>. arXiv:1111.5869
60. P. Bärnreuther, M. Czakon, A. Mitov, Percent-Level-Precision Physics at the Tevatron: Next-to-Next-to-Leading Order QCD Corrections to $q\bar{q} \rightarrow t\bar{t} + X$. Phys. Rev. Lett. **109**, 132001 (2012). <https://doi.org/10.1103/PhysRevLett.109.132001>. arXiv:1204.5201
61. M. Czakon, A. Mitov, NNLO corrections to top-pair production at hadron colliders: the all-fermionic scattering channels. JHEP **12**, 054 (2012). [https://doi.org/10.1007/JHEP12\(2012\)054](https://doi.org/10.1007/JHEP12(2012)054). arXiv:1207.0236
62. M. Czakon, A. Mitov, NNLO corrections to top pair production at hadron colliders: the quark-gluon reaction. JHEP **01**, 080 (2013). [https://doi.org/10.1007/JHEP01\(2013\)080](https://doi.org/10.1007/JHEP01(2013)080). arXiv:1210.6832
63. M. Czakon, P. Fiedler, A. Mitov, Total Top-Quark Pair-Production Cross Section at Hadron Colliders Through $O(\alpha_s^4)$. Phys. Rev. Lett. **110**, 252004 (2013). <https://doi.org/10.1103/PhysRevLett.110.252004>. arXiv:1303.6254
64. M. Czakon, A. Mitov, Top++: A program for the calculation of the top-pair cross-section at hadron colliders. Comput. Phys. Commun. **185**, 2930 (2014). <https://doi.org/10.1016/j.cpc.2014.06.021>. arXiv:1112.5675
65. M. Aliev et al., HATHOR - HAdronic Top and Heavy quarks crOss section calculatoR. Comput. Phys. Commun. **182**, 1034 (2011). <https://doi.org/10.1016/j.cpc.2010.12.040>. arXiv:1007.1327
66. P. Kant et al., HATHOR for single top-quark production: Updated predictions and uncertainty estimates for single top-quark production in hadronic collisions. Comput. Phys. Commun. **191**, 74 (2015). <https://doi.org/10.1016/j.cpc.2015.02.001>. arXiv:1406.4403
67. N. Kidonakis, Two-loop soft anomalous dimensions for single top quark associated production with a W^- or H^- . Phys. Rev. D **82**, 054018 (2010). <https://doi.org/10.1103/PhysRevD.82.054018>. arXiv:1005.4451 [hep-ph]
68. N. Kidonakis, 'Top Quark Production', Proceedings, Helmholtz International Summer School on Physics of Heavy Quarks and Hadrons (HQ 2013): JINR, Dubna, Russia, July 15-28, 2013, 2014 139, <https://doi.org/10.3204/DESY-PROC-2013-03/Kidonakis>, arXiv:1311.0283 [hep-ph]
69. M. Bahr et al., Herwig++ physics and manual. Eur. Phys. J. C **58**, 639 (2008). <https://doi.org/10.1140/epjc/s10052-008-0798-9>. arXiv:0803.0883
70. J. Bellm et al., Herwig 7.0/Herwig++ 3.0 release note, Eur. Phys. J. C **76** (2016) 196, [10.1140/epjc/s10052-016-4018-8](https://doi.org/10.1140/epjc/s10052-016-4018-8), arXiv:1512.01178
71. D. de Florian et al., Handbook of LHC Higgs Cross Sections: 4. Deciphering the Nature of the Higgs Sector, (2016), <https://doi.org/10.23731/CYRM-2017-002>, arXiv:1610.07922
72. D.J. Lange, The EvtGen particle decay simulation package. Nucl. Instrum. Meth. A **462**, 152 (2001). [https://doi.org/10.1016/S0168-9002\(01\)00089-4](https://doi.org/10.1016/S0168-9002(01)00089-4)
73. ATLAS Collaboration, The ATLAS Simulation Infrastructure, Eur. Phys. J. C **70**, 823, (2010), <https://doi.org/10.1140/epjc/s10052-010-1429-9>, arXiv:1005.4568 [physics.ins-det]
74. GEANT4 Collaboration, S. Agostinelli et al., GEANT4 - a simulation toolkit, Nucl. Instrum. Meth. A **506**, 250, (2003), [https://doi.org/10.1016/S0168-9002\(03\)01368-8](https://doi.org/10.1016/S0168-9002(03)01368-8)
75. ATLAS Collaboration, The simulation principle and performance of the ATLAS fast calorimeter simulation FastCaloSim, ATL-PHYS-PUB-2010-013 (2010), URL: <https://cds.cern.ch/record/1300517>
76. T. Sjöstrand, S. Mrenna and P. Skands, A brief introduction to PYTHIA 8.1, Comput. Phys. Commun. **178** (2008) 852. <https://doi.org/10.1016/j.cpc.2008.01.036>. arXiv:0710.3820
77. ATLAS Collaboration, The Pythia 8 A3 tune description of ATLAS minimum bias and inelastic measurements incorporating the Donnachie-Landshoff diffractive model, ATL-PHYS-PUB-2016-017, 2016, URL: <https://cds.cern.ch/record/2206965>
78. ATLAS Collaboration, Electron and photon performance measurements with the ATLAS detector using the 2015-2017 LHC proton-proton collision data, JINST **14** (2019) P12006. <https://doi.org/10.1088/1748-0221/14/12/P12006>, arXiv:1908.00005
79. ATLAS Collaboration, Muon reconstruction performance of the ATLAS detector in proton-proton collision data at $\sqrt{s} = 13$ TeV, Eur. Phys. J. C **76**, 292, (2016). <https://doi.org/10.1140/epjc/s10052-016-4120-y>, arXiv:1603.05598
80. M. Cacciari, G.P. Salam, G. Soyez, The anti- k_t jet clustering algorithm. JHEP **04**, 063 (2008). <https://doi.org/10.1088/1126-6708/2008/04/063>. arXiv:0802.1189
81. M. Cacciari, G.P. Salam, G. Soyez, FastJet user manual. Eur. Phys. J. C **72**, 1896 (2012). <https://doi.org/10.1140/epjc/s10052-012-1896-2>. arXiv:1111.6097 [hep-ph]
82. ATLAS Collaboration, Jet reconstruction and performance using particle flow with the ATLAS Detector, Eur. Phys. J. C **77**, 466, (2017), <https://doi.org/10.1140/epjc/s10052-017-5031-2>, arXiv:1703.10485
83. ATLAS Collaboration, Jet energy scale and resolution measured in proton-proton collisions at $\sqrt{s} = 13$ TeV with the ATLAS detector, (2020), arXiv:2007.02645
84. ATLAS Collaboration, Topological cell clustering in the ATLAS calorimeters and its performance in LHC Run 1, Eur. Phys. J. C **77**, 490, (2017), <https://doi.org/10.1140/epjc/s10052-017-5004-5>, arXiv:1603.02934 [hep-ex]
85. ATLAS Collaboration, Performance of pile-up mitigation techniques for jets in pp collisions at $\sqrt{s} = 8$ TeV using the ATLAS detector, Eur. Phys. J. C **76** (2016) 581, <https://doi.org/10.1140/epjc/s10052-016-4395-z>, arXiv:1510.03823
86. D. Krohn, J. Thaler, L.-T. Wang, Jet trimming. JHEP **02**, 084 (2010). [https://doi.org/10.1007/JHEP02\(2010\)084](https://doi.org/10.1007/JHEP02(2010)084). arXiv:0912.1342
87. S. Catani, Y.L. Dokshitzer, M. Olsson, G. Turnock, B. Webber, New clustering algorithm for multijet cross-sections in e^+e^- annihilation. Phys. Lett. B **269**, 432 (1991). [https://doi.org/10.1016/0370-2693\(91\)90196-W](https://doi.org/10.1016/0370-2693(91)90196-W)
88. S.D. Ellis, D.E. Soper, Successive combination jet algorithm for hadron collisions. Phys. Rev. D **48**, 3160 (1993). <https://doi.org/10.1103/PhysRevD.48.3160>. arXiv:hep-ph/9305266
89. S. Catani, Y.L. Dokshitzer, M. Seymour, B. Webber, Longitudinally-invariant k_{\perp} -clustering algorithms for hadron-hadron collisions. Nucl. Phys. B **406**, 187 (1993). [https://doi.org/10.1016/0550-3213\(93\)90166-M](https://doi.org/10.1016/0550-3213(93)90166-M)
90. ATLAS Collaboration, Performance of jet substructure techniques for large- R jets in proton-proton collisions at $\sqrt{s} = 7$ TeV using the ATLAS detector, JHEP **09**, 076, (2013), [https://doi.org/10.1007/JHEP09\(2013\)076](https://doi.org/10.1007/JHEP09(2013)076), arXiv:1306.4945 [hep-ex]
91. J. Thaler, K.V. Tilburg, Identifying boosted objects with N-subjettiness. JHEP **03**, 015 (2011). [https://doi.org/10.1007/JHEP03\(2011\)015](https://doi.org/10.1007/JHEP03(2011)015). arXiv:1011.2268

92. J. Thaler, K.V. Tilburg, Maximizing boosted top identification by minimizing N -subjettiness. *JHEP* **02**, 093 (2012). [https://doi.org/10.1007/JHEP02\(2012\)093](https://doi.org/10.1007/JHEP02(2012)093). [arXiv:1108.2701](https://arxiv.org/abs/1108.2701)
93. ATLAS Collaboration, Measurement of k_T splitting scales in $W \rightarrow l\nu$ events at $\sqrt{s}=7$ TeV with the ATLAS detector, *Eur. Phys. J. C* **73**, 2432, (2013). <https://doi.org/10.1140/epjc/s10052-013-2432-8>, [arXiv:1302.1415](https://arxiv.org/abs/1302.1415)
94. J. Thaler, L.-T. Wang, Strategies to identify boosted tops. *JHEP* **07**, 092 (2008). <https://doi.org/10.1088/1126-6708/2008/07/092>. [arXiv:0806.0023](https://arxiv.org/abs/0806.0023)
95. ATLAS Collaboration, Performance of missing transverse momentum reconstruction with the ATLAS detector using proton–proton collisions at $\sqrt{s} = 13$ TeV, *Eur. Phys. J. C* **78**, 903, (2018), <https://doi.org/10.1140/epjc/s10052-018-6288-9>, [arXiv:1802.08168](https://arxiv.org/abs/1802.08168) [hep-ex]
96. ATLAS Collaboration, E_T^{miss} performance in the ATLAS detector using 2015–2016 LHC pp collisions, ATLAS-CONF-2018-023, 2018, URL: <https://cds.cern.ch/record/2625233>
97. ATLAS Collaboration, Performance of electron and photon triggers in ATLAS during LHC Run 2, *Eur. Phys. J. C* **80**, 47, (2020). <https://doi.org/10.1140/epjc/s10052-019-7500-2>, [arXiv:1909.00761](https://arxiv.org/abs/1909.00761) [hep-ex]
98. ATLAS Collaboration, Performance of the ATLAS muon triggers in Run 2, (2020). <https://doi.org/10.1088/1748-0221/15/09/p09015>, [arXiv:2004.13447](https://arxiv.org/abs/2004.13447) [hep-ex]
99. T. Chen, C. Guestrin, XGBoost: A Scalable Tree Boosting System, (2016), <https://doi.org/10.1145/2939672.2939785>, [arXiv:1603.02754](https://arxiv.org/abs/1603.02754)
100. M. Stone, Cross-Validatory Choice and Assessment of Statistical Predictions. *J. Roy. Stat. Soc. B* **36**, 111 (1974). <https://doi.org/10.1111/j.2517-6161.1974.tb00994.x>
101. P. Jackson, C. Rogan, Recursive jigsaw reconstruction: HEP event analysis in the presence of kinematic and combinatoric ambiguities. *Phys. Rev. D* **96**, 112007 (2017). <https://doi.org/10.1103/PhysRevD.96.112007>. [arXiv:1705.10733](https://arxiv.org/abs/1705.10733)
102. P. Baldi, K. Cranmer, T. Faucett, P. Sadowski, D. Whiteson, Parameterized neural networks for high-energy physics. *Eur. Phys. J. C* **76**, 235 (2016). <https://doi.org/10.1140/epjc/s10052-016-4099-4>. [arXiv:1601.07913](https://arxiv.org/abs/1601.07913) [hep-ex]
103. ATLAS Collaboration, Luminosity determination in pp collisions at $\sqrt{s} = 13$ TeV using the ATLAS detector at the LHC, ATLAS-CONF-2019-021, 2019, URL: <https://cds.cern.ch/record/2677054>
104. G. Avoni et al., The new LUCID-2 detector for luminosity measurement and monitoring in ATLAS, JINST **13**, P07017, (2018). <https://doi.org/10.1088/1748-0221/13/07/P07017>
105. J. Butterworth et al., PDF4LHC recommendations for LHC Run II. *J. Phys. G* **43**, 023001 (2016). <https://doi.org/10.1088/0954-3899/43/2/023001>. [arXiv:1510.03865](https://arxiv.org/abs/1510.03865)
106. K. Melnikov, F. Petriello, Electroweak gauge boson production at hadron colliders through $O(\alpha_s^2)$. *Phys. Rev. D* **74**, 114017 (2006). <https://doi.org/10.1103/PhysRevD.74.114017>. [arXiv:hep-ph/0609070](https://arxiv.org/abs/hep-ph/0609070)
107. ATLAS Collaboration, Multi-boson simulation for 13 TeV ATLAS analyses, ATL-PHYS-PUB-2016-002, 2016, URL: <https://cds.cern.ch/record/2119986>
108. ATLAS Collaboration, Modelling of the $t\bar{t}H$ and $t\bar{t}V$ ($V = W, Z$) processes for $\sqrt{s} = 13$ TeV ATLAS analyses, ATL-PHYS-PUB-2016-005, 2016, URL: <https://cds.cern.ch/record/2120826>
109. ATLAS Collaboration, Jet Calibration and Systematic Uncertainties for Jets Reconstructed in the ATLAS Detector at $\sqrt{s} = 13$ TeV, ATL-PHYS-PUB-2015-015 (2015), URL: <https://cds.cern.ch/record/2037613>
110. L. Harland-Lang, A. Martin, P. Motylinski, R. Thorne, Parton distributions in the LHC era: MMHT 2014 PDFs. *Eur. Phys. J. C* **75**, 204 (2015). <https://doi.org/10.1140/epjc/s10052-015-3397-6>. [arXiv:1412.3989](https://arxiv.org/abs/1412.3989)
111. S. Dulat et al., New parton distribution functions from a global analysis of quantum chromodynamics. *Phys. Rev. D* **93**, 033006 (2016). <https://doi.org/10.1103/PhysRevD.93.033006>. [arXiv:1506.07443](https://arxiv.org/abs/1506.07443)
112. W. Verkerke, D. Kirkby, The RooFit toolkit for data modeling, (2003), [arXiv:physics/0306116](https://arxiv.org/abs/physics/0306116)
113. W. Verkerke, D. Kirkby, RooFit Users Manual v2.91, (2008), URL: <http://roofit.sourceforge.net>
114. A.L. Read, Presentation of search results: the CL_s technique. *J. Phys. G* **28**, 2693 (2002). <https://doi.org/10.1088/0954-3899/28/10/313>
115. T. Junk, Confidence level computation for combining searches with small statistics. *Nucl. Instrum. Meth. A* **434**, 435 (1999). [https://doi.org/10.1016/S0168-9002\(99\)00498-2](https://doi.org/10.1016/S0168-9002(99)00498-2). [arXiv:hep-ex/9902006](https://arxiv.org/abs/hep-ex/9902006)
116. G. Cowan, K. Cranmer, E. Gross, O. Vitells, Asymptotic formulae for likelihood-based tests of new physics, *Eur. Phys. J. C* **71**, 1554, (2011), <https://doi.org/10.1140/epjc/s10052-011-1554-0>, [arXiv:1007.1727](https://arxiv.org/abs/1007.1727), Erratum: *Eur. Phys. J. C* **73**, 2501, (2013). <https://doi.org/10.1140/epjc/s10052-013-2501-z>
117. A.J. Larkoski, D. Neill, J. Thaler, Jet shapes with the broadening axis. *JHEP* **04**, 017 (2014). [https://doi.org/10.1007/JHEP04\(2014\)017](https://doi.org/10.1007/JHEP04(2014)017). [arXiv:1401.2158](https://arxiv.org/abs/1401.2158) [hep-ph]
118. ATLAS Collaboration, ATLAS Computing Acknowledgements, ATL-SOFT-PUB-2020-001, URL: <https://cds.cern.ch/record/2717821>

ATLAS Collaboration

G. Aad¹⁰², B. Abbott¹²⁸, D. C. Abbott¹⁰³, A. Abed Abud³⁶, K. Abeling⁵³, D. K. Abhayasinghe⁹⁴, S. H. Abidi¹⁶⁷, O. S. AbouZeid⁴⁰, N. L. Abraham¹⁵⁶, H. Abramowicz¹⁶¹, H. Abreu¹⁶⁰, Y. Abulaiti⁶, B. S. Acharya^{67a,67b,o}, B. Achkar⁵³, L. Adam¹⁰⁰, C. Adam Bourdarios⁵, L. Adamczyk^{84a}, L. Adamek¹⁶⁷, J. Adelman¹²¹, A. Adiguzel^{12c,ad}, S. Adorni⁵⁴, T. Adye¹⁴³, A. A. Affolder¹⁴⁵, Y. Afik¹⁶⁰, C. Agapopoulou⁶⁵, M. N. Agaras³⁸, A. Aggarwal¹¹⁹, C. Agheorghiesei^{27c}, J. A. Aguilar-Saavedra^{139f,139a,ac}, A. Ahmad³⁶, F. Ahmadov⁸⁰, W. S. Ahmed¹⁰⁴, X. Ai¹⁸, G. Aielli^{74a,74b}, S. Akatsuka⁸⁶, M. Akbiyik¹⁰⁰, T. P. A. Åkesson⁹⁷, E. Akilli⁵⁴, A. V. Akimov¹¹¹, K. Al Khoury⁶⁵, G. L. Alberghi^{23a,23b}, J. Albert¹⁷⁶, M. J. Alconada Verzini¹⁶¹, S. Alderweireldt³⁶, M. Aleksa³⁶, I. N. Aleksandrov⁸⁰, C. Alexa^{27b}, T. Alexopoulos¹⁰, A. Alfonsi¹²⁰, F. Alfonsi^{23a,23b}, M. Alhroob¹²⁸, B. Ali¹⁴¹, S. Ali¹⁵⁸, M. Aliev¹⁶⁶, G. Alimonti^{69a}, C. Allaire³⁶, B. M. M. Allbrooke¹⁵⁶, B. W. Allen¹³¹, P. P. Allport²¹, A. Aloisio^{70a,70b}, F. Alonso⁸⁹, C. Alpigiani¹⁴⁸, E. Alunno Camelia^{74a,74b}, M. Alvarez Estevez⁹⁹, M. G. Alviggi^{70a,70b}, Y. Amaral Coutinho^{81b}, A. Ambler¹⁰⁴, L. Ambroz¹³⁴, C. Amelung³⁶, D. Amidei¹⁰⁶, S. P. Amor Dos Santos^{139a}, S. Amoroso⁴⁶, C. S. Amrouche⁵⁴, F. An⁷⁹, C. Anastopoulos¹⁴⁹, N. Andari¹⁴⁴, T. Andeen¹¹, J. K. Anders²⁰, S. Y. Andreev^{45a,45b}, A. Andreazza^{69a,69b}, V. Andrei^{61a}, C. R. Anelli¹⁷⁶, S. Angelidakis⁹, A. Angerami³⁹, A. V. Anisenkov^{122a,122b}, A. Annovi^{72a}, C. Antel⁵⁴, M. T. Anthony¹⁴⁹, E. Antipov¹²⁹, M. Antonelli⁵¹, D. J. A. Antrim¹⁸, F. Anulli^{73a}, M. Aoki⁸², J. A. Aparisi Pozo¹⁷⁴, M. A. Aparo¹⁵⁶, L. Aperio Bella⁴⁶, N. Aranzabal³⁶, V. Araujo Ferraz^{81a}, R. Araujo Pereira^{81b}, C. Arcangeletti⁵¹, A. T. H. Arce⁴⁹, J.-F. Arguin¹¹⁰, S. Argyropoulos⁵², J.-H. Arling⁴⁶, A. J. Armbruster³⁶, A. Armstrong¹⁷¹, O. Arnaez¹⁶⁷, H. Arnold¹²⁰, Z. P. Arrabarrena Tame¹¹⁴, G. Artoni¹³⁴, H. Asada¹¹⁷, K. Asai¹²⁶, S. Asai¹⁶³, T. Asawatavonvanich¹⁶⁵, N. Asbah⁵⁹, E. M. Asimakopoulou¹⁷², L. Asquith¹⁵⁶, J. Assahsah^{35e}, K. Assamagan²⁹, R. Astalos^{28a}, R. J. Atkin^{33a}, M. Atkinson¹⁷³, N. B. Atlay¹⁹, H. Atmani⁶⁵, P. A. Atmasiddha¹⁰⁶, K. Augsten¹⁴¹, V. A. Austrup¹⁸², G. Avolio³⁶, M. K. Ayoub^{15a}, G. Azeulos^{110,ak}, D. Babal^{28a}, H. Bachacou¹⁴⁴, K. Bachas¹⁶², F. Backman^{45a,45b}, P. Bagnaia^{73a,73b}, M. Bahmani⁸⁵, H. Bahrasemani¹⁵², A. J. Bailey¹⁷⁴, V. R. Bailey¹⁷³, J. T. Baines¹⁴³, C. Bakalis¹⁰, O. K. Baker¹⁸³, P. J. Bakker¹²⁰, E. Bakos¹⁶, D. Bakshi Gupta⁸, S. Balaji¹⁵⁷, R. Balasubramanian¹²⁰, E. M. Baldin^{122a,122b}, P. Balek¹⁸⁰, F. Balli¹⁴⁴, W. K. Balunas¹³⁴, J. Balz¹⁰⁰, E. Banas⁸⁵, M. Bandieramonte¹³⁸, A. Bandyopadhyay¹⁹, Sw. Banerjee^{181j}, L. Barak¹⁶¹, W. M. Barbe³⁸, E. L. Barberio¹⁰⁵, D. Barberis^{55a,55b}, M. Barbero¹⁰², G. Barbour⁹⁵, T. Barillari¹¹⁵, M.-S. Barisits³⁶, J. Barkeloo¹³¹, T. Barklow¹⁵³, R. Barnea¹⁶⁰, B. M. Barnett¹⁴³, R. M. Barnett¹⁸, Z. Barnovska-Blenessy^{60a}, A. Baroncelli^{60a}, G. Barone²⁹, A. J. Barr¹³⁴, L. Barranco Navarro^{45a,45b}, F. Barreiro⁹⁹, J. Barreiro Guimarães da Costa^{15a}, U. Barron¹⁶¹, S. Barsov¹³⁷, F. Bartels^{61a}, R. Bartoldus¹⁵³, G. Bartolini¹⁰², A. E. Barton⁹⁰, P. Bartos^{28a}, A. Basalae⁴⁶, A. Basan¹⁰⁰, A. Bassalat^{65,ah}, M. J. Basso¹⁶⁷, R. L. Bates⁵⁷, S. Batlamous^{35f}, J. R. Batley³², B. Batool¹⁵¹, M. Battaglia¹⁴⁵, M. Bauce^{73a,73b}, F. Bauer¹⁴⁴, P. Bauer²⁴, H. S. Bawa³¹, A. Bayirli^{12c}, J. B. Beacham⁴⁹, T. Beau¹³⁵, P. H. Beauchemin¹⁷⁰, F. Becherer⁵², P. Bechtel²⁴, H. C. Beck⁵³, H. P. Beck^{20,q}, K. Becker¹⁷⁸, C. Becot⁴⁶, A. Beddall^{12d}, A. J. Beddall^{12a}, V. A. Bednyakov⁸⁰, M. Bedognetti¹²⁰, C. P. Bee¹⁵⁵, T. A. Beermann¹⁸², M. Begalli^{81b}, M. Begel²⁹, A. Behera¹⁵⁵, J. K. Behr⁴⁶, F. Beisiegel²⁴, M. Belfkir⁵, A. S. Bell⁹⁵, G. Bella¹⁶¹, L. Bellagamba^{23b}, A. Bellerive³⁴, P. Bellos⁹, K. Beloborodov^{122a,122b}, K. Belotskiy¹¹², N. L. Belyaev¹¹², D. Bencheikroun^{35a}, N. Benekos¹⁰, Y. Benhammou¹⁶¹, D. P. Benjamin⁶, M. Benoit²⁹, J. R. Bensinger²⁶, S. Bentvelsen¹²⁰, L. Beresford¹³⁴, M. Beretta⁵¹, D. Berge¹⁹, E. Bergeas Kuutmann¹⁷², N. Berger⁵, B. Bergmann¹⁴¹, L. J. Bergsten²⁶, J. Beringer¹⁸, S. Berlendis⁷, G. Bernardi¹³⁵, C. Bernius¹⁵³, F. U. Bernlochner²⁴, T. Berry⁹⁴, P. Berta¹⁰⁰, A. Berthold⁴⁸, I. A. Bertram⁹⁰, O. Bessidskaia Bylund¹⁸², N. Besson¹⁴⁴, S. Bethke¹¹⁵, A. Betti⁴², A. J. Bevan⁹³, J. Beyer¹¹⁵, S. Bhatta¹⁵⁵, D. S. Bhattacharya¹⁷⁷, P. Bhattacharai²⁶, V. S. Bhopatkar⁶, R. Bi¹³⁸, R. M. Bianchi¹³⁸, O. Biebel¹¹⁴, D. Biedermann¹⁹, R. Bielski³⁶, K. Bierwagen¹⁰⁰, N. V. Biesuz^{72a,72b}, M. Biglietti^{75a}, T. R. V. Billoud¹⁴¹, M. Bindi⁵³, A. Bingul^{12d}, C. Bini^{73a,73b}, S. Biondi^{23a,23b}, C. J. Birch-sykes¹⁰¹, M. Birman¹⁸⁰, T. Bisanz³⁶, J. P. Biswal³, D. Biswas^{181j}, A. Bitadze¹⁰¹, C. Bittrich⁴⁸, K. Björke¹³³, T. Blazek^{28a}, I. Bloch⁴⁶, C. Blocker²⁶, A. Blue⁵⁷, U. Blumenschein⁹³, G. J. Bobbink¹²⁰, V. S. Bobrovnikov^{122a,122b}, S. S. Bocchetta⁹⁷, D. Bogavac¹⁴, A. G. Bogdanchikov^{122a,122b}, C. Bohm^{45a}, V. Boisvert⁹⁴, P. Bokan^{172,53}, T. Bold^{84a}, A. E. Bolz^{61b}, M. Bomben¹³⁵, M. Bona⁹³, J. S. Bonilla¹³¹, M. Boonekamp¹⁴⁴, C. D. Booth⁹⁴, A. G. Borbély⁵⁷, H. M. Borecka-Bielska⁹¹, L. S. Borgna⁹⁵, A. Borisov¹²³, G. Borissov⁹⁰, D. Bortoletto¹³⁴, D. Boscherini^{23b}, M. Bosman¹⁴, J. D. Bossio Sola¹⁰⁴, K. Bouaouda^{35a}, J. Boudreau¹³⁸, E. V. Bouhova-Thacker⁹⁰, D. Boumediene³⁸, A. Boveia¹²⁷, J. Boyd³⁶

E. B. Diehl¹⁰⁶, J. Dietrich¹⁹, S. Díez Cornell⁴⁶, C. Diez Pardos¹⁵¹, A. Dimitrievska¹⁸, W. Ding^{15b}, J. Dingfelder²⁴, S. J. Dittmeier^{61b}, F. Dittus³⁶, F. Djama¹⁰², T. Djobava^{159b}, J. I. Djuvsland¹⁷, M. A. B. Do Vale¹⁴⁷, M. Dobre^{27b}, D. Dodsworth²⁶, C. Doglioni⁹⁷, J. Dolejsi¹⁴², Z. Dolezal¹⁴², M. Donadelli^{81c}, B. Dong^{60c}, J. Donini³⁸, A. D'Onofrio^{15c}, M. D'Onofrio⁹¹, J. Dopke¹⁴³, A. Doria^{70a}, M. T. Dova⁸⁹, A. T. Doyle⁵⁷, E. Drechsler¹⁵², E. Dreyer¹⁵², T. Dreyer⁵³, A. S. Drobac¹⁷⁰, D. Du^{60b}, T. A. du Pree¹²⁰, Y. Duan^{60d}, F. Dubinin¹¹¹, M. Dubovsky^{28a}, A. Dubreuil⁵⁴, E. Duchovni¹⁸⁰, G. Duckeck¹¹⁴, O. A. Ducu^{36,27b}, D. Duda¹¹⁵, A. Dudarev³⁶, A. C. Dudder¹⁰⁰, E. M. Duffield¹⁸, M. D'uffizi¹⁰¹, L. Duflost⁶⁵, M. Dührssen³⁶, C. Dülsen¹⁸², M. Dumancic¹⁸⁰, A. E. Dumitriu^{27b}, M. Dunford^{61a}, S. Dungs⁴⁷, A. Duperrin¹⁰², H. Duran Yildiz^{4a}, M. Düren⁵⁶, A. Durglishvili^{159b}, D. Duschinger⁴⁸, B. Dutta⁴⁶, D. Duvnjak¹, G. I. Dyckes¹³⁶, M. Dyndal³⁶, S. Dysch¹⁰¹, B. S. Dziedzic⁸⁵, M. G. Eggleston⁴⁹, T. Eifert⁸, G. Eigen¹⁷, K. Einsweiler¹⁸, T. Ekelof¹⁷², H. El Jarrari^{35f}, V. Ellajosyula¹⁷², M. Ellert¹⁷², F. Ellinghaus¹⁸², A. A. Elliot⁹³, N. Ellis³⁶, J. Elmsheuser²⁹, M. Elsing³⁶, D. Emelianov¹⁴³, A. Emerman³⁹, Y. Enari¹⁶³, M. B. Epland⁴⁹, J. Erdmann⁴⁷, A. Ereditato²⁰, P. A. Erland⁸⁵, M. Errenst¹⁸², M. Escalier⁶⁵, C. Escobar¹⁷⁴, O. Estrada Pastor¹⁷⁴, E. Etzion¹⁶¹, G. Evans^{139a}, H. Evans⁶⁶, M. O. Evans¹⁵⁶, A. Ezhilov¹³⁷, F. Fabbri⁵⁷, L. Fabbri^{23a,23b}, V. Fabiani¹¹⁹, G. Facini¹⁷⁸, R. M. Fakhruddinov¹²³, S. Falciano^{73a}, P. J. Falke²⁴, S. Falke³⁶, J. Faltova¹⁴², Y. Fang^{15a}, Y. Fang^{15a}, G. Fanourakis⁴⁴, M. Fanti^{69a,69b}, M. Faraj^{67a,67c}, A. Farbin⁸, A. Farilla^{75a}, E. M. Farina^{71a,71b}, T. Farooque¹⁰⁷, S. M. Farrington⁵⁰, P. Farthouat³⁶, F. Fassi^{35f}, P. Fassnacht³⁶, D. Fassouliotis⁹, M. Faucci Giannelli⁵⁰, W. J. Fawcett³², L. Fayard⁶⁵, O. L. Fedin^{137,p}, W. Fedorko¹⁷⁵, A. Fehr²⁰, M. Feickert¹⁷³, L. Felgioni¹⁰², A. Fell¹⁴⁹, C. Feng^{60b}, M. Feng⁴⁹, M. J. Fenton¹⁷¹, A. B. Fenjuk¹²³, S. W. Ferguson⁴³, J. Ferrando⁴⁶, A. Ferrari¹⁷², P. Ferrari¹²⁰, R. Ferrari^{71a}, D. E. Ferreira de Lima^{61b}, A. Ferrer¹⁷⁴, D. Ferrere⁵⁴, C. Ferretti¹⁰⁶, F. Fiedler¹⁰⁰, A. Filipčić⁹², F. Filthaut¹¹⁹, K. D. Finelli²⁵, M. C. N. Fiolhais^{139a,139c,a}, L. Fiorini¹⁷⁴, F. Fischer¹¹⁴, J. Fischer¹⁰⁰, W. C. Fisher¹⁰⁷, T. Fitschen²¹, I. Fleck¹⁵¹, P. Fleischmann¹⁰⁶, T. Flick¹⁸², B. M. Flierl¹¹⁴, L. Flores¹³⁶, L. R. Flores Castillo^{63a}, F. M. Follega^{76a,76b}, N. Fomin¹⁷, J. H. Foo¹⁶⁷, G. T. Forcolin^{76a,76b}, B. C. Forland⁶⁶, A. Formica¹⁴⁴, F. A. Förster¹⁴, A. C. Forti¹⁰¹, E. Fortin¹⁰², M. G. Foti¹³⁴, D. Fournier⁶⁵, H. Fox⁹⁰, P. Francavilla^{72a,72b}, S. Francescato^{73a,73b}, M. Franchini^{23a,23b}, S. Franchino^{61a}, D. Francis³⁶, L. Franco⁵, L. Franconi²⁰, M. Franklin⁵⁹, G. Frattari^{73a,73b}, A. N. Fray⁹³, P. M. Freeman²¹, B. Freund¹¹⁰, W. S. Freund^{81b}, E. M. Freundlich⁴⁷, D. C. Frizzell¹²⁸, D. Froidevaux³⁶, J. A. Frost¹³⁴, M. Fujimoto¹²⁶, C. Fukunaga¹⁶⁴, E. Fullana Torregrosa¹⁷⁴, T. Fusayasu¹¹⁶, J. Fuster¹⁷⁴, A. Gabrielli^{23a,23b}, A. Gabrielli³⁶, S. Gadatsch⁵⁴, P. Gadov¹¹⁵, G. Gagliardi^{55a,55b}, L. G. Gagnon¹¹⁰, G. E. Gallardo¹³⁴, E. J. Gallas¹³⁴, B. J. Gallop¹⁴³, R. Gamboa Goni⁹³, K. K. Gan¹²⁷, S. Ganguly¹⁸⁰, J. Gao^{60a}, Y. Gao⁵⁰, Y. S. Gao^{31,m}, F. M. Garay Walls^{146a}, C. García¹⁷⁴, J. E. García Navarro¹⁷⁴, J. A. García Pascual^{15a}, C. Garcia-Argos⁵², M. Garcia-Sciveres¹⁸, R. W. Gardner³⁷, N. Garelli¹⁵³, S. Gargiulo⁵², C. A. Garner¹⁶⁷, V. Garonne¹³³, S. J. Gasiorowski¹⁴⁸, P. Gaspar^{81b}, A. Gaudiello^{55a,55b}, G. Gaudio^{71a}, P. Gauzzi^{73a,73b}, I. L. Gavrilenko¹¹¹, A. Gavriluk¹²⁴, C. Gay¹⁷⁵, G. Gaycken⁴⁶, E. N. Gazis¹⁰, A. A. Geanta^{27b}, C. M. Gee¹⁴⁵, C. N. P. Gee¹⁴³, J. Geisen⁹⁷, M. Geisen¹⁰⁰, C. Gemme^{55b}, M. H. Genest⁵⁸, C. Geng¹⁰⁶, S. Gentile^{73a,73b}, S. George⁹⁴, T. Gerialis⁴⁴, L. O. Gerlach⁵³, P. Gessinger-Befurt¹⁰⁰, G. Gessner⁴⁷, M. Ghasemi Bostanabad¹⁷⁶, M. Ghneimat¹⁵¹, A. Ghosh⁶⁵, A. Ghosh⁷⁸, B. Giacobbe^{23b}, S. Giagu^{73a,73b}, N. Giangiacomi¹⁶⁷, P. Giannetti^{72a}, A. Giannini^{70a,70b}, G. Giannini¹⁴, S. M. Gibson⁹⁴, M. Gignac¹⁴⁵, D. T. Gil^{84b}, B. J. Gilbert³⁹, D. Gillberg³⁴, G. Gilles¹⁸², N. E. K. Gillwald⁴⁶, D. M. Gingrich^{3,ak}, M. P. Giordani^{67a,67c}, P. F. Giraud¹⁴⁴, G. Giugliarelli^{67a,67c}, D. Giugni^{69a}, F. Giuli^{74a,74b}, S. Gkaitatzis¹⁶², I. Gkialas^{9,h}, E. L. Gkougkousis¹⁴, P. Gkoutoumis¹⁰, L. K. Gladilin¹¹³, C. Glasman⁹⁹, J. Glatzer¹⁴, P. C. F. Glaysher⁴⁶, A. Glazov⁴⁶, G. R. Gledhill¹³¹, I. Gnesi^{41b,c}, M. Goblirsch-Kolb²⁶, D. Godin¹¹⁰, S. Goldfarb¹⁰⁵, T. Golling⁵⁴, D. Golubkov¹²³, A. Gomes^{139a,139b}, R. Goncalves Gama⁵³, R. Gonçalves^{139a,139c}, G. Gonella¹³¹, L. Gonella²¹, A. Gongadze⁸⁰, F. Gonnella²¹, J. L. Gonski³⁹, S. González de la Hoz¹⁷⁴, S. Gonzalez Fernandez¹⁴, R. Gonzalez Lopez⁹¹, C. Gonzalez Renteria¹⁸, R. Gonzalez Suarez¹⁷², S. Gonzalez-Sevilla⁵⁴, G. R. Gonzalvo Rodriguez¹⁷⁴, L. Goossens³⁶, N. A. Gorasia²¹, P. A. Gorbounov¹²⁴, H. A. Gordon²⁹, B. Gorini³⁶, E. Gorini^{68a,68b}, A. Gorišek⁹², A. T. Goshaw⁴⁹, M. I. Gostkin⁸⁰, C. A. Gottardo¹¹⁹, M. Gouighri^{35b}, A. G. Goussiou¹⁴⁸, N. Govender^{33c}, C. Goy⁵, I. Grabowska-Bold^{84a}, E. C. Graham⁹¹, J. Gramling¹⁷¹, E. Gramstad¹³³, S. Grancagnolo¹⁹, M. Grandi¹⁵⁶, V. Gratchev¹³⁷, P. M. Gravila^{27f}, F. G. Gravili^{68a,68b}, C. Gray⁵⁷, H. M. Gray¹⁸, C. Greife²⁴, K. Gregersen⁹⁷, I. M. Gregor⁴⁶, P. Grenier¹⁵³, K. Grevtsov⁴⁶, C. Grieco¹⁴, N. A. Grieser¹²⁸, A. A. Grillo¹⁴⁵, K. Grimm^{31,l}, S. Grinstein^{14,w}, J.-F. Grivaz⁶⁵, S. Groh¹⁰⁰, E. Gross¹⁸⁰

J. Grosse-Knetter⁵³, Z. J. Grout⁹⁵, C. Grud¹⁰⁶, A. Grummer¹¹⁸, J. C. Grundy¹³⁴, L. Guan¹⁰⁶, W. Guan¹⁸¹, C. Gubbels¹⁷⁵, J. Guenther⁷⁷, A. Guerguichon⁶⁵, J. G. R. Guerrero Rojas¹⁷⁴, F. Guescini¹¹⁵, D. Guest⁷⁷, R. Gugel¹⁰⁰, A. Guida⁴⁶, T. Guillemain⁵, S. Guindon³⁶, J. Guo^{60c}, W. Guo¹⁰⁶, Y. Guo^{60a}, Z. Guo¹⁰², R. Gupta⁴⁶, S. Gurbuz^{12c}, G. Gustavino¹²⁸, M. Guth⁵², P. Gutierrez¹²⁸, C. Gutsche⁹⁵, C. Guyot¹⁴⁴, C. Gwenlan¹³⁴, C. B. Gwilliam⁹¹, E. S. Haaland¹³³, A. Haas¹²⁵, C. Haber¹⁸, H. K. Hadavand⁸, A. Hadeef¹⁰⁰, M. Haleem¹⁷⁷, J. Haley¹²⁹, J. J. Hall¹⁴⁹, G. Halladjian¹⁰⁷, G. D. Hallewell¹⁰², K. Hamano¹⁷⁶, H. Hamdaoui^{35f}, M. Hamer²⁴, G. N. Hamity⁵⁰, K. Han^{60a}, L. Han^{15c}, L. Han^{60a}, S. Han¹⁸, Y. F. Han¹⁶⁷, K. Hanagaki^{82,u}, M. Hance¹⁴⁵, D. M. Handl¹¹⁴, M. D. Hank³⁷, R. Hankache¹³⁵, E. Hansen⁹⁷, J. B. Hansen⁴⁰, J. D. Hansen⁴⁰, M. C. Hansen²⁴, P. H. Hansen⁴⁰, E. C. Hanson¹⁰¹, K. Hara¹⁶⁹, T. Harenberg¹⁸², S. Harkusha¹⁰⁸, P. F. Harrison¹⁷⁸, N. M. Hartman¹⁵³, N. M. Hartmann¹¹⁴, Y. Hasegawa¹⁵⁰, A. Hasib⁵⁰, S. Hassani¹⁴⁴, S. Haug²⁰, R. Hauser¹⁰⁷, M. Havranek¹⁴¹, C. M. Hawkes²¹, R. J. Hawkins³⁶, S. Hayashida¹¹⁷, D. Hayden¹⁰⁷, C. Hayes¹⁰⁶, R. L. Hayes¹⁷⁵, C. P. Hays¹³⁴, J. M. Hays⁹³, H. S. Hayward⁹¹, S. J. Haywood¹⁴³, F. He^{60a}, Y. He¹⁶⁵, M. P. Heath⁵⁰, V. Hedberg⁹⁷, A. L. Heggelund¹³³, N. D. Hehir⁹³, C. Heidegger⁵², K. K. Heidegger⁵², W. D. Heidorn⁷⁹, J. Heilman³⁴, S. Heim⁴⁶, T. Heim¹⁸, B. Heinemann^{46,ai}, J. G. Heinlein¹³⁶, J. J. Heinrich¹³¹, L. Heinrich³⁶, J. Hejbal¹⁴⁰, L. Helary⁴⁶, A. Held¹²⁵, S. Hellesund¹³³, C. M. Helling¹⁴⁵, S. Hellman^{45a,45b}, C. Helsens³⁶, R. C. W. Henderson⁹⁰, L. Henkelmann³², A. M. Henriques Correia³⁶, H. Herde²⁶, Y. Hernández Jiménez^{33e}, H. Herr¹⁰⁰, M. G. Herrmann¹¹⁴, T. Herrmann⁴⁸, G. Herten⁵², R. Hertenberger¹¹⁴, L. Hervas³⁶, G. G. Hesketh⁹⁵, N. P. Hessey^{168a}, H. Hibi⁸³, S. Higashino⁸², E. Higón-Rodríguez¹⁷⁴, K. Hildebrand³⁷, J. C. Hill³², K. K. Hill²⁹, K. H. Hiller⁴⁶, S. J. Hillier²¹, M. Hils⁴⁸, I. Hinchliffe¹⁸, F. Hinterkeuser²⁴, M. Hirose¹³², S. Hirose¹⁶⁹, D. Hirschbuehl¹⁸², B. Hiti⁹², O. Hladik¹⁴⁰, J. Hobbs¹⁵⁵, R. Hobincu^{27e}, N. Hod¹⁸⁰, M. C. Hodgkinson¹⁴⁹, A. Hoecker³⁶, D. Hohn⁵², D. Hohov⁶⁵, T. Holm²⁴, T. R. Holmes³⁷, M. Holzbock¹¹⁵, L. B. A. H. Hommels³², T. M. Hong¹³⁸, J. C. Honig⁵², A. Hönle¹¹⁵, B. H. Hooberman¹⁷³, W. H. Hopkins⁶, Y. Horii¹¹⁷, P. Horn⁴⁸, L. A. Horyn³⁷, S. Hou¹⁵⁸, A. Houmada^{35a}, J. Howarth⁵⁷, J. Hoya⁸⁹, M. Hrabovsky¹³⁰, J. Hrivnac⁶⁵, A. Hrynevich¹⁰⁹, T. Hryn'ova⁵, P. J. Hsu⁶⁴, S.-C. Hsu¹⁴⁸, Q. Hu³⁹, S. Hu^{60c}, Y. F. Hu^{15a,15d,am}, D. P. Huang⁹⁵, X. Huang^{15c}, Y. Huang^{60a}, Y. Huang^{15a}, Z. Hubacek¹⁴¹, F. Hubaut¹⁰², M. Huebner²⁴, F. Huegging²⁴, T. B. Huffman¹³⁴, M. Huhtinen³⁶, R. Hulsken⁵⁸, R. F. H. Hunter³⁴, N. Huseynov^{80,ab}, J. Huston¹⁰⁷, J. Huth⁵⁹, R. Hyneman¹⁵³, S. Hyrych^{28a}, G. Iacobucci⁵⁴, G. Iakovidis²⁹, I. Ibragimov¹⁵¹, L. Iconomidou-Fayard⁶⁵, P. Iengo³⁶, R. Ignazzi⁴⁰, R. Iguchi¹⁶³, T. Iizawa⁵⁴, Y. Ikegami⁸², M. Ikeno⁸², N. Ilic^{119,167,aa}, F. Iltzsche⁴⁸, H. Iman^{35a}, G. Introzzi^{71a,71b}, M. Iodice^{75a}, K. Iordanidou^{168a}, V. Ippolito^{73a,73b}, M. F. Isacson¹⁷², M. Ishino¹⁶³, W. Islam¹²⁹, C. Issever^{19,46}, S. Istin¹⁶⁰, J. M. Iturbe Ponce^{63a}, R. Iuppa^{76a,76b}, A. Ivina¹⁸⁰, J. M. Izen⁴³, V. Izzo^{70a}, P. Jacka¹⁴⁰, P. Jackson¹, R. M. Jacobs⁴⁶, B. P. Jaeger¹⁵², V. Jain², G. Jäkel¹⁸², K. B. Jakobi¹⁰⁰, K. Jakobs⁵², T. Jakoubek¹⁸⁰, J. Jamieson⁵⁷, K. W. Janas^{84a}, R. Jansky⁵⁴, M. Janus⁵³, P. A. Janus^{84a}, G. Jarlskog⁹⁷, A. E. Jaspan⁹¹, N. Javadov^{80,ab}, T. Javůrek³⁶, M. Javurkova¹⁰³, F. Jeanneau¹⁴⁴, L. Jeanty¹³¹, J. Jejelava^{159a}, P. Jenni^{52,d}, N. Jeong⁴⁶, S. Jézéquel⁵, J. Jia¹⁵⁵, Z. Jia^{15c}, H. Jiang⁷⁹, Y. Jiang^{60a}, Z. Jiang¹⁵³, S. Jiggins⁵², F. A. Jimenez Morales³⁸, J. Jimenez Pena¹¹⁵, S. Jin^{15c}, A. Jinaru^{27b}, O. Jinnouchi¹⁶⁵, H. Jivan^{33e}, P. Johansson¹⁴⁹, K. A. Johns⁷, C. A. Johnson⁶⁶, E. Jones¹⁷⁸, R. W. L. Jones⁹⁰, S. D. Jones¹⁵⁶, T. J. Jones⁹¹, J. Jovicevic³⁶, X. Ju¹⁸, J. J. Junggeburth¹¹⁵, A. Juste Rozas^{14,w}, A. Kaczmarska⁸⁵, M. Kado^{73a,73b}, H. Kagan¹²⁷, M. Kagan¹⁵³, A. Kahn³⁹, C. Kahra¹⁰⁰, T. Kaji¹⁷⁹, E. Kajomovitz¹⁶⁰, C. W. Kalderon²⁹, A. Kaluza¹⁰⁰, A. Kamenshchikov¹²³, M. Kaneda¹⁶³, N. J. Kang¹⁴⁵, S. Kang⁷⁹, Y. Kano¹¹⁷, J. Kanzaki⁸², L. S. Kaplan¹⁸¹, D. Kar^{33e}, K. Karava¹³⁴, M. J. Kareem^{168b}, I. Karkanas¹⁶², S. N. Karpov⁸⁰, Z. M. Karpova⁸⁰, V. Kartvelishvili⁹⁰, A. N. Karyukhin¹²³, E. Kasimi¹⁶², A. Kastanas^{45a,45b}, C. Kato^{60d}, J. Katzy⁴⁶, K. Kawade¹⁵⁰, K. Kawagoe⁸⁸, T. Kawaguchi¹¹⁷, T. Kawamoto¹⁴⁴, G. Kawamura⁵³, E. F. Kay¹⁷⁶, F. I. Kaya¹⁷⁰, S. Kazakov¹⁴, V. F. Kazanin^{122a,122b}, J. M. Keaveney^{33a}, R. Keeler¹⁷⁶, J. S. Keller³⁴, E. Kellermann⁹⁷, D. Kelsey¹⁵⁶, J. J. Kempster²¹, J. Kendrick²¹, K. E. Kennedy³⁹, O. Kepka¹⁴⁰, S. Kersten¹⁸², B. P. Kerševan⁹², S. Ketabchi Haghighat¹⁶⁷, F. Khalil-Zada¹³, M. Khandoga¹⁴⁴, A. Khanov¹²⁹, A. G. Kharlamov^{122a,122b}, T. Kharlamova^{122a,122b}, E. E. Khoda¹⁷⁵, T. J. Khoo⁷⁷, G. Khoraiuli¹⁷⁷, E. Khramov⁸⁰, J. Khubua^{159b}, S. Kido⁸³, M. Kiehn³⁶, E. Kim¹⁶⁵, Y. K. Kim³⁷, N. Kimura⁹⁵, A. Kirchhoff⁵³, D. Kirchmeier⁴⁸, J. Kirk¹⁴³, A. E. Kiryunin¹¹⁵, T. Kishimoto¹⁶³, D. P. Kisliuk¹⁶⁷, V. Kitali⁴⁶, C. Kitsaki¹⁰, O. Kivernyk²⁴, T. Klapdor-Kleingrothaus⁵², M. Klassen^{61a}, C. Klein³⁴, M. H. Klein¹⁰⁶, M. Klein⁹¹, U. Klein⁹¹, K. Kleinknecht¹⁰⁰, P. Klimek³⁶, A. Klimentov²⁹, F. Klimpel³⁶, T. Klingl²⁴, T. Klioutchnikova³⁶, F. F. Klitzner¹¹⁴, P. Kluit¹²⁰, S. Kluth¹¹⁵, E. Kneringer⁷⁷, E. B. F. G. Knoops¹⁰², A. Knue⁵², D. Kobayashi⁸⁸, M. Kobel⁴⁸, M. Kocian¹⁵³, T. Kodama¹⁶³, P. Kodys¹⁴², D. M. Koeck¹⁵⁶

P. T. Koenig²⁴, T. Koffas³⁴, N. M. Köhler³⁶, M. Kolb¹⁴⁴, I. Koletsou⁵, T. Komarek¹³⁰, T. Kondo⁸², K. Köneke⁵², A. X. Y. Kong¹, A. C. König¹¹⁹, T. Kono¹²⁶, V. Konstantinides⁹⁵, N. Konstantinidis⁹⁵, B. Konya⁹⁷, R. Kopeliansky⁶⁶, S. Koperny^{84a}, K. Korcyl⁸⁵, K. Kordas¹⁶², G. Koren¹⁶¹, A. Korn⁹⁵, I. Korolkov¹⁴, E. V. Korolkova¹⁴⁹, N. Korotkova¹¹³, O. Kortner¹¹⁵, S. Kortner¹¹⁵, V. V. Kostyukhin^{149,166}, A. Kotsokechagia⁶⁵, A. Kotwal⁴⁹, A. Koulouris¹⁰, A. Kourkoumeli-Charalampidi^{71a,71b}, C. Kourkoumelis⁹, E. Kourlitis⁶, V. Kouskoura²⁹, R. Kowalewski¹⁷⁶, W. Kozanecki¹⁰¹, A. S. Kozhin¹²³, V. A. Kramarenko¹¹³, G. Kramberger⁹², D. Krasnopevtsev^{60a}, M. W. Krasny¹³⁵, A. Krasznahorkay³⁶, D. Krauss¹¹⁵, J. A. Kremer¹⁰⁰, J. Kretzschmar⁹¹, K. Kreul¹⁹, P. Krieger¹⁶⁷, F. Krieter¹¹⁴, S. Krishnamurthy¹⁰³, A. Krishnan^{61b}, M. Krivos¹⁴², K. Krizka¹⁸, K. Kroeninger⁴⁷, H. Kroha¹¹⁵, J. Kroll¹⁴⁰, J. Kroll¹³⁶, K. S. Krowpman¹⁰⁷, U. Kruchonak⁸⁰, H. Krüger²⁴, N. Krumnack⁷⁹, M. C. Kruse⁴⁹, J. A. Krzysiak⁸⁵, A. Kubota¹⁶⁵, O. Kuchinskaia¹⁶⁶, S. Kuday^{4b}, D. Kuechler⁴⁶, J. T. Kuechler⁴⁶, S. Kuehn³⁶, T. Kuhl⁴⁶, V. Kukhtin⁸⁰, Y. Kulchitsky^{108,ae}, S. Kuleshov^{146b}, Y. P. Kulinich¹⁷³, M. Kuna⁵⁸, A. Kupco¹⁴⁰, T. Kupfer⁴⁷, O. Kuprash⁵², H. Kurashige⁸³, L. L. Kurchaninov^{168a}, Y. A. Kurochkin¹⁰⁸, A. Kurova¹¹², M. G. Kurth^{15a,15d}, E. S. Kuwertz³⁶, M. Kuze¹⁶⁵, A. K. Kvam¹⁴⁸, J. Kvita¹³⁰, T. Kwan¹⁰⁴, C. Lacasta¹⁷⁴, F. Lacava^{73a,73b}, D. P. J. Lack¹⁰¹, H. Lacker¹⁹, D. Lacour¹³⁵, E. Ladygin⁸⁰, R. Lafaye⁵, B. Laforge¹³⁵, T. Lagouri^{146c}, S. Lai⁵³, I. K. Lakomicz^{84a}, J. E. Lambert¹²⁸, S. Lammers⁶⁶, W. Lampl⁷, C. Lampoudis¹⁶², E. Lançon²⁹, U. Landgraf⁵², M. P. J. Landon⁹³, V. S. Lang⁵², J. C. Lange⁵³, R. J. Langenberg¹⁰³, A. J. Lankford¹⁷¹, F. Lanni²⁹, K. Lantzsch²⁴, A. Lanza^{71a}, A. Lapertosa^{55a,55b}, J. F. Laporte¹⁴⁴, T. Lari^{69a}, F. Lasagni Manghi^{23a,23b}, M. Lassnig³⁶, V. Latonova¹⁴⁰, T. S. Lau^{63a}, A. Laudrain¹⁰⁰, A. Laurier³⁴, M. Lavorgna^{70a,70b}, S. D. Lawlor⁹⁴, M. Lazzaroni^{69a,69b}, B. Le¹⁰¹, E. Le Guirriec¹⁰², A. Lebedev⁷⁹, M. LeBlanc⁷, T. LeCompte⁶, F. Ledroit-Guillon⁵⁸, A. C. A. Lee⁹⁵, C. A. Lee²⁹, G. R. Lee¹⁷, L. Lee⁵⁹, S. C. Lee¹⁵⁸, S. Lee⁷⁹, B. Lefebvre^{168a}, H. P. Lefebvre⁹⁴, M. Lefebvre¹⁷⁶, C. Leggett¹⁸, K. Lehmann¹⁵², N. Lehmann²⁰, G. Lehmann Miotto³⁶, W. A. Leight⁴⁶, A. Leisos^{162,v}, M. A. L. Leite^{81c}, C. E. Leitgeb¹¹⁴, R. Leitner¹⁴², K. J. C. Leney⁴², T. Lenz²⁴, S. Leone^{72a}, C. Leonidopoulos⁵⁰, A. Leopold¹³⁵, C. Leroy¹¹⁰, R. Les¹⁰⁷, C. G. Lester³², M. Levchenko¹³⁷, J. Levêque⁵, D. Levin¹⁰⁶, L. J. Levinson¹⁸⁰, D. J. Lewis²¹, B. Li^{15b}, B. Li¹⁰⁶, C-Q. Li^{60c,60d}, F. Li^{60c}, H. Li^{60a}, H. Li^{60b}, J. Li^{60c}, K. Li¹⁴⁸, L. Li^{60c}, M. Li^{15a,15d}, Q. Y. Li^{60a}, S. Li^{60d,60c,b}, X. Li⁴⁶, Y. Li⁴⁶, Z. Li^{60b}, Z. Li¹³⁴, Z. Li¹⁰⁴, Z. Li⁹¹, Z. Liang^{15a}, M. Liberatore⁴⁶, B. Liberti^{74a}, K. Lie^{63c}, S. Lim²⁹, C. Y. Lin³², K. Lin¹⁰⁷, R. A. Linck⁶⁶, R. E. Lindley⁷, J. H. Lindon²¹, A. Linss⁴⁶, A. L. Lioni⁵⁴, E. Lipeles¹³⁶, A. Lipniacka¹⁷, T. M. Liss^{173,aj}, A. Lister¹⁷⁵, J. D. Little⁸, B. Liu⁷⁹, B. X. Liu¹⁵², H. B. Liu²⁹, J. B. Liu^{60a}, J. K. K. Liu³⁷, K. Liu^{60d,60c}, M. Liu^{60a}, M. Y. Liu^{60a}, P. Liu^{15a}, X. Liu^{60a}, Y. Liu⁴⁶, Y. Liu^{15a,15d}, Y. L. Liu¹⁰⁶, Y. W. Liu^{60a}, M. Livan^{71a,71b}, A. Lleres⁵⁸, J. Llorente Merino¹⁵², S. L. Lloyd⁹³, C. Y. Lo^{63b}, E. M. Lobodzinska⁴⁶, P. Loch⁷, S. Loffredo^{74a,74b}, T. Lohse¹⁹, K. Lohwasser¹⁴⁹, M. Lokajicek¹⁴⁰, J. D. Long¹⁷³, R. E. Long⁹⁰, I. Longarini^{73a,73b}, L. Longo³⁶, I. Lopez Paz¹⁰¹, A. Lopez Solis¹⁴⁹, J. Lorenz¹¹⁴, N. Lorenzo Martinez⁵, A. M. Lory¹¹⁴, A. Lösle⁵², X. Lou^{45a,45b}, X. Lou^{15a}, A. Lounis⁶⁵, J. Love⁶, P. A. Love⁹⁰, J. J. Lozano Bahilo¹⁷⁴, M. Lu^{60a}, Y. J. Lu⁶⁴, H. J. Lubatti¹⁴⁸, C. Luci^{73a,73b}, F. L. Lucio Alves^{15c}, A. Lucotte⁵⁸, F. Luehring⁶⁶, I. Luise¹⁵⁵, L. Luminari^{73a}, B. Lund-Jensen¹⁵⁴, N. A. Luongo¹³¹, M. S. Lutz¹⁶¹, D. Lynn²⁹, H. Lyons⁹¹, R. Lysak¹⁴⁰, E. Lytken⁹⁷, F. Lyu^{15a}, V. Lyubushkin⁸⁰, T. Lyubushkina⁸⁰, H. Ma²⁹, L. L. Ma^{60b}, Y. Ma⁹⁵, D. M. Mac Donnell¹⁷⁶, G. Maccarrone⁵¹, C. M. Macdonald¹⁴⁹, J. C. MacDonald¹⁴⁹, J. Machado Miguens¹³⁶, R. Madar³⁸, W. F. Mader⁴⁸, M. Madugoda Ralalage Don¹²⁹, N. Madysa⁴⁸, J. Maeda⁸³, T. Maeno²⁹, M. Maerker⁴⁸, V. Magerl⁵², N. Magini⁷⁹, J. Magro^{67a,67c,r}, D. J. Mahon³⁹, C. Maidantchik^{81b}, A. Maio^{139a,139b,139d}, K. Maj^{84a}, O. Majersky^{28a}, S. Majewski¹³¹, Y. Makida⁸², N. Makovec⁶⁵, B. Malaescu¹³⁵, Pa. Malecki⁸⁵, V. P. Maleev¹³⁷, F. Malek⁵⁸, D. Malito^{41a,41b}, U. Mallik⁷⁸, C. Malone³², S. Maltezos¹⁰, S. Malyukov⁸⁰, J. Mamuzic¹⁷⁴, G. Mancini⁵¹, J. P. Mandalia⁹³, I. Mandić⁹², L. Manhaes de Andrade Filho^{81a}, I. M. Maniatis¹⁶², J. Manjarres Ramos⁴⁸, K. H. Mankinen⁹⁷, A. Mann¹¹⁴, A. Manousos⁷⁷, B. Mansoulie¹⁴⁴, I. Manthos¹⁶², S. Manzoni¹²⁰, A. Marantis¹⁶², G. Marceca³⁰, L. Marchese¹³⁴, G. Marchiori¹³⁵, M. Marcisovsky¹⁴⁰, L. Marcoccia^{74a,74b}, C. Marcon⁹⁷, M. Marjanovic¹²⁸, Z. Marshall¹⁸, M. U. F. Martensson¹⁷², S. Marti-Garcia¹⁷⁴, C. B. Martin¹²⁷, T. A. Martin¹⁷⁸, V. J. Martin⁵⁰, B. Martin dit Latour¹⁷, L. Martinelli^{75a,75b}, M. Martinez^{14,w}, P. Martinez Agullo¹⁷⁴, V. I. Martinez Outschoorn¹⁰³, S. Martin-Haugh¹⁴³, V. S. Martoiu^{27b}, A. C. Martyniuk⁹⁵, A. Marzin³⁶, S. R. Maschek¹¹⁵, L. Masetti¹⁰⁰, T. Mashimo¹⁶³, R. Mashinistov¹¹¹, J. Masik¹⁰¹, A. L. Maslennikov^{122a,122b}, L. Massa^{23a,23b}, P. Massarotti^{70a,70b}, P. Mastrandrea^{72a,72b}, A. Mastroberardino^{41a,41b}, T. Masubuchi¹⁶³, D. Matakias²⁹, A. Matic¹¹⁴, N. Matsuzawa¹⁶³, P. Mättig²⁴, J. Maurer^{27b}, B. Maček⁹², D. A. Maximov^{122a,122b}

R. Mazini¹⁵⁸, I. Maznas¹⁶², S. M. Mazza¹⁴⁵, J. P. Mc Gowan¹⁰⁴, S. P. Mc Kee¹⁰⁶, T. G. McCarthy¹¹⁵, W. P. McCormack¹⁸, E. F. McDonald¹⁰⁵, A. E. McDougall¹²⁰, J. A. Mcfayden¹⁸, G. Mchedlidze^{159b}, M. A. McKay⁴², K. D. McLean¹⁷⁶, S. J. McMahon¹⁴³, P. C. McNamara¹⁰⁵, C. J. McNicol¹⁷⁸, R. A. McPherson^{176,aa}, J. E. Mdhluhi^{33e}, Z. A. Meadows¹⁰³, S. Meehan³⁶, T. Megy³⁸, S. Mehlhase¹¹⁴, A. Mehta⁹¹, B. Meirose⁴³, D. Melini¹⁶⁰, B. R. Mellado Garcia^{33e}, J. D. Mellenthin⁵³, M. Melo^{28a}, F. Meloni⁴⁶, A. Melzer²⁴, E. D. Mendes Gouveia^{139a,139e}, A. M. Mendes Jacques Da Costa²¹, H. Y. Meng¹⁶⁷, L. Meng³⁶, X. T. Meng¹⁰⁶, S. Menke¹¹⁵, E. Meoni^{41a,41b}, S. Mergelmeyer¹⁹, S. A. M. Merkt¹³⁸, C. Merlassino¹³⁴, P. Mermod⁵⁴, L. Merola^{70a,70b}, C. Meroni^{69a}, G. Merz¹⁰⁶, O. Meshkov^{113,111}, J. K. R. Meshreki¹⁵¹, J. Metcalfe⁶, A. S. Mete⁶, C. Meyer⁶⁶, J.-P. Meyer¹⁴⁴, M. Michetti¹⁹, R. P. Middleton¹⁴³, L. Mijović⁵⁰, G. Mikenberg¹⁸⁰, M. Mikesstikova¹⁴⁰, M. Mikuz⁹², H. Mildner¹⁴⁹, A. Milic¹⁶⁷, C. D. Milke⁴², D. W. Miller³⁷, L. S. Miller³⁴, A. Milov¹⁸⁰, D. A. Milstead^{45a,45b}, A. A. Minaenko¹²³, I. A. Minashvili^{159b}, L. Mince⁵⁷, A. I. Mincer¹²⁵, B. Mindur^{84a}, M. Mineev⁸⁰, Y. Minegishi¹⁶³, Y. Mino⁸⁶, L. M. Mir¹⁴, M. Mironova¹³⁴, T. Mitani¹⁷⁹, J. Mitrevski¹¹⁴, V. A. Mitsou¹⁷⁴, M. Mittal^{60c}, O. Miu¹⁶⁷, A. Miucci²⁰, P. S. Miyagawa⁹³, A. Mizukami⁸², J. U. Mjörnmark⁹⁷, T. Mkrtychyan^{61a}, M. Mlynarikova¹²¹, T. Moa^{45a,45b}, S. Mobius⁵³, K. Mochizuki¹¹⁰, P. Moder⁴⁶, P. Mogg¹¹⁴, S. Mohapatra³⁹, R. Moles-Valls²⁴, K. Mönig⁴⁶, E. Monnier¹⁰², A. Montalbano¹⁵², J. Montejo Berlingen³⁶, M. Montella⁹⁵, F. Monticelli⁸⁹, S. Monzani^{69a}, N. Morange⁶⁵, A. L. Moreira De Carvalho^{139a}, D. Moreno^{22a}, M. Moreno Llácer¹⁷⁴, C. Moreno Martinez¹⁴, P. Morettini^{55b}, M. Morgenstern¹⁶⁰, S. Morgenstern⁴⁸, D. Mori¹⁵², M. Morii⁵⁹, M. Morinaga¹⁷⁹, V. Morisbak¹³³, A. K. Morley³⁶, G. Mornacchi³⁶, A. P. Morris⁹⁵, L. Morvaj³⁶, P. Moschovakos³⁶, B. Moser¹²⁰, M. Mosidze^{159b}, T. Moskalets¹⁴⁴, P. Moskvitina¹¹⁹, J. Moss^{31,n}, E. J. W. Moyse¹⁰³, S. Muanza¹⁰², J. Mueller¹³⁸, R. S. P. Mueller¹¹⁴, D. Muenstermann⁹⁰, G. A. Mullier⁹⁷, D. P. Mungo^{69a,69b}, J. L. Munoz Martinez¹⁴, F. J. Munoz Sanchez¹⁰¹, P. Murin^{28b}, W. J. Murray^{178,143}, A. Murrone^{69a,69b}, J. M. Muse¹²⁸, M. Muškinja¹⁸, C. Mwewa^{33a}, A. G. Myagkov^{123,af}, A. A. Myers¹³⁸, G. Myers⁶⁶, J. Myers¹³¹, M. Myska¹⁴¹, B. P. Nachman¹⁸, O. Nackenhorst⁴⁷, A. Nag Nag⁴⁸, K. Nagai¹³⁴, K. Nagano⁸², Y. Nagasaka⁶², J. L. Nagle²⁹, E. Nagy¹⁰², A. M. Nairz³⁶, Y. Nakahama¹¹⁷, K. Nakamura⁸², T. Nakamura¹⁶³, H. Nanjo¹³², F. Napolitano^{61a}, R. F. Naranjo Garcia⁴⁶, R. Narayan⁴², I. Naryshkin¹³⁷, M. Naseri³⁴, T. Naumann⁴⁶, G. Navarro^{22a}, P. Y. Nechaeva¹¹¹, F. Nechansky⁴⁶, T. J. Neep²¹, A. Negri^{71a,71b}, M. Negrini^{23b}, C. Nellist¹¹⁹, C. Nelson¹⁰⁴, M. E. Nelson^{45a,45b}, S. Nemecek¹⁴⁰, M. Nessi^{36,f}, M. S. Neubauer¹⁷³, F. Neuhaus¹⁰⁰, M. Neumann¹⁸², R. Newhouse¹⁷⁵, P. R. Newman²¹, C. W. Ng¹³⁸, Y. S. Ng¹⁹, Y. W. Y. Ng¹⁷¹, B. Ngair^{35f}, H. D. N. Nguyen¹⁰², T. Nguyen Manh¹¹⁰, E. Nibigira³⁸, R. B. Nickerson¹³⁴, R. Nicolaidou¹⁴⁴, D. S. Nielsen⁴⁰, J. Nielsen¹⁴⁵, M. Niemeyer⁵³, N. Nikiforou¹¹, V. Nikolaenko^{123,af}, I. Nikolic-Audit¹³⁵, K. Nikolopoulos²¹, P. Nilsson²⁹, H. R. Nindhito⁵⁴, A. Nisati^{73a}, N. Nishu^{60c}, R. Nisius¹¹⁵, I. Nitsche⁴⁷, T. Nitta¹⁷⁹, T. Nobe¹⁶³, D. L. Noel³², Y. Noguchi⁸⁶, I. Nomidis¹³⁵, M. A. Nomura²⁹, M. Nordberg³⁶, J. Novak⁹², T. Novak⁹², O. Novgorodova⁴⁸, R. Novotny¹¹⁸, L. Nozka¹³⁰, K. Ntekas¹⁷¹, E. Nurse⁹⁵, F. G. Oakham^{34,ak}, J. Ocariz¹³⁵, A. Ochi⁸³, I. Ochoa^{139a}, J. P. Ochoa-Ricoux^{146a}, K. O'Connor²⁶, S. Oda⁸⁸, S. Odaka⁸², S. Oerdek⁵³, A. Ogrodnik^{84a}, A. Oh¹⁰¹, C. C. Ohm¹⁵⁴, H. Oide¹⁶⁵, R. Oishi¹⁶³, M. L. Ojeda¹⁶⁷, H. Okawa¹⁶⁹, Y. Okazaki⁸⁶, M. W. O'Keefe⁹¹, Y. Okumura¹⁶³, A. Olariu^{27b}, L. F. Oleiro Seabra^{139a}, S. A. Olivares Pino^{146a}, D. Oliveira Damazio²⁹, J. L. Oliver¹, M. J. R. Olsson¹⁷¹, A. Olszewski⁸⁵, J. Olszowska⁸⁵, Ö.O. Öncel²⁴, D. C. O'Neil¹⁵², A. P. O'Neill¹³⁴, A. Onofre^{139a,139e}, P. U. E. Onyisi¹¹, H. Oppen¹³³, R. G. Oreamuno Madriz¹²¹, M. J. Oreglia³⁷, G. E. Orellana⁸⁹, D. Orestano^{75a,75b}, N. Orlando¹⁴, R. S. Orr¹⁶⁷, V. O'Shea⁵⁷, R. Ospanov^{60a}, G. Otero y Garzon³⁰, H. Otono⁸⁸, P. S. Ott^{61a}, G. J. Ottino¹⁸, M. Ouchrif^{35e}, J. Ouellette²⁹, F. Ould-Saada¹³³, A. Ouraou^{144,*}, Q. Ouyang^{15a}, M. Owen⁵⁷, R. E. Owen¹⁴³, V. E. Ozcan^{12c}, N. Ozturk⁸, J. Pacalt¹³⁰, H. A. Pacey³², K. Pachal⁴⁹, A. Pacheco Pages¹⁴, C. Padilla Aranda¹⁴, S. Pagan Griso¹⁸, G. Palacino⁶⁶, S. Palazzo⁵⁰, S. Palestini³⁶, M. Palka^{84b}, P. Palni^{84a}, C. E. Pandini⁵⁴, J. G. Panduro Vazquez⁹⁴, P. Pani⁴⁶, G. Panizzo^{67a,67c}, L. Paolozzi⁵⁴, C. Papadatos¹¹⁰, K. Papageorgiou^{9,h}, S. Parajuli⁴², A. Paramonov⁶, C. Paraskevopoulos¹⁰, D. Paredes Hernandez^{63b}, S. R. Paredes Saenz¹³⁴, B. Parida¹⁸⁰, T. H. Park¹⁶⁷, A. J. Parker³¹, M. A. Parker³², F. Parodi^{55a,55b}, E. W. Parrish¹²¹, J. A. Parsons³⁹, U. Parzefall⁵², L. Pascual Dominguez¹³⁵, V. R. Pascuzzi¹⁸, J. M. P. Pasner¹⁴⁵, F. Pasquali¹²⁰, E. Pasqualucci^{73a}, S. Passaggio^{55b}, F. Pastore⁹⁴, P. Pasuwan^{45a,45b}, S. Patariaia¹⁰⁰, J. R. Pater¹⁰¹, A. Pathak^{181,j}, J. Patton⁹¹, T. Pauly³⁶, J. Parkes¹⁵³, M. Pedersen¹³³, L. Pedraza Diaz¹¹⁹, R. Pedro^{139a}, T. Peiffer⁵³, S. V. Peleganchuk^{122a,122b}, O. Penc¹⁴⁰, C. Peng^{63b}, H. Peng^{60a}, B. S. Peralva^{81a}, M. M. Perego⁶⁵, A. P. Pereira Peixoto^{139a}, L. Pereira Sanchez^{45a,45b}, D. V. Perreletisa²⁹, E. Perez Codina^{168a}, L. Perini^{69a,69b}, H. Pernegger³⁶, S. Perrella³⁶, A. Perrevoort¹²⁰

K. Peters⁴⁶, R. F. Y. Peters¹⁰¹, B. A. Petersen³⁶, T. C. Petersen⁴⁰, E. Petit¹⁰², V. Petousis¹⁴¹, C. Petridou¹⁶², F. Petrucci^{75a,75b}, M. Pettee¹⁸³, N. E. Pettersson¹⁰³, K. Petukhova¹⁴², A. Peyaud¹⁴⁴, R. Pezoa^{146d}, L. Pezzotti^{71a,71b}, T. Pham¹⁰⁵, P. W. Phillips¹⁴³, M. W. Phipps¹⁷³, G. Piacquadio¹⁵⁵, E. Pianori¹⁸, A. Picazio¹⁰³, R. H. Pickles¹⁰¹, R. Piegaia³⁰, D. Pietreanu^{27b}, J. E. Pilcher³⁷, A. D. Pilkington¹⁰¹, M. Pinamonti^{67a,67c}, J. L. Pinfold³, C. Pitman Donaldson⁹⁵, M. Pitt¹⁶¹, L. Pizzimento^{74a,74b}, A. Pizzini¹²⁰, M.-A. Pleier²⁹, V. Plesanovs⁵², V. Pleskot¹⁴², E. Plotnikova⁸⁰, P. Podberczko^{122a,122b}, R. Poettgen⁹⁷, R. Poggi⁵⁴, L. Poggioli¹³⁵, I. Pogrebnyak¹⁰⁷, D. Pohl²⁴, I. Pokharel⁵³, G. Polesello^{71a}, A. Poley^{152,168a}, A. Policicchio^{73a,73b}, R. Polifka¹⁴², A. Polini^{23b}, C. S. Pollard⁴⁶, V. Polychronakos²⁹, D. Ponomarenko¹¹², L. Pontecorvo³⁶, S. Popa^{27a}, G. A. Popeneciu^{27d}, L. Portales⁵, D. M. Portillo Quintero⁵⁸, S. Pospisil¹⁴¹, K. Potamianos⁴⁶, I. N. Potrap⁸⁰, C. J. Potter³², H. Potti¹¹, T. Poulsen⁹⁷, J. Poveda¹⁷⁴, T. D. Powell¹⁴⁹, G. Pownall⁴⁶, M. E. Pozo Astigarraga³⁶, A. Prades Ibanez¹⁷⁴, P. Pralavorio¹⁰², M. M. Prapa⁴⁴, S. Prell⁷⁹, D. Price¹⁰¹, M. Primavera^{68a}, M. L. Proffitt¹⁴⁸, N. Proklova¹¹², K. Prokofiev^{63c}, F. Prokoshin⁸⁰, S. Protopopescu²⁹, J. Proudfoot⁶, M. Przybycien^{84a}, D. Pudzha¹³⁷, A. Puri¹⁷³, P. Puzo⁶⁵, D. Pyatiizbyantseva¹¹², J. Qian¹⁰⁶, Y. Qin¹⁰¹, A. Quadt⁵³, M. Queitsch-Maitland³⁶, G. Rabanal Bolanos⁵⁹, M. Racko^{28a}, F. Ragusa^{69a,69b}, G. Rahal⁹⁸, J. A. Raine⁵⁴, S. Rajagopalan²⁹, A. Ramirez Morales⁹³, K. Ran^{15a,15d}, D. F. Rassloff^{61a}, D. M. Rauch⁴⁶, F. Rauscher¹¹⁴, S. Rave¹⁰⁰, B. Ravina⁵⁷, I. Ravinovich¹⁸⁰, J. H. Rawling¹⁰¹, M. Raymond³⁶, A. L. Read¹³³, N. P. Readioff¹⁴⁹, M. Reale^{68a,68b}, D. M. Rebuffi^{71a,71b}, G. Redlinger²⁹, K. Reeves⁴³, D. Reikher¹⁶¹, A. Reiss¹⁰⁰, A. Rej¹⁵¹, C. Rembser³⁶, A. Renardi⁴⁶, M. Renda^{27b}, M. B. Rendel¹¹⁵, A. G. Rennie⁵⁷, S. Resconi^{69a}, E. D. Resseguie¹⁸, S. Rettie⁹⁵, B. Reynolds¹²⁷, E. Reynolds²¹, O. L. Rezanova^{122a,122b}, P. Reznicek¹⁴², E. Ricci^{76a,76b}, R. Richter¹¹⁵, S. Richter⁴⁶, E. Richter-Was^{84b}, M. Ridel¹³⁵, P. Rieck¹¹⁵, O. Rifki⁴⁶, M. Rijssenbeek¹⁵⁵, A. Rimoldi^{71a,71b}, M. Rimoldi⁴⁶, L. Rinaldi^{23b}, T. T. Rinn¹⁷³, G. Ripellino¹⁵⁴, I. Riu¹⁴, P. Rivadeneira⁴⁶, J. C. Rivera Vergara¹⁷⁶, F. Rizatdinova¹²⁹, E. Rizvi⁹³, C. Rizzi³⁶, S. H. Robertson^{104,aa}, M. Robin⁴⁶, D. Robinson³², C. M. Robles Gajardo^{146d}, M. Robles Manzano¹⁰⁰, A. Robson⁵⁷, A. Rocchi^{74a,74b}, C. Roda^{72a,72b}, S. Rodriguez Bosca¹⁷⁴, A. Rodriguez Rodriguez⁵², A. M. Rodríguez Vera^{168b}, S. Roe³⁶, J. Roggel¹⁸², O. Røhne¹³³, R. Röhrig¹¹⁵, R. A. Rojas^{146d}, B. Roland⁵², C. P. A. Roland⁶⁶, J. Roloff²⁹, A. Romaniouk¹¹², M. Romano^{23a,23b}, N. Rompotis⁹¹, M. Ronzani¹²⁵, L. Roos¹³⁵, S. Rosati^{73a}, G. Rosin¹⁰³, B. J. Rosser¹³⁶, E. Rossi⁴⁶, E. Rossi^{75a,75b}, E. Rossi^{70a,70b}, L. P. Rossi^{55b}, L. Rossini⁴⁶, R. Rosten¹⁴, M. Rotaru^{27b}, B. Rottler⁵², D. Rousseau⁶⁵, G. Rovelli^{71a,71b}, A. Roy¹¹, D. Roy^{33c}, A. Rozanov¹⁰², Y. Rozen¹⁶⁰, X. Ruan^{33e}, T. A. Ruggeri¹, F. Rühr⁵², A. Ruiz-Martinez¹⁷⁴, A. Rummler³⁶, Z. Rurikova⁵², N. A. Rusakovich⁸⁰, H. L. Russell¹⁰⁴, L. Rustige^{38,47}, J. P. Rutherford⁷, E. M. Rüttinger¹⁴⁹, M. Rybar¹⁴², G. Rybkin⁶⁵, E. B. Rye¹³³, A. Ryzhov¹²³, J. A. Sabater Iglesias⁴⁶, P. Sabatini¹⁷⁴, L. Sabetta^{73a,73b}, S. Sacerdoti⁶⁵, H.F.-W. Sadrozinski¹⁴⁵, R. Sadykov⁸⁰, F. Safai Tehrani^{73a}, B. Safarzadeh Samani¹⁵⁶, M. Safdari¹⁵³, P. Saha¹²¹, S. Saha¹⁰⁴, M. Sahinsoy¹¹⁵, A. Sahu¹⁸², M. Saimpert³⁶, M. Saito¹⁶³, T. Saito¹⁶³, H. Sakamoto¹⁶³, D. Salamani⁵⁴, G. Salamanna^{75a,75b}, A. Salnikov¹⁵³, J. Salt¹⁷⁴, A. Salvador Salas¹⁴, D. Salvatore^{41a,41b}, F. Salvatore¹⁵⁶, A. Salvucci^{63a}, A. Salzburger³⁶, J. Samarati³⁶, D. Sammel⁵², D. Sampsonidis¹⁶², D. Sampsonidou^{60d,60c}, J. Sánchez¹⁷⁴, A. Sanchez Pineda^{67a,36,67c}, H. Sandaker¹³³, C. O. Sander⁴⁶, I. G. Sanderswood⁹⁰, M. Sandhoff¹⁸², C. Sandoval^{22b}, D. P. C. Sankey¹⁴³, M. Sannino^{55a,55b}, Y. Sano¹¹⁷, A. Sansoni⁵¹, C. Santoni³⁸, H. Santos^{139a,139b}, S. N. Santpur¹⁸, A. Santra¹⁷⁴, K. A. Saoucha¹⁴⁹, A. Sapronov⁸⁰, J. G. Saraiva^{139a,139d}, O. Sasaki⁸², K. Sato¹⁶⁹, F. Sauerburger⁵², E. Sauvan⁵, P. Savard^{167,ak}, R. Sawada¹⁶³, C. Sawyer¹⁴³, L. Sawyer⁹⁶, I. Sayago Galvan¹⁷⁴, C. Sbarra^{23b}, A. Sbrizzi^{67a,67c}, T. Scanlon⁹⁵, J. Schaarschmidt¹⁴⁸, P. Schacht¹¹⁵, D. Schaefer³⁷, L. Schaefer¹³⁶, U. Schäfer¹⁰⁰, A. C. Schaffer⁶⁵, D. Schaile¹¹⁴, R. D. Schamberger¹⁵⁵, E. Schanel¹¹⁴, C. Scharf¹⁹, N. Scharmberg¹⁰¹, V. A. Schegelsky¹³⁷, D. Scheirich¹⁴², F. Schenck¹⁹, M. Schernau¹⁷¹, C. Schiavi^{55a,55b}, L. K. Schildgen²⁴, Z. M. Schillaci²⁶, E. J. Schioppa^{68a,68b}, M. Schioppa^{41a,41b}, K. E. Schleicher⁵², S. Schlenker³⁶, K. R. Schmidt-Sommerfeld¹¹⁵, K. Schmieden¹⁰⁰, C. Schmitt¹⁰⁰, S. Schmitt⁴⁶, L. Schoeffel¹⁴⁴, A. Schoening^{61b}, P. G. Scholer⁵², E. Schopf¹³⁴, M. Schott¹⁰⁰, J. F. P. Schouwenberg¹¹⁹, J. Schovancova³⁶, S. Schramm⁵⁴, F. Schroeder¹⁸², A. Schulte¹⁰⁰, H.-C. Schultz-Coulon^{61a}, M. Schumacher⁵², B. A. Schumm¹⁴⁵, Ph. Schune¹⁴⁴, A. Schwartzman¹⁵³, T. A. Schwarz¹⁰⁶, Ph. Schwemling¹⁴⁴, R. Schwienhorst¹⁰⁷, A. Sciandra¹⁴⁵, G. Sciolla²⁶, F. Scuri^{72a}, F. Scutti¹⁰⁵, L. M. Scyboz¹¹⁵, C. D. Sebastiani⁹¹, K. Sedlaczek⁴⁷, P. Seema¹⁹, S. C. Seidel¹¹⁸, A. Seiden¹⁴⁵, B. D. Seidlitz²⁹, T. Seiss³⁷, C. Seitz⁴⁶, J. M. Seixas^{81b}, G. Sekhniaidze^{70a}, S. J. Sekula⁴², N. Semprini-Cesari^{23a,23b}, S. Sen⁴⁹, C. Serfon²⁹, L. Serin⁶⁵, L. Serkin^{67a,67b}, M. Sessa^{60a}, H. Severini¹²⁸, S. Sevova¹⁵³, F. Sforza^{55a,55b}, A. Sfyrta⁵⁴, E. Shabalina⁵³, J. D. Shahinian¹³⁶, N. W. Shaikh^{45a,45b}

D. Shaked Renous¹⁸⁰, L. Y. Shan^{15a}, M. Shapiro¹⁸, A. Sharma³⁶, A. S. Sharma¹, P. B. Shatalov¹²⁴, K. Shaw¹⁵⁶, S. M. Shaw¹⁰¹, M. Shehade¹⁸⁰, Y. Shen¹²⁸, A. D. Sherman²⁵, P. Sherwood⁹⁵, L. Shi⁹⁵, C. O. Shimmin¹⁸³, Y. Shimogama¹⁷⁹, M. Shimojima¹¹⁶, J. D. Shinner⁹⁴, I. P. J. Shipsey¹³⁴, S. Shirabe¹⁶⁵, M. Shiyakova^{80.y}, J. Shlomi¹⁸⁰, A. Shmeleva¹¹¹, M. J. Shochet³⁷, J. Shojaii¹⁰⁵, D. R. Shope¹⁵⁴, S. Shrestha¹²⁷, E. M. Shrif^{33e}, M. J. Shroff¹⁷⁶, E. Shulga¹⁸⁰, P. Sicho¹⁴⁰, A. M. Sickles¹⁷³, E. Sideras Haddad^{33e}, O. Sidiropoulou³⁶, A. Sidoti^{23a,23b}, F. Siegert⁴⁸, Dj. Sijacki¹⁶, M. Jr. Silva¹⁸¹, M. V. Silva Oliveira³⁶, S. B. Silverstein^{45a}, S. Simion⁶⁵, R. Simoniello¹⁰⁰, C. J. Simpson-allsoy²¹, S. Simsek^{12b}, P. Sinervo¹⁶⁷, V. Sinetckii¹¹³, S. Singh¹⁵², S. Sinha^{33e}, M. Sioli^{23a,23b}, I. Siral¹³¹, S. Yu. Sivoklov¹¹³, J. Sjölin^{45a,45b}, A. Skaf⁵³, E. Skorda⁹⁷, P. Skubic¹²⁸, M. Slawinska⁸⁵, K. Sliwa¹⁷⁰, V. Smakhtin¹⁸⁰, B. H. Smart¹⁴³, J. Smiesko^{28b}, N. Smirnov¹¹², S. Yu. Smirnov¹¹², Y. Smirnov¹¹², L. N. Smirnova^{113.s}, O. Smirnova⁹⁷, E. A. Smith³⁷, H. A. Smith¹³⁴, M. Smizanska⁹⁰, K. Smolek¹⁴¹, A. Smykiewicz⁸⁵, A. A. Snesarev¹¹¹, H. L. Snoek¹²⁰, I. M. Snyder¹³¹, S. Snyder²⁹, R. Sobie^{176,aa}, A. Soffer¹⁶¹, A. Sogaard⁵⁰, F. Sohns⁵³, C. A. Solans Sanchez³⁶, E. Yu. Soldatov¹¹², U. Soldevila¹⁷⁴, A. A. Solodkov¹²³, A. Soloshenko⁸⁰, O. V. Solovyanov¹²³, V. Solovyev¹³⁷, P. Sommer¹⁴⁹, H. Son¹⁷⁰, A. Sonay¹⁴, W. Song¹⁴³, W. Y. Song^{168b}, A. Sopczak¹⁴¹, A. L. Sopio⁹⁵, F. Sopkova^{28b}, S. Sottocornola^{71a,71b}, R. Soualah^{67a,67c}, A. M. Soukharev^{122a,122b}, D. South⁴⁶, S. Spagnolo^{68a,68b}, M. Spalla¹¹⁵, M. Spangenberg¹⁷⁸, F. Spanò⁹⁴, D. Sperlich⁵², T. M. Spieker^{61a}, G. Spigo³⁶, M. Spina¹⁵⁶, D. P. Spiteri⁵⁷, M. Spousta¹⁴², A. Stabile^{69a,69b}, B. L. Stamas¹²¹, R. Stamen^{61a}, M. Stamenkovic¹²⁰, A. Stampeki²¹, E. Stanecka⁸⁵, B. Stanislaus¹³⁴, M. M. Stanitzki⁴⁶, M. Stankaityte¹³⁴, B. Stapf¹²⁰, E. A. Starchenko¹²³, G. H. Stark¹⁴⁵, J. Stark⁵⁸, P. Staroba¹⁴⁰, P. Starovoitov^{61a}, S. Stärz¹⁰⁴, R. Staszewski⁸⁵, G. Stavropoulos⁴⁴, M. Stegler⁴⁶, P. Steinberg²⁹, A. L. Steinhebel¹³¹, B. Stelzer^{152,168a}, H. J. Stelzer¹³⁸, O. Stelzer-Chilton^{168a}, H. Stenzel⁵⁶, T. J. Stevenson¹⁵⁶, G. A. Stewart³⁶, M. C. Stockton³⁶, G. Stoicea^{27b}, M. Stolarski^{139a}, S. Stonjek¹¹⁵, A. Straessner⁴⁸, J. Strandberg¹⁵⁴, S. Strandberg^{45a,45b}, M. Strauss¹²⁸, T. Streblner¹⁰², P. Strizenec^{28b}, R. Ströhmer¹⁷⁷, D. M. Strom¹³¹, R. Stroynowski⁴², A. Strubig^{45a,45b}, S. A. Stucci²⁹, B. Stugu¹⁷, J. Stupak¹²⁸, N. A. Styles⁴⁶, D. Su¹⁵³, W. Su^{60d,148,60c}, X. Su^{60a}, N. B. Suarez¹³⁸, V. V. Sulini¹¹¹, M. J. Sullivan⁹¹, D. M. S. Sultan⁵⁴, S. Sultansoy^{4c}, T. Sumida⁸⁶, S. Sun¹⁰⁶, X. Sun¹⁰¹, C. J. E. Suster¹⁵⁷, M. R. Sutton¹⁵⁶, S. Suzuki⁸², M. Svatos¹⁴⁰, M. Swiatlowski^{168a}, S. P. Swift², T. Swirski¹⁷⁷, A. Sydorenko¹⁰⁰, I. Sykora^{28a}, M. Sykora¹⁴², T. Sykora¹⁴², D. Ta¹⁰⁰, K. Tackmann^{46,x}, J. Taenzer¹⁶¹, A. Taffard¹⁷¹, R. Tafirout^{168a}, E. Tagiev¹²³, R. H. M. Taibah¹³⁵, R. Takashima⁸⁷, K. Takeda⁸³, T. Takeshita¹⁵⁰, E. P. Takeva⁵⁰, Y. Takubo⁸², M. Talby¹⁰², A. A. Talyshev^{122a,122b}, K. C. Tam^{63b}, N. M. Tamir¹⁶¹, J. Tanaka¹⁶³, R. Tanaka⁶⁵, S. Tapia Araya¹⁷³, S. Tapprogge¹⁰⁰, A. Tarek Abouelfadl Mohamed¹⁰⁷, S. Tarem¹⁶⁰, K. Tariq^{60b}, G. Tarna^{27b,c}, G. F. Tartarelli^{69a}, P. Tas¹⁴², M. Tasevsky¹⁴⁰, E. Tassi^{41a,41b}, G. Tateno¹⁶³, A. Tavares Delgado^{139a}, Y. Tayalati^{35f}, A. J. Taylor⁵⁰, G. N. Taylor¹⁰⁵, W. Taylor^{168b}, H. Teagle⁹¹, A. S. Tee⁹⁰, R. Teixeira De Lima¹⁵³, P. Teixeira-Dias⁹⁴, H. Ten Kate³⁶, J. J. Teoh¹²⁰, K. Terashi¹⁶³, J. Terron⁹⁹, S. Terzo¹⁴, M. Testa⁵¹, R. J. Teuscher^{167,aa}, N. Themistokleous⁵⁰, T. Thevenaux-Pelzer¹⁹, D. W. Thomas⁹⁴, J. P. Thomas²¹, E. A. Thompson⁴⁶, P. D. Thompson²¹, E. Thomson¹³⁶, E. J. Thorpe⁹³, V. O. Tikhomirov^{111,ag}, Yu. A. Tikhonov^{122a,122b}, S. Timoshenko¹¹², P. Tipton¹⁸³, S. Tisserant¹⁰², K. Todome^{23a,23b}, S. Todorova-Nova¹⁴², S. Todt⁴⁸, J. Tojo⁸⁸, S. Tokár^{28a}, K. Tokushuku⁸², E. Tolley¹²⁷, R. Tombs³², K. G. Tomiwa^{33e}, M. Tomoto^{82,117}, L. Tompkins¹⁵³, P. Tornambe¹⁰³, E. Torrence¹³¹, H. Torres⁴⁸, E. Torró Pastor¹⁷⁴, M. Toscani³⁰, C. Toscini¹³⁴, J. Toth^{102,z}, D. R. Tovey¹⁴⁹, A. Traet¹⁷, C. J. Treado¹²⁵, T. Trefzger¹⁷⁷, F. Tresoldi¹⁵⁶, A. Tricoli²⁹, I. M. Trigger^{168a}, S. Trincaz-Duvoid¹³⁵, D. A. Trischuk¹⁷⁵, W. Trischuk¹⁶⁷, B. Trocmé⁵⁸, A. Trofymov⁶⁵, C. Troncon^{69a}, F. Trovato¹⁵⁶, L. Truong^{33c}, M. Trzebinski⁸⁵, A. Trzupek⁸⁵, F. Tsai⁴⁶, P. V. Tsiarehka^{108,ae}, A. Tsirigotis^{162,v}, V. Tsiskaridze¹⁵⁵, E. G. Tskhadadze^{159a}, M. Tsopoulou¹⁶², I. I. Tsukerman¹²⁴, V. Tsulaia¹⁸, S. Tsuno⁸², D. Tsybychev¹⁵⁵, Y. Tu^{63b}, A. Tudorache^{27b}, V. Tudorache^{27b}, A. N. Tuna³⁶, S. Turchikhin⁸⁰, D. Turgeman¹⁸⁰, I. Turk Cakir^{4b,t}, R. J. Turner²¹, R. Turra^{69a}, P. M. Tuts³⁹, S. Tzamarias¹⁶², E. Tzovara¹⁰⁰, K. Uchida¹⁶³, F. Ukegawa¹⁶⁹, G. Unal³⁶, M. Unal¹¹, A. Undrus²⁹, G. Unel¹⁷¹, F. C. Ungaro¹⁰⁵, Y. Unno⁸², K. Uno¹⁶³, J. Urban^{28b}, P. Urquijo¹⁰⁵, G. Usai⁸, Z. Uysal^{12d}, V. Vacek¹⁴¹, B. Vachon¹⁰⁴, K. O. H. Vadla¹³³, T. Vafeiadis³⁶, A. Vaidya⁹⁵, C. Valderanis¹¹⁴, E. Valdes Santurio^{45a,45b}, M. Valente^{168a}, S. Valentinetti^{23a,23b}, A. Valero¹⁷⁴, L. Valéry⁴⁶, R. A. Vallance²¹, A. Vallier³⁶, J. A. Valls Ferrer¹⁷⁴, T. R. Van Daalen¹⁴, P. Van Gemmeren⁶, S. Van Stroud⁹⁵, I. Van Vulpen¹²⁰, M. Vanadia^{74a,74b}, W. Vandelli³⁶, M. Vandenbroucke¹⁴⁴, E. R. Vandewall¹²⁹, D. Vannicola^{73a,73b}, R. Vari^{73a}, E. W. Varnes⁷, C. Varni^{55a,55b}, T. Varol¹⁵⁸, D. Varouchas⁶⁵, K. E. Varvell¹⁵⁷, M. E. Vasile^{27b}, G. A. Vasquez¹⁷⁶, F. Vazeille³⁸, D. Vazquez Furelos¹⁴, T. Vazquez Schroeder³⁶, J. Veatch⁵³, V. Vecchio¹⁰¹, M. J. Veen¹²⁰, L. M. Veloce¹⁶⁷

F. Veloso^{139a,139c}, S. Veneziano^{73a}, A. Ventura^{68a,68b}, A. Verbytskyi¹¹⁵, V. Vercesi^{71a}, M. Verducci^{72a,72b}, C. M. Vergel Infante⁷⁹, C. Vergis²⁴, W. Verkerke¹²⁰, A. T. Vermeulen¹²⁰, J. C. Vermeulen¹²⁰, C. Vernieri¹⁵³, P. J. Verschuur⁹⁴, M. C. Vetterli^{152.ak}, N. Viaux Maira^{146d}, T. Vickey¹⁴⁹, O. E. Vickey Boeriu¹⁴⁹, G. H. A. Viehhauser¹³⁴, L. Vigani^{61b}, M. Villa^{23a,23b}, M. Villaplana Perez¹⁷⁴, E. M. Villhauer⁵⁰, E. Vilucchi⁵¹, M. G. Vincter³⁴, G. S. Virdee²¹, A. Vishwakarma⁵⁰, C. Vittori^{23a,23b}, I. Vivarelli¹⁵⁶, M. Vogel¹⁸², P. Vokac¹⁴¹, J. Von Ahnen⁴⁶, S. E. von Buddenbrock^{33e}, E. Von Toerne²⁴, V. Vorobel¹⁴², K. VorobeV¹¹², M. Vos¹⁷⁴, J. H. Vosseveld⁹¹, M. Vozak¹⁰¹, N. Vranjes¹⁶, M. Vranjes Milosavljevic¹⁶, V. Vrba¹⁴¹, M. Vreeswijk¹²⁰, N. K. Vu¹⁰², R. Vuillermet³⁶, I. Vukotic³⁷, S. Wada¹⁶⁹, P. Wagner²⁴, W. Wagner¹⁸², J. Wagner-Kuhr¹¹⁴, S. Wahdan¹⁸², H. Wahlberg⁸⁹, R. Wakasa¹⁶⁹, V. M. Walbrecht¹¹⁵, J. Walder¹⁴³, R. Walker¹¹⁴, S. D. Walker⁹⁴, W. Walkowiak¹⁵¹, V. Wallangen^{45a,45b}, A. M. Wang⁵⁹, A. Z. Wang¹⁸¹, C. Wang^{60a}, C. Wang^{60c}, H. Wang¹⁸, H. Wang³, J. Wang^{63a}, P. Wang⁴², Q. Wang¹²⁸, R.-J. Wang¹⁰⁰, R. Wang^{60a}, R. Wang⁶, S. M. Wang¹⁵⁸, W. T. Wang^{60a}, W. Wang^{15c}, W. X. Wang^{60a}, Y. Wang^{60a}, Z. Wang¹⁰⁶, C. Wanotayaroj⁴⁶, A. Warburton¹⁰⁴, C. P. Ward³², R. J. Ward²¹, N. Warrack⁵⁷, A. T. Watson²¹, M. F. Watson²¹, G. Watts¹⁴⁸, B. M. Waugh⁹⁵, A. F. Webb¹¹, C. Weber²⁹, M. S. Weber²⁰, S. A. Weber³⁴, S. M. Weber^{61a}, Y. Wei¹³⁴, A. R. Weidberg¹³⁴, J. Weingarten⁴⁷, M. Weirich¹⁰⁰, C. Weiser⁵², P. S. Wells³⁶, T. Wenaus²⁹, B. Wendland⁴⁷, T. Wengler³⁶, S. Wenig³⁶, N. Vermes²⁴, M. Wessels^{61a}, T. D. Weston²⁰, K. Whalen¹³¹, A. M. Wharton⁹⁰, A. S. White¹⁰⁶, A. White⁸, M. J. White¹, D. Whiteson¹⁷¹, B. W. Whitmore⁹⁰, W. Wiedenmann¹⁸¹, C. Wiel⁴⁸, M. Wielers¹⁴³, N. Wieseotte¹⁰⁰, C. Wiglesworth⁴⁰, L. A. M. Wiik-Fuchs⁵², H. G. Wilkens³⁶, L. J. Wilkins⁹⁴, D. M. Williams³⁹, H. H. Williams¹³⁶, S. Williams³², S. Willocq¹⁰³, P. J. Windischhofer¹³⁴, I. Wingerter-Seez⁵, E. Winkels¹⁵⁶, F. Winklmeier¹³¹, B. T. Winter⁵², M. Wittgen¹⁵³, M. Wobisch⁹⁶, A. Wolf¹⁰⁰, R. Wölker¹³⁴, J. Wollrath⁵², M. W. Wolter⁸⁵, H. Wolters^{139a,139c}, V. W. S. Wong¹⁷⁵, A. F. Wongel⁴⁶, N. L. Woods¹⁴⁵, S. D. Worm⁴⁶, B. K. Wosiek⁸⁵, K. W. Woźniak⁸⁵, K. Wraight⁵⁷, S. L. Wu¹⁸¹, X. Wu⁵⁴, Y. Wu^{60a}, J. Wuerzinger¹³⁴, T. R. Wyatt¹⁰¹, B. M. Wynne⁵⁰, S. Xella⁴⁰, L. Xia¹⁷⁸, J. Xiang^{63c}, X. Xiao¹⁰⁶, X. Xie^{60a}, I. Xioidis¹⁵⁶, D. Xu^{15a}, H. Xu^{60a}, H. Xu^{60a}, L. Xu²⁹, R. Xu¹³⁶, T. Xu¹⁴⁴, W. Xu¹⁰⁶, Y. Xu^{15b}, Z. Xu^{60b}, Z. Xu¹⁵³, B. Yabsley¹⁵⁷, S. Yacoob^{33a}, D. P. Yallup⁹⁵, N. Yamaguchi⁸⁸, Y. Yamaguchi¹⁶⁵, A. Yamamoto⁸², M. Yamatani¹⁶³, T. Yamazaki¹⁶³, Y. Yamazaki⁸³, J. Yan^{60c}, Z. Yan²⁵, H. J. Yang^{60c,60d}, H. T. Yang¹⁸, S. Yang^{60a}, T. Yang^{63c}, X. Yang^{60a}, X. Yang^{60b,58}, Y. Yang¹⁶³, Z. Yang^{60a}, W.-M. Yao¹⁸, Y. C. Yap⁴⁶, H. Ye^{15c}, J. Ye⁴², S. Ye²⁹, I. Yeletsikh⁸⁰, M. R. Yexley⁹⁰, E. Yigitbasi²⁵, P. Yin³⁹, K. Yorita¹⁷⁹, K. Yoshihara⁷⁹, C. J. S. Young³⁶, C. Young¹⁵³, J. Yu⁷⁹, R. Yuan^{60b,i}, X. Yue^{61a}, M. Zaazoua^{35f}, B. Zabinski⁸⁵, G. Zacharis¹⁰, E. Zaffaroni⁵⁴, J. Zahreddine¹³⁵, A. M. Zaitsev^{123.af}, T. Zakareishvili^{159b}, N. Zakharchuk³⁴, S. Zambito³⁶, D. Zanzi³⁶, S. V. Zeiřner⁴⁷, C. Zeitnitz¹⁸², G. Zemaityte¹³⁴, J. C. Zeng¹⁷³, O. Zenin¹²³, T. Ženiř^{28a}, D. Zerwas⁶⁵, M. Zgubić¹³⁴, B. Zhang^{15c}, D. F. Zhang^{15b}, G. Zhang^{15b}, J. Zhang⁶, K. Zhang^{15a}, L. Zhang^{15c}, L. Zhang^{60a}, M. Zhang¹⁷³, R. Zhang¹⁸¹, S. Zhang¹⁰⁶, X. Zhang^{60c}, X. Zhang^{60b}, Y. Zhang^{15a,15d}, Z. Zhang^{63a}, Z. Zhang⁶⁵, P. Zhao⁴⁹, Y. Zhao¹⁴⁵, Z. Zhao^{60a}, A. Zhemchugov⁸⁰, Z. Zheng¹⁰⁶, D. Zhong¹⁷³, B. Zhou¹⁰⁶, C. Zhou¹⁸¹, H. Zhou⁷, M. Zhou¹⁵⁵, N. Zhou^{60c}, Y. Zhou⁷, C. G. Zhu^{60b}, C. Zhu^{15a,15d}, H. L. Zhu^{60a}, H. Zhu^{15a}, J. Zhu¹⁰⁶, Y. Zhu^{60a}, X. Zhuang^{15a}, K. Zhukov¹¹¹, V. Zhulanov^{122a,122b}, D. Zierniska⁶⁶, N. I. Zimine⁸⁰, S. Zimmermann^{52.*}, Z. Zinonos¹¹⁵, M. Ziolkowski¹⁵¹, L. Živković¹⁶, G. Zobernig¹⁸¹, A. Zoccoli^{23a,23b}, K. Zoch⁵³, T. G. Zorbass¹⁴⁹, R. Zou³⁷, L. Zwalinski³⁶

¹ Department of Physics, University of Adelaide, Adelaide, Australia
² Physics Department, SUNY Albany, Albany, NY, USA
³ Department of Physics, University of Alberta, Edmonton, AB, Canada
⁴ (a)Department of Physics, Ankara University, Ankara, Turkey; (b)Istanbul Aydin University, Application and Research Center for Advanced Studies, Istanbul, Turkey; (c)Division of Physics, TOBB University of Economics and Technology, Ankara, Turkey
⁵ LAPP, Université Grenoble Alpes, Université Savoie Mont Blanc, CNRS/IN2P3, Annecy, France
⁶ High Energy Physics Division, Argonne National Laboratory, Argonne, IL, USA
⁷ Department of Physics, University of Arizona, Tucson, AZ, USA
⁸ Department of Physics, University of Texas at Arlington, Arlington, TX, USA
⁹ Physics Department, National and Kapodistrian University of Athens, Athens, Greece
¹⁰ Physics Department, National Technical University of Athens, Zografou, Greece
¹¹ Department of Physics, University of Texas, Austin, TX, USA

- ¹² (a) Bahcesehir University, Faculty of Engineering and Natural Sciences, Istanbul, Turkey; (b) Istanbul Bilgi University, Faculty of Engineering and Natural Sciences, Istanbul, Turkey; (c) Department of Physics, Bogazici University, Istanbul, Turkey; (d) Department of Physics Engineering, Gaziantep University, Gaziantep, Turkey
- ¹³ Institute of Physics, Azerbaijan Academy of Sciences, Baku, Azerbaijan
- ¹⁴ Institut de Física d'Altes Energies (IFAE), Barcelona Institute of Science and Technology, Barcelona, Spain
- ¹⁵ (a) Institute of High Energy Physics, Chinese Academy of Sciences, Beijing, China; (b) Physics Department, Tsinghua University, Beijing, China; (c) Department of Physics, Nanjing University, Nanjing, China; (d) University of Chinese Academy of Science (UCAS), Beijing, China
- ¹⁶ Institute of Physics, University of Belgrade, Belgrade, Serbia
- ¹⁷ Department for Physics and Technology, University of Bergen, Bergen, Norway
- ¹⁸ Physics Division, Lawrence Berkeley National Laboratory and University of California, Berkeley, CA, USA
- ¹⁹ Institut für Physik, Humboldt Universität zu Berlin, Berlin, Germany
- ²⁰ Albert Einstein Center for Fundamental Physics and Laboratory for High Energy Physics, University of Bern, Bern, Switzerland
- ²¹ School of Physics and Astronomy, University of Birmingham, Birmingham, UK
- ²² (a) Facultad de Ciencias y Centro de Investigaciones, Universidad Antonio Nariño, Bogotá, Colombia; (b) Departamento de Física, Universidad Nacional de Colombia, Bogotá, Colombia
- ²³ (a) Dipartimento di Fisica, INFN Bologna and Università di Bologna, Bologna, Italy; (b) INFN Sezione di Bologna, Bologna, Italy
- ²⁴ Physikalisches Institut, Universität Bonn, Bonn, Germany
- ²⁵ Department of Physics, Boston University, Boston, MA, USA
- ²⁶ Department of Physics, Brandeis University, Waltham, MA, USA
- ²⁷ (a) Transilvania University of Brasov, Brasov, Romania; (b) Horia Hulubei National Institute of Physics and Nuclear Engineering, Bucharest, Romania; (c) Department of Physics, Alexandru Ioan Cuza University of Iasi, Iasi, Romania; (d) Physics Department, National Institute for Research and Development of Isotopic and Molecular Technologies, Cluj-Napoca, Romania; (e) University Politehnica Bucharest, Bucharest, Romania; (f) West University in Timisoara, Timisoara, Romania
- ²⁸ (a) Faculty of Mathematics, Physics and Informatics, Comenius University, Bratislava, Slovakia; (b) Department of Subnuclear Physics, Institute of Experimental Physics of the Slovak Academy of Sciences, Kosice, Slovak Republic
- ²⁹ Physics Department, Brookhaven National Laboratory, Upton, NY, USA
- ³⁰ Departamento de Física, Universidad de Buenos Aires, Buenos Aires, Argentina
- ³¹ California State University, Long Beach, CA, USA
- ³² Cavendish Laboratory, University of Cambridge, Cambridge, UK
- ³³ (a) Department of Physics, University of Cape Town, Cape Town, South Africa; (b) iThemba Labs, Western Cape, South Africa; (c) Department of Mechanical Engineering Science, University of Johannesburg, Johannesburg, South Africa; (d) University of South Africa, Department of Physics, Pretoria, South Africa; (e) School of Physics, University of the Witwatersrand, Johannesburg, South Africa
- ³⁴ Department of Physics, Carleton University, Ottawa, ON, Canada
- ³⁵ (a) Faculté des Sciences Ain Chock, Réseau Universitaire de Physique des Hautes Energies, Université Hassan II, Casablanca, Morocco; (b) Faculté des Sciences, Université Ibn-Tofail, Kenitra, Morocco; (c) Faculté des Sciences Semlalia, Université Cadi Ayyad, LPHEA-Marrakech, Marrakesh, Morocco; (d) Moroccan Foundation for Advanced Science Innovation and Research (MAScIR), Rabat, Morocco; (e) Faculté des Sciences, Université Mohamed Premier and LTPM, Oujda, Morocco; (f) Faculté des sciences, Université Mohammed V, Rabat, Morocco
- ³⁶ CERN, Geneva, Switzerland
- ³⁷ Enrico Fermi Institute, University of Chicago, Chicago, IL, USA
- ³⁸ LPC, Université Clermont Auvergne, CNRS/IN2P3, Clermont-Ferrand, France
- ³⁹ Nevis Laboratory, Columbia University, Irvington, NY, USA
- ⁴⁰ Niels Bohr Institute, University of Copenhagen, Copenhagen, Denmark
- ⁴¹ (a) Dipartimento di Fisica, Università della Calabria, Rende, Italy; (b) INFN Gruppo Collegato di Cosenza, Laboratori Nazionali di Frascati, Frascati, Italy
- ⁴² Physics Department, Southern Methodist University, Dallas, TX, USA
- ⁴³ Physics Department, University of Texas at Dallas, Richardson, TX, USA
- ⁴⁴ National Centre for Scientific Research “Demokritos”, Agia Paraskevi, Greece

- 45 ^(a)Department of Physics, Stockholm University, Stockholm, Sweden; ^(b)Oskar Klein Centre, Stockholm, Sweden
- 46 Deutsches Elektronen-Synchrotron DESY, Hamburg and Zeuthen, Germany
- 47 Lehrstuhl für Experimentelle Physik IV, Technische Universität Dortmund, Dortmund, Germany
- 48 Institut für Kern- und Teilchenphysik, Technische Universität Dresden, Dresden, Germany
- 49 Department of Physics, Duke University, Durham, NC, USA
- 50 SUPA, School of Physics and Astronomy, University of Edinburgh, Edinburgh, UK
- 51 INFN e Laboratori Nazionali di Frascati, Frascati, Italy
- 52 Physikalisches Institut, Albert-Ludwigs-Universität Freiburg, Freiburg, Germany
- 53 II. Physikalisches Institut, Georg-August-Universität Göttingen, Göttingen, Germany
- 54 Département de Physique Nucléaire et Corpusculaire, Université de Genève, Geneva, Switzerland
- 55 ^(a)Dipartimento di Fisica, Università di Genova, Genoa, Italy; ^(b)INFN Sezione di Genova, Genoa, Italy
- 56 II. Physikalisches Institut, Justus-Liebig-Universität Giessen, Giessen, Germany
- 57 SUPA, School of Physics and Astronomy, University of Glasgow, Glasgow, UK
- 58 LPSC, Université Grenoble Alpes, CNRS/IN2P3, Grenoble INP, Grenoble, France
- 59 Laboratory for Particle Physics and Cosmology, Harvard University, Cambridge, MA, USA
- 60 ^(a)Department of Modern Physics and State Key Laboratory of Particle Detection and Electronics, University of Science and Technology of China, Hefei, China; ^(b)Institute of Frontier and Interdisciplinary Science and Key Laboratory of Particle Physics and Particle Irradiation (MOE), Shandong University, Qingdao, China; ^(c)School of Physics and Astronomy, Shanghai Jiao Tong University, KLPPAC-MoE, SKLPPC, Shanghai, China; ^(d)Tsung-Dao Lee Institute, Shanghai, China
- 61 ^(a)Kirchhoff-Institut für Physik, Ruprecht-Karls-Universität Heidelberg, Heidelberg, Germany; ^(b)Physikalisches Institut, Ruprecht-Karls-Universität Heidelberg, Heidelberg, Germany
- 62 Faculty of Applied Information Science, Hiroshima Institute of Technology, Hiroshima, Japan
- 63 ^(a)Department of Physics, Chinese University of Hong Kong, Shatin, N.T., Hong Kong, China; ^(b)Department of Physics, University of Hong Kong, Hong Kong, China; ^(c)Department of Physics and Institute for Advanced Study, Hong Kong University of Science and Technology, Clear Water Bay, Kowloon, Hong Kong, China
- 64 Department of Physics, National Tsing Hua University, Hsinchu, Taiwan
- 65 IJCLab, Université Paris-Saclay, CNRS/IN2P3, 91405 Orsay, France
- 66 Department of Physics, Indiana University, Bloomington, IN, USA
- 67 ^(a)INFN Gruppo Collegato di Udine, Sezione di Trieste, Udine, Italy; ^(b)ICTP, Trieste, Italy; ^(c)Dipartimento Politecnico di Ingegneria e Architettura, Università di Udine, Udine, Italy
- 68 ^(a)INFN Sezione di Lecce, Lecce, Italy; ^(b)Dipartimento di Matematica e Fisica, Università del Salento, Lecce, Italy
- 69 ^(a)INFN Sezione di Milano, Milan, Italy; ^(b)Dipartimento di Fisica, Università di Milano, Milan, Italy
- 70 ^(a)INFN Sezione di Napoli, Naples, Italy; ^(b)Dipartimento di Fisica, Università di Napoli, Naples, Italy
- 71 ^(a)INFN Sezione di Pavia, Pavia, Italy; ^(b)Dipartimento di Fisica, Università di Pavia, Pavia, Italy
- 72 ^(a)INFN Sezione di Pisa, Pisa, Italy; ^(b)Dipartimento di Fisica E. Fermi, Università di Pisa, Pisa, Italy
- 73 ^(a)INFN Sezione di Roma, Rome, Italy; ^(b)Dipartimento di Fisica, Sapienza Università di Roma, Rome, Italy
- 74 ^(a)INFN Sezione di Roma Tor Vergata, Rome, Italy; ^(b)Dipartimento di Fisica, Università di Roma Tor Vergata, Rome, Italy
- 75 ^(a)INFN Sezione di Roma Tre, Rome, Italy; ^(b)Dipartimento di Matematica e Fisica, Università Roma Tre, Rome, Italy
- 76 ^(a)INFN-TIFPA, Trento, Italy; ^(b)Università degli Studi di Trento, Trento, Italy
- 77 Institut für Astro- und Teilchenphysik, Leopold-Franzens-Universität, Innsbruck, Austria
- 78 University of Iowa, Iowa City, IA, USA
- 79 Department of Physics and Astronomy, Iowa State University, Ames, IA, USA
- 80 Joint Institute for Nuclear Research, Dubna, Russia
- 81 ^(a)Departamento de Engenharia Elétrica, Universidade Federal de Juiz de Fora (UFJF), Juiz de Fora, Brazil ; ^(b)Universidade Federal do Rio De Janeiro COPPE/EE/IF, Rio de Janeiro, Brazil; ^(c)Instituto de Física, Universidade de São Paulo, São Paulo, Brazil
- 82 KEK, High Energy Accelerator Research Organization, Tsukuba, Japan
- 83 Graduate School of Science, Kobe University, Kobe, Japan
- 84 ^(a)AGH University of Science and Technology, Faculty of Physics and Applied Computer Science, Kraków, Poland ; ^(b)Marian Smoluchowski Institute of Physics, Jagiellonian University, Kraków, Poland
- 85 Institute of Nuclear Physics Polish Academy of Sciences, Krakow, Poland

- 86 Faculty of Science, Kyoto University, Kyoto, Japan
- 87 Kyoto University of Education, Kyoto, Japan
- 88 Research Center for Advanced Particle Physics and Department of Physics, Kyushu University, Fukuoka, Japan
- 89 Instituto de Física La Plata, Universidad Nacional de La Plata and CONICET, La Plata, Argentina
- 90 Physics Department, Lancaster University, Lancaster, UK
- 91 Oliver Lodge Laboratory, University of Liverpool, Liverpool, UK
- 92 Department of Experimental Particle Physics, Jožef Stefan Institute and Department of Physics, University of Ljubljana, Ljubljana, Slovenia
- 93 School of Physics and Astronomy, Queen Mary University of London, London, UK
- 94 Department of Physics, Royal Holloway University of London, Egham, UK
- 95 Department of Physics and Astronomy, University College London, London, UK
- 96 Louisiana Tech University, Ruston, LA, USA
- 97 Fysiska institutionen, Lunds universitet, Lund, Sweden
- 98 Centre de Calcul de l'Institut National de Physique Nucléaire et de Physique des Particules (IN2P3), Villeurbanne, France
- 99 Departamento de Física Teórica C-15 and CIAFF, Universidad Autónoma de Madrid, Madrid, Spain
- 100 Institut für Physik, Universität Mainz, Mainz, Germany
- 101 School of Physics and Astronomy, University of Manchester, Manchester, UK
- 102 CPPM, Aix-Marseille Université, CNRS/IN2P3, Marseille, France
- 103 Department of Physics, University of Massachusetts, Amherst, MA, USA
- 104 Department of Physics, McGill University, Montreal, QC, Canada
- 105 School of Physics, University of Melbourne, Melbourne, VIC, Australia
- 106 Department of Physics, University of Michigan, Ann Arbor, MI, USA
- 107 Department of Physics and Astronomy, Michigan State University, East Lansing, MI, USA
- 108 B.I. Stepanov Institute of Physics, National Academy of Sciences of Belarus, Minsk, Belarus
- 109 Research Institute for Nuclear Problems of Byelorussian State University, Minsk, Belarus
- 110 Group of Particle Physics, University of Montreal, Montreal, QC, Canada
- 111 P.N. Lebedev Physical Institute of the Russian Academy of Sciences, Moscow, Russia
- 112 National Research Nuclear University MEPhI, Moscow, Russia
- 113 D.V. Skobeltsyn Institute of Nuclear Physics, M.V. Lomonosov Moscow State University, Moscow, Russia
- 114 Fakultät für Physik, Ludwig-Maximilians-Universität München, Munich, Germany
- 115 Max-Planck-Institut für Physik (Werner-Heisenberg-Institut), Munich, Germany
- 116 Nagasaki Institute of Applied Science, Nagasaki, Japan
- 117 Graduate School of Science and Kobayashi-Maskawa Institute, Nagoya University, Nagoya, Japan
- 118 Department of Physics and Astronomy, University of New Mexico, Albuquerque, NM, USA
- 119 Institute for Mathematics, Astrophysics and Particle Physics, Radboud University/Nikhef, Nijmegen, The Netherlands
- 120 Nikhef National Institute for Subatomic Physics and University of Amsterdam, Amsterdam, The Netherlands
- 121 Department of Physics, Northern Illinois University, DeKalb, IL, USA
- 122 (a) Budker Institute of Nuclear Physics and NSU, SB RAS, Novosibirsk, Russia; (b) Novosibirsk State University Novosibirsk, Novosibirsk, Russia
- 123 Institute for High Energy Physics of the National Research Centre Kurchatov Institute, Protvino, Russia
- 124 Institute for Theoretical and Experimental Physics named by A.I. Alikhanov of National Research Centre "Kurchatov Institute", Moscow, Russia
- 125 Department of Physics, New York University, New York, NY, USA
- 126 Ochanomizu University, Otsuka, Bunkyo-ku, Tokyo, Japan
- 127 Ohio State University, Columbus, OH, USA
- 128 Homer L. Dodge Department of Physics and Astronomy, University of Oklahoma, Norman, OK, USA
- 129 Department of Physics, Oklahoma State University, Stillwater, OK, USA
- 130 Palacký University, RCPTM, Joint Laboratory of Optics, Olomouc, Czech Republic
- 131 Institute for Fundamental Science, University of Oregon, Eugene, OR, USA
- 132 Graduate School of Science, Osaka University, Osaka, Japan
- 133 Department of Physics, University of Oslo, Oslo, Norway
- 134 Department of Physics, Oxford University, Oxford, UK

- 135 LPNHE, Sorbonne Université, Université de Paris, CNRS/IN2P3, Paris, France
- 136 Department of Physics, University of Pennsylvania, Philadelphia, PA, USA
- 137 Konstantinov Nuclear Physics Institute of National Research Centre “Kurchatov Institute”, PNPI, St. Petersburg, Russia
- 138 Department of Physics and Astronomy, University of Pittsburgh, Pittsburgh, PA, USA
- 139 (a) Laboratório de Instrumentação e Física Experimental de Partículas - LIP, Lisbon, Portugal; (b) Departamento de Física, Faculdade de Ciências, Universidade de Lisboa, Lisbon, Portugal; (c) Departamento de Física, Universidade de Coimbra, Coimbra, Portugal; (d) Centro de Física Nuclear da Universidade de Lisboa, Lisbon, Portugal; (e) Departamento de Física, Universidade do Minho, Braga, Portugal; (f) Departamento de Física Teórica y del Cosmos, Universidad de Granada, Granada, Spain; (g) Dep Física and CEFITEC of Faculdade de Ciências e Tecnologia, Universidade Nova de Lisboa, Caparica, Portugal; (h) Instituto Superior Técnico, Universidade de Lisboa, Lisbon, Portugal
- 140 Institute of Physics of the Czech Academy of Sciences, Prague, Czech Republic
- 141 Czech Technical University in Prague, Prague, Czech Republic
- 142 Charles University, Faculty of Mathematics and Physics, Prague, Czech Republic
- 143 Particle Physics Department, Rutherford Appleton Laboratory, Didcot, UK
- 144 IRFU, CEA, Université Paris-Saclay, Gif-sur-Yvette, France
- 145 Santa Cruz Institute for Particle Physics, University of California Santa Cruz, Santa Cruz, CA, USA
- 146 (a) Departamento de Física, Pontificia Universidad Católica de Chile, Santiago, Chile; (b) Universidad Andres Bello, Department of Physics, Santiago, Chile; (c) Instituto de Alta Investigación, Universidad de Tarapacá, Santiago, Chile; (d) Departamento de Física, Universidad Técnica Federico Santa María, Valparaíso, Chile
- 147 Universidade Federal de São João del Rei (UFSJ), São João del Rei, Brazil
- 148 Department of Physics, University of Washington, Seattle, WA, USA
- 149 Department of Physics and Astronomy, University of Sheffield, Sheffield, UK
- 150 Department of Physics, Shinshu University, Nagano, Japan
- 151 Department Physik, Universität Siegen, Siegen, Germany
- 152 Department of Physics, Simon Fraser University, Burnaby, BC, Canada
- 153 SLAC National Accelerator Laboratory, Stanford, CA, USA
- 154 Physics Department, Royal Institute of Technology, Stockholm, Sweden
- 155 Departments of Physics and Astronomy, Stony Brook University, Stony Brook, NY, USA
- 156 Department of Physics and Astronomy, University of Sussex, Brighton, UK
- 157 School of Physics, University of Sydney, Sydney, Australia
- 158 Institute of Physics, Academia Sinica, Taipei, Taiwan
- 159 (a) E. Andronikashvili Institute of Physics, Iv. Javakhishvili Tbilisi State University, Tbilisi, Georgia; (b) High Energy Physics Institute, Tbilisi State University, Tbilisi, Georgia
- 160 Department of Physics, Technion, Israel Institute of Technology, Haifa, Israel
- 161 Raymond and Beverly Sackler School of Physics and Astronomy, Tel Aviv University, Tel Aviv, Israel
- 162 Department of Physics, Aristotle University of Thessaloniki, Thessaloniki, Greece
- 163 International Center for Elementary Particle Physics and Department of Physics, University of Tokyo, Tokyo, Japan
- 164 Graduate School of Science and Technology, Tokyo Metropolitan University, Tokyo, Japan
- 165 Department of Physics, Tokyo Institute of Technology, Tokyo, Japan
- 166 Tomsk State University, Tomsk, Russia
- 167 Department of Physics, University of Toronto, Toronto, ON, Canada
- 168 (a) TRIUMF, Vancouver, BC, Canada; (b) Department of Physics and Astronomy, York University, Toronto, ON, Canada
- 169 Division of Physics and Tomonaga Center for the History of the Universe, Faculty of Pure and Applied Sciences, University of Tsukuba, Tsukuba, Japan
- 170 Department of Physics and Astronomy, Tufts University, Medford, MA, USA
- 171 Department of Physics and Astronomy, University of California Irvine, Irvine, CA, USA
- 172 Department of Physics and Astronomy, University of Uppsala, Uppsala, Sweden
- 173 Department of Physics, University of Illinois, Urbana, IL, USA
- 174 Instituto de Física Corpuscular (IFIC), Centro Mixto Universidad de Valencia, CSIC, Valencia, Spain
- 175 Department of Physics, University of British Columbia, Vancouver, BC, Canada
- 176 Department of Physics and Astronomy, University of Victoria, Victoria, BC, Canada
- 177 Fakultät für Physik und Astronomie, Julius-Maximilians-Universität Würzburg, Würzburg, Germany
- 178 Department of Physics, University of Warwick, Coventry, UK

- 179 Waseda University, Tokyo, Japan
- 180 Department of Particle Physics and Astrophysics, Weizmann Institute of Science, Rehovot, Israel
- 181 Department of Physics, University of Wisconsin, Madison, WI, USA
- 182 Fakultät für Mathematik und Naturwissenschaften, Fachgruppe Physik, Bergische Universität Wuppertal, Wuppertal, Germany
- 183 Department of Physics, Yale University, New Haven, CT, USA
- ^a Also at Borough of Manhattan Community College, City University of New York, New York, NY, USA
- ^b Center for High Energy Physics, Peking University, China
- ^c Centro Studi e Ricerche Enrico Fermi, Rome, Italy
- ^d CERN, Geneva, Switzerland
- ^e Also at CPPM, Aix-Marseille Université, CNRS/IN2P3, Marseille, France
- ^f Also at Département de Physique Nucléaire et Corpusculaire, Université de Genève, Geneva, Switzerland
- ^g Departament de Física de la Universitat Autònoma de Barcelona, Barcelona, Spain
- ^h Also at Department of Financial and Management Engineering, University of the Aegean, Chios, Greece
- ⁱ Also at Department of Physics and Astronomy, Michigan State University, East Lansing, MI, USA
- ^j Also at Department of Physics and Astronomy, University of Louisville, Louisville, KY, USA
- ^k Also at Department of Physics, Ben Gurion University of the Negev, Beer Sheva, Israel
- ^l Also at Department of Physics, California State University, East Bay, USA
- ^m Also at Department of Physics, California State University, Fresno, USA
- ⁿ Also at Department of Physics, California State University, Sacramento, USA
- ^o Also at Department of Physics, King's College London, London, UK
- ^p Also at Department of Physics, St. Petersburg State Polytechnical University, St. Petersburg, Russia
- ^q Also at Department of Physics, University of Fribourg, Fribourg, Switzerland
- ^r Also at Dipartimento di Matematica, Informatica e Fisica, Università di Udine, Udine, Italy
- ^s Also at Faculty of Physics, M.V. Lomonosov Moscow State University, Moscow, Russia
- ^t Also at Giresun University, Faculty of Engineering, Giresun, Turkey
- ^u Also at Graduate School of Science, Osaka University, Osaka, Japan
- ^v Hellenic Open University, Patras, Greece
- ^w Also at Institutio Catalana de Recerca i Estudis Avancats, ICREA, Barcelona, Spain
- ^x Also at Institut für Experimentalphysik, Universität Hamburg, Hamburg, Germany
- ^y Institute for Nuclear Research and Nuclear Energy (INRNE) of the Bulgarian Academy of Sciences, Sofia, Bulgaria
- ^z Also at Institute for Particle and Nuclear Physics, Wigner Research Centre for Physics, Budapest, Hungary
- ^{aa} Institute of Particle Physics (IPP), Montreal, Canada
- ^{ab} Also at Institute of Physics, Azerbaijan Academy of Sciences, Baku, Azerbaijan
- ^{ac} Also at Instituto de Física Teórica, IFT-UAM/CSIC, Madrid, Spain
- ^{ad} Also at Istanbul University, Department of Physics, Istanbul, Turkey
- ^{ae} Joint Institute for Nuclear Research, Dubna, Russia
- ^{af} Moscow Institute of Physics and Technology State University, Dolgoprudny, Russia
- ^{ag} National Research Nuclear University MEPhI, Moscow, Russia
- ^{ah} Also at Physics Department, An-Najah National University, Nablus, Palestine
- ^{ai} Also at Physikalisches Institut, Albert-Ludwigs-Universität Freiburg, Freiburg, Germany
- ^{aj} The City College of New York, New York, NY, USA
- ^{ak} TRIUMF, Vancouver, BC, Canada
- ^{al} Università di Napoli Parthenope, Naples, Italy
- ^{am} University of Chinese Academy of Sciences (UCAS), Beijing, China
- * Deceased